

The Effect of Ivy Leaf Dry Extract EA 575[®] on the Signalling of Adenosine Receptor A_{2B}

Dissertation

zur Erlangung des Doktorgrades (Dr. rer. nat.)
der Mathematisch-Naturwissenschaftlichen Fakultät
der Rheinischen Friedrich-Wilhelms-Universität Bonn

vorgelegt von

Fabio Gian-Luca Meurer

aus Lohmar

Bonn 2024

Angefertigt mit Genehmigung der Mathematisch-Naturwissenschaftlichen Fakultät
der Rheinischen Friedrich-Wilhelms-Universität Bonn

1. Gutachter: Prof. Dr. Hanns Häberlein

2. Gutachter: Prof. Dr. Gerd Bendas

Tag der Promotion: 16.05.2024

Erscheinungsjahr: 2024

Die vorliegende Arbeit wurde in der Zeit von Januar 2019 bis Januar 2024 am Institut für Biochemie und Molekularbiologie der Rheinischen Friedrich-Wilhelms-Universität Bonn unter der Leitung von Herrn Prof. Dr. Hanns Häberlein angefertigt.

*“When the sun burns out will it all be worth it?
Will the stars fall down into you?
No one knows”*

While She Sleeps – YOU ARE ALL YOU NEED

Abstract*

Ivy leaf dry extract EA 575[®] is used to alleviate the symptoms associated with chronic inflammatory bronchial diseases and acute inflammation of the respiratory tract accompanied by coughing. Its mechanism of action has so far been explained by influencing β_2 -adrenergic signal transduction. The present study investigated the effect of EA 575[®] on the signalling of adenosine receptor A_{2B} (A_{2B}AR), as it has been described to play a significant and detrimental role in chronic inflammatory airway diseases. This part of the study has already been published [1]. In addition, this study approached to identify the compounds of EA 575[®] responsible for the observed effects. Moreover, a HEK293 cell line expressing HiBiT-tagged A_{2B}AR at an endogenous expression level was generated, with the aim to conduct experiments on the receptor's behaviour under the influence of EA 575[®].

The influence of EA 575[®] on A_{2B}AR signalling was assessed using various cellular assays targeting different events in the signalling cascade. Initially, the effect on the cellular reaction following A_{2B}AR stimulation was investigated by measurements of dynamic mass redistribution. Subsequently, the effects on A_{2B}AR-mediated second messenger cAMP levels, β -arrestin 2 recruitment, and cAMP response element (CRE) activation were examined using luciferase-based HEK293 reporter cell lines. Lastly, the impact on A_{2B}AR-mediated IL-6 release in Calu-3 epithelial lung cells was investigated via Lumit[™] Immunoassay. Additionally, the adenosine receptor subtype mediating these effects was specified. Bioassay-guided fractionation of EA 575[®] was performed, combining HPLC methods with cAMP measurements and LC-MS/MS analyses, for the identification and isolation of bioactive compounds. CRISPR/Cas9-mediated homology-directed repair (HDR) was utilised for the expression of HiBiT-tagged A_{2B}AR under endogenous promotion in HEK293 cells.

* Parts of this study, in particular the cellular assays investigating the influence of EA 575[®] on A_{2B}AR signalling, have been published recently within the scope of my doctoral studies [1]. For the sake of completeness and readability, these parts were incorporated into this work. This chapter therefore contains text passages from the referenced publication, which were revised and supplemented where necessary. Further information can be found in 10.4.

The results demonstrate the inhibitory effect of EA 575[®] on A_{2B}AR-mediated general cellular response, cAMP levels, β -arrestin 2 recruitment, CRE activation, and IL-6 release. Since these EA 575[®]-mediated effects occurred within a time frame of several hours of incubation, its mode of action may be described as indirect. The data presented here are the first to describe an inhibitory effect of EA 575[®] on A_{2B}AR signalling. Thus, a novel mechanism of action of EA 575[®] was revealed. Additionally, two bioactive sub-fractions of EA 575[®] were obtained that showed effects similar to the total extract, allowing to narrow down potential candidates responsible for the newly discovered effects of EA 575[®]. The HEK293 cell line expressing HiBiT-tagged A_{2B}AR at an endogenous expression level was successfully generated using CRISPR/Cas9-mediated HDR. However, due to insufficient signals, it could not be utilised for the additional experiments on the receptor's behaviour.

The findings of this study offer an explanation for initial positive clinical effects associated with EA 575[®] in adjuvant asthma therapy. Furthermore, they provide a rationale to conduct additional studies in animals or human subjects to explore further effects on chronic airway diseases such as asthma or COPD.

Table of Contents

Abstract	IV
Table of Contents	VI
Abbreviations	VIII
List of Figures	XII
List of Tables	XIV
1 Introduction	1
2 Aim and Approach	4
3 Materials	5
3.1 <i>Cell lines</i>	5
3.1.1 Bought cell lines	5
3.1.2 Genetically modified cell lines	6
3.2 <i>Solutions</i>	7
3.2.1 Bought solutions	7
3.2.2 Self-made solutions	8
3.3 <i>Chemicals</i>	10
4 Methods	13
4.1 <i>Cell culture</i>	13
4.2 <i>Transformation</i>	13
4.3 <i>Dynamic mass redistribution measurements</i>	14
4.4 <i>cAMP measurements</i>	15
4.4.1 Transfection	15
4.4.2 Assay procedure	15
4.5 <i>Measurements of β-arrestin 2 recruitment</i>	16
4.5.1 Plasmid generation	16
4.5.2 Transfection	16
4.5.3 Assay procedure	17
4.6 <i>Measurements of CRE activation</i>	17
4.6.1 Transfection	17
4.6.2 Assay procedure	17
4.7 <i>IL-6 measurements</i>	18
4.8 <i>Measurements of NFκB transcriptional activity</i>	18
4.8.1 Plasmid generation	18
4.8.2 Transfection	19
4.8.3 Assay procedure	19
4.9 <i>Identification of active constituents</i>	19
4.9.1 HPLC analysis	19
4.9.2 Characterisation of EA 575 [®]	20

4.9.3	Compound combinations	21
4.10	<i>Bioassay-guided fractionation</i>	22
4.10.1	Fractionation of EA 575 [®]	22
4.10.2	Sub-fractionation of fraction I	24
4.10.3	Mass spectrometry (LC-MS/MS)	24
4.11	<i>Generation of a HEK HiBiT-A_{2B}AR cell line using CRISPR/Cas9-mediated HDR</i>	25
4.11.1	CRISPR/Cas9 lipofection	25
4.11.2	PCR analyses	26
4.11.3	PCR screening	27
4.11.4	RNA analysis	27
4.11.5	Measurements of HiBiT-tagged A _{2B} AR	28
4.12	<i>Generation of an overexpressing HEK HiBiT-A_{2B}AR cell line</i>	28
4.12.1	Plasmid generation	28
4.12.2	Transfection	29
4.12.3	Measurements of HiBiT-tagged A _{2B} AR	29
4.13	<i>Statistical analysis</i>	29
5	Results	30
5.1	<i>Influence of EA 575[®] on A_{2B}AR-mediated intracellular dynamic mass redistribution</i>	30
5.2	<i>Influence of EA 575[®] on A_{2B}AR-mediated intracellular cAMP levels</i>	34
5.3	<i>Influence of EA 575[®] on β-arrestin 2 recruitment to A_{2B}AR</i>	37
5.4	<i>Influence of EA 575[®] on CRE activation and determination of the responsible receptor subtype</i>	39
5.5	<i>Influence of EA 575[®] on IL-6 release and determination of the responsible receptor subtype</i>	41
5.6	<i>Influence of adenosine receptor signalling on NFκB transcriptional activity</i>	44
5.7	<i>Identification of active constituents contained in EA 575[®]</i>	45
5.8	<i>Bioassay-guided fractionation of EA 575[®]</i>	50
5.9	<i>Generation and investigation of a HEK HiBiT-A_{2B}AR cell line using CRISPR/Cas9-mediated HDR</i>	59
5.10	<i>Generation and investigation of an overexpressing HEK HiBiT-A_{2B}AR cell line</i>	64
6	Discussion	65
7	Conclusion and Outlook	81
8	References	84
9	Supplemental Material	96
10	Appendix	118
10.1	<i>Publikationen und Poster</i>	118
10.2	<i>Danksagung</i>	119
10.3	<i>Eidesstattliche Erklärung</i>	120
10.4	<i>Zusammenfassung der Publikation nach PromO § 9 (4) und Erklärung zu teil-kumulativer Dissertation</i>	121

Abbreviations

A _{2A} AR	Adenosine receptor A _{2A}
A _{2B} AR	Adenosine receptor A _{2B}
ADA	Adenosine deaminase
ADORA2B	Gene coding for adenosine receptor A _{2B}
ANOVA	Analysis of variance
ARRB2	β-arrestin 2
AUC	Area under the curve
BALF	Bronchoalveolar lavage fluid
BC	Baseline-corrected
BODE index	Body-mass index, airflow obstruction, dyspnea and exercise capacity index in chronic obstructive pulmonary disease
cAMP	Cyclic adenosine monophosphate
Cas9	CRISPR-associated protein 9
CD39	Ectonucleoside triphosphate diphosphohydrolase-1
CD73	5'-Nucleotidase
cDNA	Complementary DNA
COPD	Chronic obstructive pulmonary disease
CMV	Cytomegalovirus
CRE	cAMP response element
CRISPR	Clustered Regularly Interspaced Short Palindromic Repeats
crRNA	CRISPR RNA

DQA	Dicaffeoylquinic acid
DER	Drug extract ratio
DMEM	Dulbecco's Modified Eagle Medium
DMEM/F-12	Dulbecco's Modified Eagle Medium/Nutrient Mixture F-12
DMR	Dynamic mass redistribution
DNA	Deoxyribonucleic acid
EBC	Exhaled breath condensate
EC ₅₀	Half maximal effective concentration
ERK	Extracellular signal-regulated kinases
FBS	Fetal bovine serum
FC	Fold change
FEV ₁	Forced expiratory volume in 1 second
FSK	Forskolin
G418	Geneticin
GFP	Green fluorescent protein
GOLD	Global Initiative for Chronic Obstructive Lung Disease
GPCR	G protein-coupled receptor
GRK2	G protein-coupled receptor kinase 2
gRNA	Guide RNA
HBSS	Hanks' Balanced Salt Solution
HDR	Homology-directed repair
HEK	Human embryonic kidney
HEPES	4-(2-Hydroxyethyl)piperazine-1-ethanesulfonic acid

Abbreviations

HPLC	High-performance liquid chromatography
I κ B α	Inhibitor of nuclear factor 'kappa-light-chain-enhancer' of activated B-cells, alpha
IL-6	Interleukin-6
LB medium	Lysogeny broth medium
LC-MS/MS	Liquid chromatography coupled with tandem mass spectrometry
mRNA	Messenger RNA
NanoLuc [®] -PEST / NlucP	NanoLuc [®] luciferase destabilised through proline (P), glutamate (E), serine (S), and threonine (T)
NECA	5'-N-Ethylcarboxamidoadenosine
NF κ B	Nuclear factor 'kappa-light-chain-enhancer' of activated B-cells
PAH	Pulmonary arterial hypertension
PAM	Protospacer adjacent motif
PCR	Polymerase chain reaction
PDL	Poly-D-lysine hydrobromide
PEI	Branched polyethylenimine
PKA	Protein kinase A
PKC	Protein kinase C
RLU	Relative light unit
RNA	Ribonucleic acid
RNP	Ribonucleoprotein
RP	Reversed-phase

RT	Room temperature
SC	Stimulated control
secNluc	Secreted NanoLuc [®] luciferase
SEM	Standard error of the mean
TNF α	Tumor necrosis factor alpha
tracrRNA	Trans-activating CRISPR RNA
UTC	Untreated control
wt	Wild-type
YFP	Yellow fluorescent protein
β_2 -AR	β_2 -adrenergic receptor

List of Figures

Figure 1:	Schematic overview of the preparation of the compound combinations	21
Figure 2:	Flowchart of the fractionation of EA 575 [®]	22
Figure 3:	Principle of DMR detection	31
Figure 4:	Dose-response curve of BAY 60-6583 in the DMR measurements	32
Figure 5:	Influence of EA 575 [®] (A) and different incubation periods thereof (B) on the cellular reaction of HEK GloSensor™ cells evoked by stimulation of A _{2B} AR	33
Figure 6:	Principle of the GloSensor™ technology	34
Figure 7:	Dose-response curve of BAY 60-6583 in the cAMP level measurements	35
Figure 8:	Influence of EA 575 [®] (A) and different incubation periods thereof (B) on the intracellular cAMP levels in HEK GloSensor™ cells elicited by stimulation of A _{2B} AR	36
Figure 9:	Principle of the measurements of β-arrestin 2 recruitment	37
Figure 10:	Influence of EA 575 [®] on the recruitment of β-arrestin 2 to A _{2B} AR in transiently transfected HEK cells following stimulation with NECA or BAY 60-6583	38
Figure 11:	Influence of EA 575 [®] (A,B) or the antagonists PSB-603 and SCH 442416 (C) on the CRE activation in transiently transfected HEK cells mediated by stimulation with adenosine (A,C,D), BAY 60-6583 (B,D) or CGS 21680 (D)	40
Figure 12:	Principle of the Lumit™ IL-6 (Human) Immunoassay	41
Figure 13:	Influence of adenosine, BAY 60-6583, and TNFα on the IL-6 release in Calu-3 cells	42
Figure 14:	Influence of EA 575 [®] (A,B) or the antagonists PSB-603 and SCH 442416 (C) on the IL-6 release of Calu-3 cells mediated by stimulation with adenosine (A,C), BAY 60-6583 (B,D) or CGS 21680 (D)	43
Figure 15:	Influence of different adenosine receptor agonists on the NFκB transcriptional activity	44
Figure 16:	HPLC chromatogram of EA 575 [®] at 205 nm with structural formulae of the main components	46
Figure 17:	HPLC chromatogram of compound combination 1 at 205 nm	48
Figure 18:	Influence of the compound combinations on the intracellular cAMP levels in HEK GloSensor™ cells elicited by stimulation of A _{2B} AR	49
Figure 19:	Influence of the fractions (A) and different concentrations of fraction I (B) on the intracellular cAMP levels in HEK GloSensor™ cells elicited by stimulation of A _{2B} AR	50
Figure 20:	HPLC chromatogram of fraction I at 205 nm	52
Figure 21:	HPLC chromatogram of sub-fraction I-2 at 205 nm	53
Figure 22:	HPLC chromatogram of sub-fraction I-3 at 205 nm	54

Figure 23:	Influence of the sub-fractions (A) and combinations thereof (B) on the intracellular cAMP levels in HEK GloSensor™ cells elicited by stimulation of A _{2B} AR	55
Figure 24:	Influence of chlorogenic acid, neochlorogenic acid, and a combination thereof on the intracellular cAMP levels in HEK GloSensor™ cells elicited by stimulation of A _{2B} AR	58
Figure 25:	Principle of the CRISPR/Cas9-mediated HDR DNA knock-in	60
Figure 26:	Agarose gel electrophoresis of HEK CRISPR HiBiT-A _{2B} AR DNA	61
Figure 27:	Agarose gel electrophoresis of HEK CRISPR HiBiT-A _{2B} AR cDNA	62
Figure 28:	Quantification of HiBiT-tagged A _{2B} AR on the cell surface (A) and in the cell lysate (B) of HEK CRISPR HiBiT-A _{2B} AR cells	63
Figure 29:	Quantification of HiBiT-tagged A _{2B} AR on the cell surface of HEK HiBiT-A _{2B} AR cells	64
Figure 30:	Schematic illustration of the proposed mode of action of EA 575® on A _{2B} AR signalling	82
Figure S 1:	Protocol of the NucleoBond™ Xtra Midi kit by Macherey-Nagel	96
Figure S 2:	Plasmid map of pGloSensor™-22F cAMP	97
Figure S 3:	Protocol for electroporation of HEK cells by Lonza	97
Figure S 4:	Protocol for single-cell cloning by Corning	98
Figure S 5:	Plasmid map of pCMV_ADORA2B-LgBiT	99
Figure S 6:	Plasmid map of pcDNA™3.1/Zeo ⁽⁺⁾ _SmBiT-ARRB2	99
Figure S 7:	Plasmid map of pNL_CRE-NlucP	100
Figure S 8:	Protocol of Nano-Glo® Vivazine™ Live Cell Substrate by Promega	101
Figure S 9:	Protocol of Lumit™ IL-6 (Human) Immunoassay by Promega	102
Figure S 10:	Plasmid map of pcDNA™3.1 ⁽⁺⁾ _NFκB-secNluc	103
Figure S 11:	Protocol of Metafectene® Pro by Biontex	104
Figure S 12:	Protocol of Nano-Glo® Luciferase Assay System by Promega	105
Figure S 13:	HPLC chromatogram of EA 575® at 205 nm applying the method without phosphoric acid	106
Figure S 14:	Overlay of the fraction chromatograms	107
Figure S 15:	Overlay of the sub-fraction chromatograms	108
Figure S 16:	Protocol of Nano-Glo® HiBiT Extracellular Detection System by Promega	109
Figure S 17:	Protocol of Nano-Glo® HiBiT Extracellular Detection System by Promega	110
Figure S 18:	Protocol of the NucleoSpin® RNA XS kit by Macherey Nagel	111
Figure S 19:	Protocol of the First Strand cDNA Synthesis Kit by Thermo Fisher Scientific	112
Figure S 20:	Plasmid map of pcDNA™3.1/Zeo ⁽⁺⁾ _HiBiT-ADORA2B	113

List of Tables

Table 1:	Bought cell lines	5
Table 2:	Genetically modified cell lines	6
Table 3:	Bought solutions	7
Table 4:	Self-made solutions	8
Table 5:	Chemicals and kits	10
Table 6:	HPLC gradient	20
Table 7:	Collected fractions of EA 575 [®]	23
Table 8:	Primer combinations used for the detection of genome-edited clones	26
Table 9:	Identification and quantification of the compounds in EA 575 [®] and analysis of compound combination 1	47
Table S 1:	PCR cycling parameters	114
Table S 2:	Presumed substances identified in sub-fraction I-2 via LC-MS/MS (positive ionisation mode)	114
Table S 3:	Presumed substances identified in sub-fraction I-2 via LC-MS/MS (negative ionisation mode)	115
Table S 4:	Presumed substances identified in sub-fraction I-3 via LC-MS/MS (positive ionisation mode)	116
Table S 5:	Presumed substances identified in sub-fraction I-3 via LC-MS/MS (negative ionisation mode)	117

1 Introduction*

The use of medicinal products containing ivy leaf (*Hedera helix* L.) dry extract EA 575[®] is recommended for the treatment of chronic inflammatory airway diseases and acute respiratory tract inflammation accompanied by coughing [2–5]. Two recent publications, a comprehensive review and a meta-analysis, underline the efficacy and tolerability of EA 575[®] in the treatment of acute and chronic cough across all age groups [6,7].

Chronic respiratory diseases are among the most important health issues. For example, asthma affects 1–29 % of the population in different countries, while the global prevalence of chronic obstructive pulmonary disease (COPD) is estimated to be 10.3 %. Both diseases are associated with coughing [8,9]. To date, the guidelines do not recommend any phytopharmaceuticals, but initial studies have indicated positive effects from adjuvant treatment with EA 575[®] on lung function in children with asthma [3,10].

Until now, the main mechanism of action of EA 575[®] has been explained by its influence on the β_2 -adrenergic receptor (β_2 -AR). It has been shown that α -hederin identified in EA 575[®] indirectly inhibits GRK2-mediated phosphorylation of β_2 -AR [11], which is the reason for the decrease in recruitment of β -arrestin 2 by EA 575[®] [12]. This leads to the inhibition of β_2 -AR internalisation [13–15], which in turn results in increased β_2 -adrenergic responsiveness, as evidenced by a corresponding increase in receptor binding and cAMP formation [12,14]. This biased signalling by EA 575[®] offers an explanation for the bronchospasmolytic and secretolytic effects, as well as the reduction in β -arrestin-mediated negative adverse effects [12]. The anti-inflammatory effects of EA 575[®] are substantiated by β -arrestin-independent inhibition of NF κ B, presumably by the inhibition of I κ B α phosphorylation, leading to decreased IL-6 release [12,16,17].

* Parts of this study, in particular the cellular assays investigating the influence of EA 575[®] on A_{2B}AR signalling, have been published recently within the scope of my doctoral studies [1]. For the sake of completeness and readability, these parts were incorporated into this work. This chapter therefore contains text passages from the referenced publication, which were revised and supplemented where necessary. Further information can be found in 10.4.

As additional receptor classes are involved in the pathogenesis of these respiratory diseases, it is essential to explore other signalling pathways that may be affected by EA 575[®]. These pathways could provide explanations for its beneficial effects in the treatment of inflammatory airway diseases. Many authors have described the harmful influence of adenosine via its adenosine receptor A_{2B} (A_{2B}AR) in chronic inflammatory airway diseases [18–21], based on the following findings.

Elevated adenosine concentrations were found in the bronchoalveolar lavage fluid (BALF) and exhaled breath condensate (EBC) of patients with chronic respiratory diseases such as asthma and chronic obstructive pulmonary disease (COPD), indicating increased adenosine levels in the lungs [22–25]. These elevations in adenosine were correlated with decreased forced expiratory volumes in 1 second (FEV₁) and higher Global Initiative for Chronic Obstructive Lung Disease (GOLD) stages [25,26]. Inhalation of adenosine or adenosine monophosphate (AMP) caused bronchoconstriction in patients with asthma and COPD but not in healthy subjects [27–29]. Remarkably, elevated transcript levels of A_{2B}AR were recovered from the lung tissues of patients with severe COPD, pulmonary fibrosis, and pulmonary arterial hypertension (PAH) [30,31]. Further elevation of transcript and A_{2B}AR protein levels was observed in the lung tissues of patients with COPD when accompanied by pulmonary hypertension, indicating a correlation with disease severity [32].

Several experiments in mouse models have provided additional evidence for the detrimental impact of adenosine and A_{2B}AR signalling on airway diseases such as asthma, COPD, and pulmonary fibrosis. Genetically-altered adenosine deaminase (ADA)-deficient mice developed severe pulmonary inflammation and airway remodelling as observed in these disorders [33,34]. Lowering adenosine concentrations via ADA enzyme therapy ameliorated lung injury, indicating a correlation between adenosine levels and inflammation, as well as fibrosis in the lungs [35,36]. Attenuation of pulmonary inflammation, fibrosis, and airway enlargement could also be achieved by administration of specific A_{2B}AR antagonists [32,37]. Transcript levels of A_{2B}AR were also increased in this model and could be decreased by specific antagonism of A_{2B}AR [34,37,38].

Similar observations have been made in another mouse model. Mice treated with bleomycin had elevated levels of adenosine and transcripts of A_{2B}AR in their lungs and developed pulmonary fibrosis and inflammation. This disease progression could be counteracted with specific A_{2B}AR antagonists [37,39].

The proinflammatory and profibrotic cytokine interleukin-6 (IL-6) is associated with the signalling of adenosine via A_{2B}AR and also plays a pivotal role in these pulmonary disorders [19,40]. Patients with asthma exhibited elevated levels of IL-6 in their sputum and BALF compared to healthy subjects [41–43] and compared to asymptomatic asthmatics [44,45], who already have higher serum IL-6 concentrations [46]. A further IL-6 increase in serum and BALF occurred after allergen inhalation and during allergic attacks [46,47]. Most remarkably, the sputum IL-6 levels in asthmatics inversely correlated with FEV₁ and peak expiratory flow [43,48,49].

Elevations of IL-6 have also been found in the sputum and serum of patients with COPD compared to healthy controls [50,51], further increasing during exacerbations [52]. As in asthmatics, higher IL-6 levels inversely correlated with lung function [51,52]. Furthermore, correlations with disease severity [53], GOLD stage and BODE index [50], and even mortality [54] have been described.

Correspondingly, genetic IL-6-knockout or anti-IL-6 antibody treatment led to reduced pulmonary inflammation and fibrosis in both of the aforementioned mouse models [55,56]. Further evidence for the deleterious interaction of IL-6 and A_{2B}AR has been provided by experiments using genetic A_{2B}AR-knockouts. While the adenosine receptor agonist NECA caused increased IL-6 secretion in mouse macrophages, reduced IL-6 levels were found in A_{2B}AR-knockout mice [57,58]. Bleomycin-treated mice also exhibited elevated IL-6 levels, which could be decreased by A_{2B}AR-knockout, resulting in improved lung function, as well as attenuated pulmonary fibrosis and hypertension [31,39,59]. Moreover, ADA enzyme therapy in ADA-deficient mice was able to reduce IL-6 levels [56].

2 Aim and Approach

The primary aim of this study was to investigate whether the ivy leaf dry extract EA 575[®] has an influence on adenosine receptor A_{2B} signalling and the subsequent release of IL-6. These processes have been described to play a significant and detrimental role in chronic inflammatory pulmonary diseases. For this purpose, cellular assays should be conducted examining the effect of EA 575[®] on various mechanisms within the A_{2B}AR signalling cascade. The findings could offer an explanation for the initial positive clinical effects of EA 575[®] in adjuvant asthma therapy, possibly by the inhibition of A_{2B}AR signalling. Furthermore, this could provide a rationale for conducting further clinical studies with EA 575[®] in patients with chronic respiratory diseases.

The second aim of the present study was to identify the constituents of EA 575[®] responsible for the potential effects. Two different approaches were considered for this purpose. Initially, major compounds identified previously should be tested. Then, bioassay-guided fractionation should be employed. The identification could enhance the understanding of the mechanism of action of EA 575[®] on A_{2B}AR signalling. This could provide a basis for the use of an EA 575[®] extract, enriched specifically with the bioactive substances.

The third aim of this work was to assess the behaviour of A_{2B}AR under the influence of EA 575[®], particularly internalisation measurements and single-particle tracking experiments. To enable the use of these techniques, the application of receptor tags is required. Since overexpression of receptors can lead to artificial results, this study approached to generate HEK cells expressing A_{2B}AR with a small protein tag at an endogenous expression level. To accomplish this, CRISPR/Cas9-mediated homology-directed repair (HDR) should be used to integrate the tag into the genome while preserving the endogenous promotion of the receptor. This could provide the ability to study the natural behaviour of the receptor in order to further explore the mechanism of action of EA 575[®].

3 Materials

3.1 Cell lines

3.1.1 Bought cell lines

Table 1: Bought cell lines

Name	Cell type	Supplied by	Reference number
Calu-3	Human epithelial lung cancer cells	ATCC, Manassas, VA	HTB-55
HEK293	Human embryonic kidney cells	Deutsche Sammlung von Mikroorganismen und Zellkulturen (DSMZ) GmbH, Braunschweig, Germany	ACC 305

3.1.2 Genetically modified cell lines

Table 2: Genetically modified cell lines

Name	Expressed genetic information	Transfection Method
Calu-3 NFκB secNluc	secreted NanoLuc [®] luciferase under control of a NFκB binding sequence	Lipofection (Metafectene [®] Pro)
HEK A _{2B} AR-LgBiT/SmBiT-ARRB2	A _{2B} AR with N-terminal LgBiT & β-arrestin 2 with C-terminal SmBiT	PEI (<i>transient</i>)
HEK CRE NlucP	Destabilised NanoLuc [®] luciferase under control of a promoter with CRE	PEI (<i>transient</i>)
HEK CRISPR HiBiT+Spacer-A _{2B} AR	A _{2B} AR with N-terminal HiBiT and Spacer in between at an endogenous expression level	CRISPR/Cas9-mediated HDR via Lipofection (Lipofectamine [™] CRISPRMAX [™])
HEK HiBiT+Spacer-A _{2B} AR	Overexpressed A _{2B} AR with N-terminal HiBiT and Spacer in between	PEI
HEK GloSensor [™]	Luciferase-based live-cell biosensor for cAMP activity	Electroporation

3.2 Solutions

3.2.1 Bought solutions

Table 3: Bought solutions

Name	Abbreviation	Supplied by	Reference number
Dulbecco's Modified Eagle Medium	DMEM	Thermo Fisher Scientific, Waltham, MA	31885049
Dulbecco's Modified Eagle Medium/ Nutrient Mixture F-12	DMEM/F-12	Thermo Fisher Scientific	21331046
Dulbecco's Modified Eagle Medium/ Nutrient Mixture F-12, no phenol red	DMEM/F-12 without phenol red	Thermo Fisher Scientific	21041025
Fetal bovine serum	FBS	Thermo Fisher Scientific	10270106
GlutaMAX™	-	Thermo Fisher Scientific	35050061
Hanks' Balanced Salt Solution	HBSS	Thermo Fisher Scientific	14025050
Opti-MEM™	-	Thermo Fisher Scientific	31985062
Penicillin-Streptomycin (10.000 U/ml)	P/S	Thermo Fisher Scientific	15140122
Phosphate buffered saline	PBS	Thermo Fisher Scientific	10010056

Materials

Trypsin-EDTA (0.05 %)	T/E	Thermo Fisher Scientific	25300104
-----------------------	-----	--------------------------	----------

3.2.2 Self-made solutions

Table 4: Self-made solutions

Name	Composition
Calu-3 medium	DMEM/F-12 1 % (v/v) GlutaMAX™ 100 units/ml penicillin 100 µg/ml streptomycin 15 % (v/v) FBS
Electroporation buffer	5 mM KCl 15 mM MgCl ₂ 15 mM HEPES 50 mM NaCl 150 mM Na ₂ HPO ₄ /NaH ₂ PO ₄ pH 7.2
HEK medium	DMEM 100 units/ml penicillin 100 µg/ml streptomycin 10 % (v/v) FBS
HEPES-buffered medium	50 % fully supplemented HEK medium 50 % HEPES-buffered HBSS

HEPES-buffered HBSS	20 mM HEPES 500 ml HBSS adjusted with NaOH to pH 7.4
Lysis buffer (slightly modified from [60])	50 mM KCl 10 mM TRIS pH 8.0 2.5 mM MgCl ₂ 0.45 % (v/v) NP-40 0.45 % (v/v) Tween 20 400 µg/ml Proteinase K
LB medium	1 % (w/v) Bacto™ Tryptone 0.5 % (w/v) Bacto™ Yeast extract 1 % (w/v) NaCl adjusted with NaOH to pH 7.0

3.3 Chemicals

Table 5: Chemicals and kits

Name	Supplied by	Reference number
3,4-Dicaffeoylquinic acid	Phytolab, Vestenbergsgreuth, Germany	80425
3,5-Dicaffeoylquinic acid	Phytolab	80426
4,5-Dicaffeoylquinic acid	Phytolab	80427
Acetonitrile	VWR International GmbH, Langenfeld, Germany	20060.320
Adenosine	Sigma-Aldrich, Crailsheim, Germany	A9251
Ampicillin	Sigma-Aldrich	A0166
Alt-R™ CRISPR-Cas9 System Kit (containing crRNA, tracrRNA, Cas9, Nuclease-Free Duplex Buffer, and HDR Enhancer)	Integrated DNA Technologies (IDT), Coralville, IA	-
BAY 60-6583	Sigma-Aldrich	SML1958
CGS 21680	Biomol, Hamburg, Germany	Cay17126
Chlorogenic acid	Phytolab	89175
Coelenterazine h	Prolume, Pinetop-Lakeside, AZ	CAT#301
Cryptochlorogenic acid	Phytolab	80393
Lipofectamine™ CRISPRMAX™ Cas9 Transfection Reagent	Thermo Fisher Scientific	CMAX00

EA 575 [®] (DER 5-7.5:1, 30 % ethanol; batch number 14B0310)	Engelhard Arzneimittel, Niederdorfelden, Germany	-
First Strand cDNA Synthesis Kit	Thermo Fisher Scientific	K1612
Formic acid	Sigma-Aldrich	5.33002
Forskolin	Sigma-Aldrich	F6886
G418	Thermo Fisher Scientific	11811064
GeneRuler 100 bp Plus DNA Ladder	Thermo Fisher Scientific	SM0321
GloSensor™ Assay Reagent	Promega, Mannheim, Germany	E1290
Hederacoside B	Hölzel Diagnostika, Cologne, Germany	A14663
Hederacoside C	Phytolab	89221
Hederacoside D	Phytolab	84218
HEPES	AppliChem, Darmstadt, Germany	A1069
Hygromycin B Gold	InvivoGen, San Diego, CA	ant-hg-1
Kanamycin	Sigma-Aldrich	K1377
Lumit™ IL-6 (Human) Immunoassay	Promega	W6030
Metafectene [®] Pro	Biontex, Munich, Germany	T040
Nano-Glo [®] HiBiT Extracellular Detection System	Promega	N2420

Materials

Nano-Glo [®] HiBiT Lytic Detection System	Promega	N3030
Nano-Glo [®] Luciferase Assay System	Promega	N1110
Nano-Glo [®] Vivazine [™] Live Cell Substrate	Promega	N2580
NECA	Sigma-Aldrich	119140
Neochlorogenic acid	Phytolab	80504
Nicotiflorin	Phytolab	80700
NucleoBond [™] Xtra Midi	Macherey-Nagel, Düren, Germany	740410
NucleoSpin [®] RNA XS	Macherey-Nagel	740990
PEI	Sigma-Aldrich	408727
PDL	Sigma-Aldrich	P0899
Phosphoric acid	Sigma-Aldrich	79606
PSB-603	Biomol	Cay25637
Q5 High-Fidelity 2X Master Mix	New England Biolabs, Ipswich, MA	M0492
Rutin	Phytolab	89270
SCH 442416	Sigma-Aldrich	S6451
T4 DNA ligase	Thermo Fisher Scientific	EL0011
TNF α	Merck, Darmstadt, Germany	GF314
Zeocin	Thermo Fisher Scientific	R25001
α -Hederin	Carl Roth, Karlsruhe, Germany	9970

4 Methods*

4.1 Cell culture

Human embryonic kidney cells (HEK293), subsequently called HEK cells, and all constructed clones were cultivated at 37 °C with 5 % CO₂ in DMEM supplemented with 100 units/ml penicillin, 100 µg/ml streptomycin, and 10 % (v/v) fetal bovine serum (FBS). The cells were subcultured 1:10 every 3–4 days in 10 cm cell culture dishes.

Calu-3 cells and all constructed clones were cultivated at 37 °C with 5 % CO₂ in DMEM/F-12 supplemented with 1 % (v/v) GlutaMAX™, 100 units/ml penicillin, 100 µg/ml streptomycin, and 15 % (v/v) FBS. The cells were subcultured 1:5 every 5–7 days in 10 cm cell culture dishes.

Cultivation and handling of cells was performed under sterile conditions. Additionally, all cell lines used were regularly tested for mycoplasma contamination using an established PCR method [61,62].

4.2 Transformation

All cloned plasmids were amplified by transformation into competent XL1-blue bacteria. Approximately 1 ng of DNA was added to 100 µl of frozen XL1-blue bacteria and gently mixed by pipette tip rotation. This bacteria-DNA-mix was kept on ice for 30 min prior to heat shock at 42 °C for 1 min, followed by cooling on ice for another minute.

Then, 900 µl LB medium was added and the mixture was incubated in a shaker at 37 °C for 1 h. Afterwards, the suspension was centrifuged for 5 min at 3000 × g, the supernatant was discarded, and the pellet was resuspended in 50 µl LB Medium supplemented with an appropriate antibiotic (50 µg/ml ampicillin or 25 µg/ml

* Parts of this study, in particular the cellular assays investigating the influence of EA 575[®] on A_{2B}AR signalling, have been published recently within the scope of my doctoral studies [1]. For the sake of completeness and readability, these parts were incorporated into this work. This chapter therefore contains text passages from the referenced publication, which were revised and supplemented where necessary. This particularly concerns the sections 4.1, 4.3, 4.4, 4.5, 4.6, 4.7, and 4.8. Further information can be found in 10.4.

Methods

kanamycin). The bacteria were spread on agar-LB medium plates (1.5 % (w/v) agar in LB medium) containing antibiotic and incubated at 37 °C overnight.

The next day, single clones originating from single cells were picked and incubated each in 5 ml antibiotic-supplemented LB medium in a shaker at 37 °C for 8 h. Subsequently, 500 µl of this pre-culture was diluted in 150 ml of antibiotic-containing LB medium and allowed to grow overnight in a shaker at 37 °C.

Plasmid DNA was isolated using the NucleoBond™ Xtra Midi kit according to the manufacturer's instructions (Figure S 1). All resulting plasmids were verified to be correct via digestion with the appropriate restriction enzymes and subsequent agarose gel electrophoresis in comparison to a DNA standard ladder. Moreover, verification by DNA sequencing was performed by GATC services (part of Eurofins Genomics, Ebersberg, Germany).

4.3 Dynamic mass redistribution measurements

Dynamic mass redistribution (DMR) measurements were performed using a Corning Epic® biosensor, as already published [1]. HEK GloSensor™ cells were used in these experiments for better comparability with the subsequently performed cAMP measurements. The cells were seeded at a density of 3,000 cells per well in a 384-well plate by Corning (#5042; Corning, NY) and allowed to grow for at least 24 h in full growth medium.

Pre-incubation was performed with 40, 80, 160, or 240 µg/ml EA 575® for 1 or 16 h. Whenever a concentration series like this was used, the solvent content in each solution was controlled to be the same as the solution with the highest solvent concentration within that series. In this case, for example, ethanol was added to all incubation solutions to result in a concentration of 0.3 %, as this is the concentration in the 240 µg/ml EA 575® solution.

After pre-incubation, the medium was replaced with HEPES-buffered HBSS and the cells were allowed to equilibrate at 37 °C for 1 h. A baseline of 10 measurement points, totalling 5 min, was recorded before stimulation with BAY 60-6583 was conducted using a CyBi®-SELMA semi-automatic pipetting system (Analytik Jena AG, Jena, Germany) at 37 °C. Subsequently, the wavelength shift resulting from the dynamic mass redistribution of intracellular particles was measured for an additional 70 min.

4.4 cAMP measurements

The establishment of HEK cells expressing a cAMP sensor, as well as the measurement of cAMP was performed as described by Bussmann et al. (2020) [14]. The assay procedure has already been described in Meurer et al. (2023) [1].

4.4.1 Transfection

HEK cells were transfected with the pGloSensor™-22F cAMP Plasmid (E2301; Promega) (Figure S 2) via electroporation using a Nucleofector® II (Lonza, Basel, Switzerland). A cell count of 2,000,000 was diluted in 100 µl electroporation buffer with 2 µg DNA, and program Q-001 was applied (Figure S 3). Afterwards, the freshly transfected cells were transferred into 10 ml of fully supplemented DMEM on a 10 cm cell culture plate. For the selection of successfully transfected cells, the medium was replaced with fully supplemented DMEM containing 100 µg/ml hygromycin B Gold. For the generation of single-cell clones, a single-cell dilution was performed using the protocol by Corning (Figure S 4).

4.4.2 Assay procedure

HEK GloSensor™ cells were seeded in a 96-well plate coated with 0.1 mg/ml PDL at a density of 8,000 cells per well and allowed to grow for one day. Pre-incubation was carried out with 40, 80, 160, or 240 µg/ml EA 575® for up to 16 h in full growth medium. After pre-incubation, the medium was changed to a substrate solution containing 4 % GloSensor™ cAMP reagent stock solution in HEPES-buffered medium. The cells were incubated at 37 °C for 1 h and subsequently equilibrated at RT in a plate reader (Tecan Infinite® 200 PRO, Tecan, Männedorf, Switzerland) for another hour. Stimulation was performed with BAY 60-6583 and 1 µM forskolin simultaneously, and the cAMP increase was measured as luminescence for 1 h after stimulation.

4.5 Measurements of β -arrestin 2 recruitment

In general, the establishment of expression vectors and measurements of β -arrestin 2 recruitment to A_{2B} AR were performed as recently described by Saecker et al. (2023) for A_1 AR [63]. The description of the β -arrestin 2 recruitment measurements has also been included in Meurer et al. (2023) [1].

4.5.1 Plasmid generation

The plasmid coding for human adenosine receptor A_{2B} (A_{2B} AR) fused to the N-terminus of Large BiT (LgBiT) (Figure S 5) was generated by initially removing the region coding for YFP of the vector pEYFP-N1-A2BR, which was a gift from Robert Tarran (Addgene plasmid # 37202; <http://n2t.net/addgene:37202>; RRID:Addgene_37202) [64], using BamHI/NotI. The open reading frame coding for LgBiT was amplified by PCR (forward primer: 5'-GATCGGATCCAAGTGGTAGCGGGGTCTTTACCCTG-3'; reverse primer: 5'-GATCGCGGCCGCTAGCTACCACCGCATCC-3'; Table S 1: PCR 1). The PCR product was cut with BamHI/NotI and inserted into the vector via ligation. Therefore, approximately 20 ng of vector DNA and a 5-fold amount of insert DNA were incubated for 30 min with 1 U T4 DNA ligase in 1X ligase buffer.

For the expression of rat β -arrestin 2 with an N-terminal Small BiT (SmBiT) (Figure S 6), the coding sequence was taken from pECFP-N1-r β -arrestin-2 (a kind gift from M. Bouvier, Montreal, Canada) by restriction with NheI/SalI. The fragment was introduced into the pcDNATM3.1/Zeo⁽⁺⁾ Mammalian Expression Vector (Invitrogen, Waltham, MA) containing the information for SmBit via NheI and XhoI sites.

4.5.2 Transfection

HEK cells were co-transfected to transiently express A_{2B} AR-LgBiT and SmBiT- β -arrestin 2 using branched polyethylenimine (PEI). For this purpose, the cells were seeded in a 6-well plate at a density of 350,000 per well and allowed to grow for one day. For each DNA, 1.5 μ g was diluted into 200 μ l of 150 mM NaCl, then 7.5 μ l of a 1 mg/ml PEI solution was added, and the mixture was vortexed immediately for 10 s. After 10 min at RT, the DNA/PEI mixture was added to the cells and incubated for 24 h.

4.5.3 Assay procedure

The transiently transfected cells were seeded in a 96-well plate at a density of 15,000 cells per well and allowed to grow for one day in full growth medium. Pre-incubation was carried out with 160 µg/ml EA 575[®] for 16 h. Afterwards, the medium was replaced with a solution of 2.5 µM coelenterazine h in HEPES-buffered HBSS. A baseline of three measurement points, totalling 3 min, was recorded before stimulation with 10 µM NECA or 10 µM BAY 60-6583 was performed. Subsequently, luminescence corresponding to the recruitment of β -arrestin 2 was measured for another 27 min using a Tecan Spark[®] plate reader.

4.6 Measurements of CRE activation

The procedures to measure CRE activation have already been incorporated into a recent publication [1].

4.6.1 Transfection

A plasmid expressing NanoLuc[®]-PEST (NlucP) under control of a promoter containing cAMP response elements (CRE) was received by Promega (Figure S 7). HEK cells were transiently transfected with this construct using PEI. For this purpose, the cells were seeded in a 12-well plate at a density of 175,000 per well and allowed to grow for one day. After the dilution of 2 µg DNA in 100 µl of 150 mM NaCl, 5 µl of a 1 mg/ml PEI solution was added, and the mixture was vortexed immediately for 10 s. After 10 min at RT, the DNA/PEI mixture was added to the cells and incubated for 24 h.

4.6.2 Assay procedure

Transiently transfected HEK cells were seeded in a 96-well plate at a density of 20,000 cells per well and allowed to grow for one day in fully supplemented medium. Pre-incubation was conducted with 40, 80, 160, or 240 µg/ml EA 575[®] in full growth medium for 16 h. Pre-incubation with antagonists was carried out for only 2 h, simultaneously with the substrate incubation.

Nano-Glo[®] Vivazine[™] Live Cell Substrate was prepared according to the manufacturer's instructions (Figure S 8) using HEPES-buffered medium. The cells were incubated with the substrate for 2 h at 37 °C in a Tecan Spark[®] plate reader already recording baseline luminescence. Stimulation was then conducted by adding

adenosine, BAY 60-6583 or CGS 21680 and measurement was performed for another 22 h.

4.7 IL-6 measurements

Measurement of IL-6 release was performed using the Lumit™ IL-6 (Human) Immunoassay, as already described in Meurer et al. (2023) [1]. Calu-3 cells were seeded in a 96-well plate at a density of 20,000 cells per well and allowed to grow for at least two days to a confluency of 80–90 % in full growth medium. Pre-incubation was carried out with 40, 80, 160, or 240 µg/ml EA 575® in DMEM/F-12 without phenol red supplemented with GlutaMAX™ and 5 % FBS for 16 h. Pre-incubation with antagonists was conducted for only 1 h.

IL-6 release was then provoked by adding adenosine, BAY 60-6583, or CGS 21680 for the following 24 h. Subsequently, the measurement of IL-6 was performed according to the manufacturer's instructions (Figure S 9) using a Tecan Spark® plate reader.

4.8 Measurements of NFκB transcriptional activity

The description of the NFκB transcriptional activity measurements can also be found in Meurer et al. (2023) [1].

4.8.1 Plasmid generation

For the generation of a reporter construct expressing secreted NanoLuc® under control of an NFκB response element (Figure S 10), the pNFκB-d2EGFP vector (Clontech, Mountain View, CA) was used as a first template. Destabilised GFP was removed from the vector by PCR (forward primer: 5'-TCGGATATCTCGAGCCGGAATTCGGGGAAGCTTC-3'; reverse primer: 5'-GTTTCAGGGGGAGGTGTG-3'; Table S 1: PCR 2) and restriction with BamHI/XhoI. The open reading frame coding for the secreted NanoLuc® luciferase was cut from the pNL1.3[secNluc] vector (Promega) using BamHI/XhoI and introduced into the vector via ligation, as described in 4.5.1.

In a second step, this secreted NanoLuc® reporter vector under control of an NFκB response element was cloned into the pcDNA™3.1 (+) Mammalian Expression Vector (Invitrogen) to enable the selection of stably transfected cells with G418. Therefore, the CMV promoter was removed from the vector by restriction with BamHI/BglII and

re-ligation. The vector was then re-cut with NotI/XhoI. The insert was isolated from the plasmid generated in the first step using NotI/SalI and introduced into the vector via ligation, as described in 4.5.1.

4.8.2 Transfection

Calu-3 cells were transfected using Metafectene[®] Pro according to the manufacturer's instructions (Figure S 11). For the selection of successfully transfected cells, the medium was changed to fully supplemented DMEM/F-12 containing 600 µg/ml G418.

4.8.3 Assay procedure

The cells were seeded in a 96-well plate at a density of 25,000 cells per well and allowed to grow for at least two days to a confluency of 80–90 % in full growth medium. Before stimulation with TNF α , adenosine, NECA or BAY 60-6583 for 3 h, the cells were starved overnight. Measurement of NF κ B transcriptional activity was performed in a Tecan Spark[®] plate reader using the Nano-Glo[®] Luciferase Assay System according to the manufacturer's instructions (Figure S 12).

4.9 Identification of active constituents

4.9.1 HPLC analysis

HPLC analyses were performed using an Agilent Series 1200 HPLC system (Agilent Technologies, Santa Clara, CA) equipped with a degasser (G1322A), a quaternary pump (G1311A), an autosampler (G1329A), and a photodiode array detector (G1315D). The column used was a YMC-Triart C18 (TA12S05-2546WT; 5 µm, 250 × 4.6 mm) (YMC, Dinslaken, Germany). The detection was conducted at 205 nm. The following linear gradient was employed for all HPLC procedures in this work (Table 6). The chromatograms were registered and analysed with the software Agilent Chemstation Rev. B.04.01. The presented chromatograms were prepared using Bruker Compass DataAnalysis 4.0 (Bruker Daltonik GmbH, Bremen, Germany).

Table 6: HPLC gradient

Time [min]	Flow [ml/min]	Eluent A [%]	Eluent B [%]
0	1	100	0
9	1	100	0
10	1	94	6
25	1	85	15
50	1	40	60
51	1.5	0	100
65	1.5	0	100

4.9.2 Characterisation of EA 575[®]

Eluent A was water/acetonitrile (22/1; v/v) adjusted to pH 2.0 with phosphoric acid. Eluent B was acetonitrile. EA 575[®] was dissolved in 50 % ethanol at a concentration of 40 mg/ml and diluted to 2 mg/ml with water prior to injection of 40 µl, resulting in an injected amount of 80 µg EA 575[®].

The compounds rutin, nicotiflorin, 3,4-dicaffeoylquinic acid (3,4-DQA), 3,5-dicaffeoylquinic acid (3,5-DQA), 4,5-dicaffeoylquinic acid (4,5-DQA), hederacoside C, hederacoside D, hederacoside B, and α-hederin were identified by comparison with UV spectra and retention times of reference substances. The concentrations of these compounds contained in the extract were calculated by comparing the peak areas determined in the extract with solutions of reference substances of known concentrations.

4.9.3 Compound combinations

Seven combinations of these compounds were prepared according to their chemical class, as shown below (Figure 1), with concentrations corresponding to those contained in the stock solution of EA 575®.

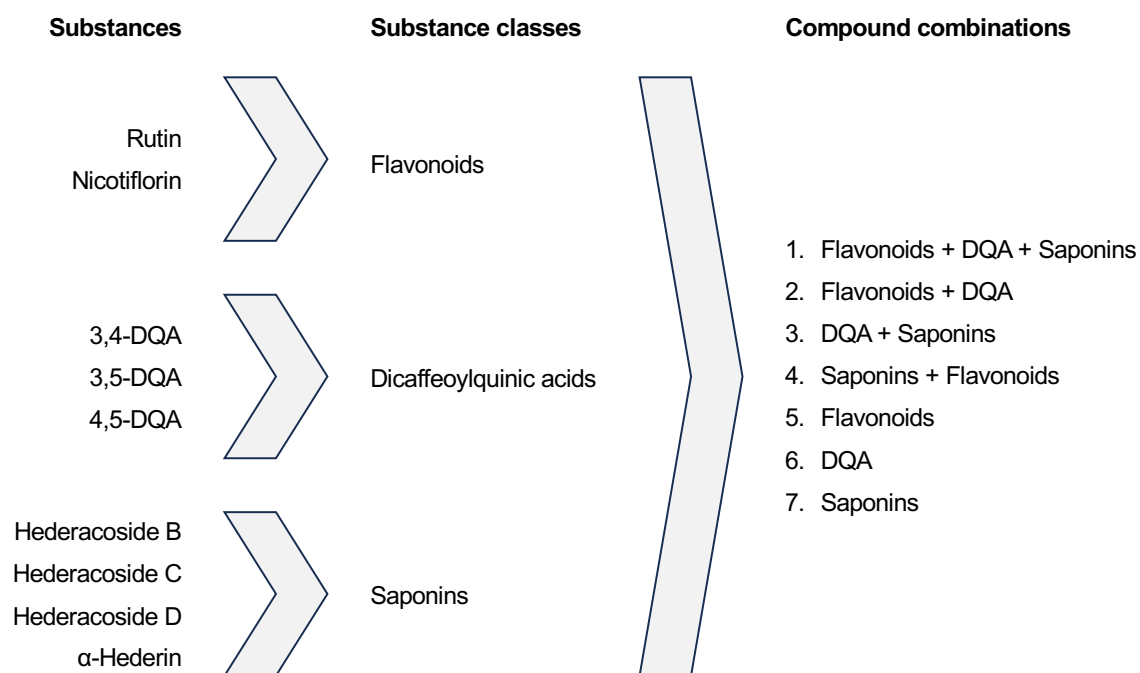


Figure 1: Schematic overview of the preparation of the compound combinations

These compound combinations were analysed by HPLC, and the peak areas were compared to those in the total extract. The pharmacological activity of the compound combinations at concentrations corresponding to 160 µg/ml EA 575® was then tested using the GloSensor™ cAMP assay described in 4.4.

4.10 Bioassay-guided fractionation

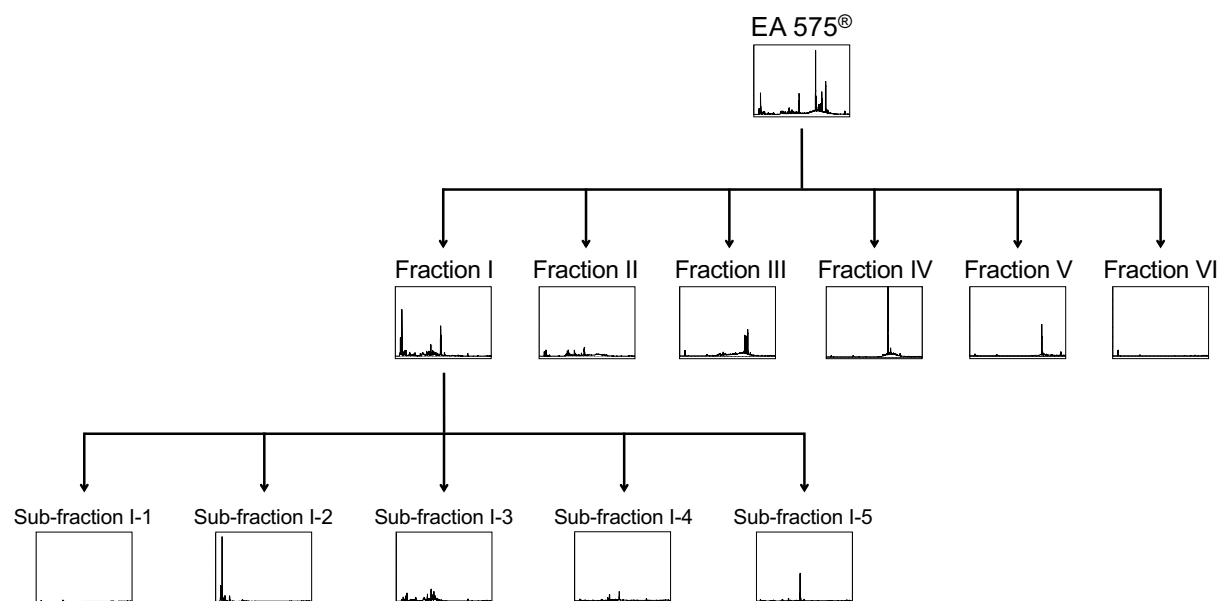


Figure 2: Flowchart of the fractionation of EA 575[®]. The corresponding chromatogram at 205 nm is displayed for each fraction. For a more detailed view of the chromatograms see Figure S 14 & Figure S 15.

4.10.1 Fractionation of EA 575[®]

For the determination of the pharmacologically active ingredients, a bioassay-guided fractionation was performed. Therefore, EA 575[®] was split up into several fractions using the HPLC method described in 4.9.1 and a Bio-Rad Model 2110 Fraction Collector (Bio-Rad Laboratories, Düsseldorf, Germany). In order to enable the use of the collected fractions in cell-based assays, the phosphoric acid in eluent A was omitted. Thus, eluent A was water/acetonitrile (22/1; v/v), eluent B was still acetonitrile. EA 575[®] was dissolved in 50 % ethanol at a concentration of 40 mg/ml prior to injection. The fractions were collected as follows, roughly based on the previously mentioned substance classes, identified by comparison with the reference substances as described above.

Table 7: Collected fractions of EA 575[®]

Name	Collection time [min after injection]	Characterised by
Fraction I	0–10	–
Fraction II	10–20	–
Fraction III	20–30	DQA
Fraction IV	30–38	Flavonoids
Fraction V	38–52	Saponins
Fraction VI	52–60	–

The solvent contained in the collected fractions was removed using an Eppendorf Concentrator plus™ (Eppendorf, Hamburg, Germany) applying the program V-AQ at 45 °C.

The resulting fraction pellets were redissolved in 50 % ethanol to perform additional HPLC analyses using eluent A supplemented with phosphoric acid. Subsequently, the chromatograms were employed to calculate the concentrations of the fractions. For this purpose, the peak areas of specific substances were used as references for the entire fraction. For fraction III, 4,5-DQA was chosen, rutin served for fraction IV, and hederacoside C was used for fraction V. Since fractions I, II, and VI did not contain any of the substances identified in the previous analyses, they were treated equally as fraction III.

Based on these calculations, the fractions were redissolved in the calculated amounts of 50 % ethanol, resulting in solutions with concentrations theoretically corresponding to those contained in the stock solution of EA 575[®]. The pharmacological activity of the fractions at concentrations equivalent to 160 µg/ml EA 575[®] and a concentration series of fraction I were investigated with the GloSensor™ cAMP assay described in 4.4.

4.10.2 Sub-fractionation of fraction I

The separation of fraction I into sub-fractions was conducted using the method described above, except for different collection times. The switch of the collection vessel was set to 2 min, yielding five sub-fractions of the originally called fraction I. The peak areas of three representative peaks, eluting at 3.7 min, 19.3 min, and 24.6 min, were chosen as references for the calculation of the concentration. The latter two of these peaks were present in two sub-fractions each, therefore the sum of the peak areas in both sub-fractions was used for the calculation.

The sub-fraction solutions were prepared to correspond to the concentration of fraction I, and thus to the stock solution of EA 575[®]. Subsequently, they were tested with the GloSensor[™] cAMP assay described in 4.4, using solutions corresponding to 240 µg/ml EA 575[®]. In addition, combinations of these sub-fractions were examined.

4.10.3 Mass spectrometry (LC-MS/MS)

Sub-fractions I-2 and I-3 were dissolved in water/acetonitrile (9/1; v/v) with 0.1 % formic acid and filtered through a 0.45 µm membrane filter. A volume of 3 µl was injected onto a C18 analytical column (350 mm length, 100 µm inner diameter, ReproSil-Pur 120 C18-AQ, 3 µm) using a Dionex Ultimate 3000 RSLC nano HPLC system (Dionex, Idstein, Germany). Analytes were separated using a linear gradient of acetonitrile/water (9/1; v/v) with 0.1 % formic acid, ranging from 5 % to 99 %, at a flow rate of 300 nl/min within 30 minutes.

The nanoHPLC was coupled online to an Orbitrap Fusion Lumos mass spectrometer (Thermo Fisher Scientific) operated in positive or negative mode. Data-dependent acquisition was performed on ions between 100 and 1000 m/z scanned in the Orbitrap detector every 2.5 s with a resolution of 60,000 (gain control target 400,000, maximum inject time 50 ms). The Easy-IC module was used for internal calibration. In a top-speed method, singly to triply charged ions were subjected to higher-energy collision-induced dissociation (HCD: 1.0 Da isolation, threshold intensity 25,000, stepped collision energies 15, 30, 50 %) and fragments analysed in the Orbitrap (R = 15,000) with gain control target 50,000 and maximum inject time 35 ms. Fragmented ions were excluded from repeat analysis for 15 s.

Analysis of the LC-MS/MS data was performed manually using the software FreeStyle™ 1.8 (Thermo Fisher Scientific). For each fraction, both positive and negative ionisation mode data were analysed. Possible molecular formulae for the most abundant masses found in these data were calculated by the software. The identified chemical formulae were then manually compared with the PubChem database. Substances that are mentioned by name were verified by analysis of MS2 spectra in comparison with literature data.

Following the LC-MS/MS measurements, chlorogenic acid and its isomers neochlorogenic acid and cryptochlorogenic acid were analysed via HPLC in comparison to EA 575® in order to estimate their abundances in the sub-fractions. Subsequently, chlorogenic acid and neochlorogenic acid were tested for a possible activity on A_{2B}AR signalling using the GloSensor™ cAMP assay described in 4.4.

4.11 Generation of a HEK HiBiT-A_{2B}AR cell line using CRISPR/Cas9-mediated HDR

4.11.1 CRISPR/Cas9 lipofection

In order to generate a HEK cell line expressing a HiBiT-tagged A_{2B}AR at an endogenous expression level, genome editing via CRISPR/Cas9-mediated HDR was performed. Therefore, the protocol “Alt-R CRISPR-Cas9 System: Cationic lipid delivery of CRISPR ribonucleoprotein complexes into mammalian cells” (version 4) by IDT (www.idtdna.com/crispr-cas9) was applied, which is briefly explained in the following paragraphs.

In a first step, crRNA and tracrRNA were mixed at equimolar concentrations of 1 µM in Nuclease-Free Duplex Buffer and heated at 95 °C for 5 min to form crRNA:tracrRNA duplexes. To produce the RNP complex, 1.5 µl of these gRNA oligonucleotides were combined with 1.5 µl of 1 µM Cas9 enzyme, 0.6 µl Cas9 PLUS™ Reagent (from CRISPRMAX™ kit), and 19.9 µl Opti-MEM and allowed to assemble for 5 min at RT.

Then, 1.5 µl of 0.3 µM donor DNA (5'-CGGCTGCCCTCGCCGGCGCGCCTTCGG TAGGGGGCGCCCGGGGCCAGCTGGCCCGCCATGGTGAGCGGCTGGCGCC TGTTCAAGAAGATTAGCTCGGGTGGATCCTCGGGAGGTAGCTCGCTAGCCACCG CGCTGCTGGAGACACAGGACGCGCTGTACGTGGCGCTGGAGCTGGTCATCGC CGCGCTTTCGGTGG-3') was added and the mixture was transferred into a well of a

Methods

96-well plate. Following the addition of 1.2 μ l CRISPRMAX™ transfection reagent and 23.8 μ l Opti-MEM, transfection complexes were allowed to form for 20 min at RT.

During the incubation, HEK cells were prepared to obtain a suspension containing 400,000 cells/ml in antibiotic-free medium. After completion of the incubation, 100 μ l of the cell dilution and 1.5 μ l Alt-R™ HDR Enhancer were combined with the transfection complexes in the 96-well plate. The cells were then incubated at 37 °C with 5 % CO₂ for 48 h.

4.11.2 PCR analyses

PCR analyses were conducted for the detection of genome-edited clones that were genetically modified successfully. For this purpose, the cycling parameters described in Table S 1: PCR 3 and the following primer combinations were used.

Table 8: Primer combinations used for the detection of genome-edited clones

	Forward primer	Reverse Primer	PCR product	Purpose
1	5'-CAGGGTTAGC CTGGAGTGAG-3'	5'-CTTAGAGCGA CGCGCATCTG-3'	1139 bp (wt: 1067 bp)	Positive control of the PCR, yields PCR product with wild-type DNA
2	5'-CAGGGTTAGC CTGGAGTGAG-3'	5'-AGGTATCTGTC GACTGCCACG-3'	904 bp (wt: 832 bp)	
3	5'-CAGGGTTAGC CTGGAGTGAG-3'	5'-GCTAATCTTCTT GAACAGGCGC-3'	554 bp	Detection of HiBiT sequence, yields PCR product only with HiBiT-tagged ADORA2B
4	5'-GCGCCTGTTCA AGAAGATTAGC-3'	5'-CTTAGAGCGA CGCGCATCTG-3'	607 bp	
5	5'-GCGCCTGTTCA AGAAGATTAGC-3'	5'-AGGTATCTGTC GACTGCCACG-3'	372 bp	

Primer combinations 3–5 yielded a PCR product only for HiBiT-tagged ADORA2B, since one of the primers of these combinations binds to the HiBiT sequence. Furthermore, primer combinations 3 and 4 were specific for HiBiT-tagged ADORA2B exclusively introduced via CRISPR/Cas9-mediated HDR, as one of the primers of

these combinations binds to the HiBiT sequence and the other binds to an intron sequence.

All resulting PCR products were verified to be correct by agarose gel electrophoresis in comparison to a DNA standard ladder. Moreover, verification of the inserted sequence was performed via DNA sequencing by GATC services. These verifications were performed after each step in which a new clone was obtained.

4.11.3 PCR screening

Due to the lack of resistance, successfully modified cells could not be isolated with an antibiotic. The transfected cells were therefore screened for genome-edited clones via PCR. For this purpose, the cells were seeded in a 96-well plate at a density of 10 per well and allowed to grow for approximately two weeks.

The cells were then detached using T/E and resuspended in medium to transfer half of the suspension into PCR tubes. The other half was returned to the incubator. The cells in the tubes were centrifuged at $300 \times g$ for 3 min, and the supernatant was discarded to lyse the cells using a self-made lysis buffer. The tubes were heated at $56\text{ }^{\circ}\text{C}$ for 30 min for lysis and then heat shocked at $95\text{ }^{\circ}\text{C}$ for 5 min to deactivate Proteinase K.

For the PCR, 1 μl of this cell lysate was used without further purification. Primer combination 4, along with the cycling parameters described in Table S 1: PCR 3, was chosen to specifically yield a PCR product that contains the genetic information for CRISPR/Cas9-modified HiBiT-tagged $A_{2B}\text{AR}$. PCR products were analysed by agarose gel electrophoresis in comparison to a DNA standard ladder. Genome-edited clones were allowed to grow until sufficient cell material was available to perform single-cell dilution using the protocol by Corning (Figure S 4).

4.11.4 RNA analysis

To examine whether the modified receptor was expressed in the obtained cell line, the total RNA was extracted and analysed for mRNA encoding HiBiT-tagged $A_{2B}\text{AR}$. In a first step, the RNA of 50,000 previously seeded cells was isolated using the NucleoSpin[®] RNA XS kit according to the manufacturer's instructions (Figure S 18). The second step was the conversion of the RNA to cDNA in order to perform PCR analyses. For this purpose, the First Strand cDNA Synthesis Kit was used according

to the manufacturer's instructions (Figure S 19). Subsequently, PCR was performed using the forward primer: 5'-GGGCGCTATGGCCATG-3' and the reverse primer: 5'-GACCCAGAGGACAGCAATG-3', with the cycling parameters described in Table S 1: PCR 4.

The correct PCR product for HiBiT-tagged ADORA2B has a size of 558 bp, wild-type cDNA yields a PCR product of 486 bp. The use of a forward primer that binds upstream of the start codon ensured that both the wild-type and modified DNA were amplified. The use of a reverse primer that binds to a sequence located in exon II ensured that only cDNA but not genomic DNA is detected. The PCR products were verified to be correct via agarose gel electrophoresis in comparison to a DNA standard ladder and DNA sequencing by GATC services.

4.11.5 Measurements of HiBiT-tagged A_{2B}AR

In order to investigate HiBiT-tagged receptors expressed on the cell surface, Nano-Glo[®] HiBiT Extracellular Detection System was used. In addition, Nano-Glo[®] HiBiT Lytic Detection System was utilized to quantify the total amount of expressed receptors. For both assays, cells were seeded in a 96-well plate at a density of 20,000 per well and allowed to grow for one day in full growth medium. Subsequently, the measurements were performed according to the manufacturer's instructions (Figure S 16 & Figure S 17) using a Tecan Spark[®] plate reader.

4.12 Generation of an overexpressing HEK HiBiT-A_{2B}AR cell line

4.12.1 Plasmid generation

The plasmid coding for HiBiT fused to the N-terminus of A_{2B}AR, separated by a spacer (Figure S 20), was cloned to match the sequence generated by CRISPR/Cas9-mediated HDR described in 4.11.1. The sequence for HiBiT fused to a spacer was obtained by annealed oligo cloning. This technique is an efficient way to insert short DNA sequences into vectors. For this purpose, the oligonucleotides 5'-GTACCGCCACCATGGTGAGCGGCTGGCGCCTGTTCAAGAAGATTAGCTCGGG TGGATCCTCGGGAGGTAGCTCG-3' and 5'-CTAGCGAGCTACCTCCCGAGGA TCCACCCGAGCTAATCTTCTTGAACAGGCGCCAGCCGCTCACCATGGTGGCG-3' were annealed by mixing and heating 10 μM of each at 95 °C for 5 min. After cooling to RT, this double-stranded DNA was introduced into the pcDNA[™]3.1/Zeo⁽⁺⁾

Mammalian Expression Vector containing the information for A_{2B}AR by ligation via NheI and Acc65I sites.

4.12.2 Transfection

HEK cells were transfected using the PEI method, as described in 4.6.1. Following the DNA/PEI incubation, the medium was changed to fully supplemented DMEM containing 100 µg/ml Zeocin for the selection of successfully transfected cells. To generate single-cell clones, single-cell dilution was performed using the protocol by Corning (Figure S 4).

4.12.3 Measurements of HiBiT-tagged A_{2B}AR

To examine differences in expression rates compared to the CRISPR/Cas9-modified cells, measurements of HiBiT-tagged A_{2B}AR on the cell surface were conducted using Nano-Glo[®] HiBiT Extracellular Detection System, as described for the CRISPR/Cas9-modified cells in 4.11.5.

4.13 Statistical analysis

For statistical analysis, one-way analysis of variance (ANOVA) with Dunnett's multiple comparisons test was performed using Prism software version 6.01 (GraphPad Software, San Diego, CA). Results were considered to be significant for p -values < 0.05.

5 Results*

5.1 Influence of EA 575[®] on A_{2B}AR-mediated intracellular dynamic mass redistribution

Dynamic mass redistribution (DMR) measurements were performed in order to test the hypothesis of EA 575[®] influencing the signalling of the adenosine receptor A_{2B} (A_{2B}AR). This technology uses broadband light to illuminate a biosensor in the bottom of the microplates interacting with the cell layer. A specific wavelength that is in resonance with this optical system is reflected, while the other wavelengths are transmitted. The reflected light passes through the lower 150 nm of the cell and the outgoing wavelength is recorded. When the cells react to test compounds by redistributing intracellular particles (dynamic mass redistribution), the outgoing wavelength shifts relative to the baseline value. This shift can be detected in both directions and is recorded in pm (Figure 3) [65].

* Parts of this study, in particular the cellular assays investigating the influence of EA 575[®] on A_{2B}AR signalling, have been published recently within the scope of my doctoral studies [1]. For the sake of completeness and readability, these parts were incorporated into this work. This chapter therefore contains text passages from the referenced publication, which were revised and supplemented where necessary. This particularly concerns the sections 5.1, 5.2, 5.3, 5.4, 5.5, and 5.6. Further information can be found in 10.4.

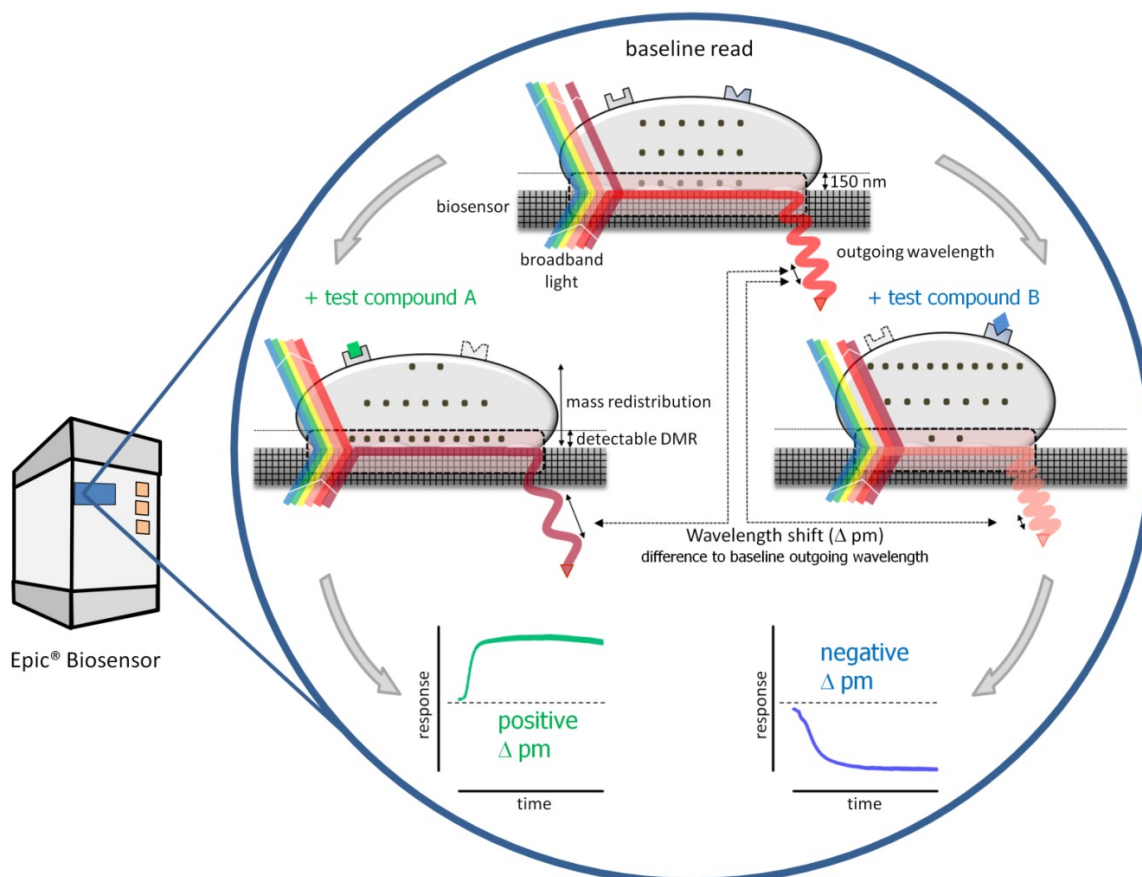


Figure 3: Principle of DMR detection. Illustration taken from Schröder et al. (2010) [65].

A dose-response curve of the wavelength shift evoked by stimulation of $A_{2B}AR$ with BAY 60-6583 was determined prior to the experiments with EA 575[®]. The cellular reaction of HEK GloSensor[™] cells to 0.01–10 μM BAY 60-6583 resulted in a dose-dependent positive wavelength shift with an EC_{50} of 0.306 μM , with the 95 % confidence interval ranging from 0.233 μM to 0.401 μM (Figure 4).

Results

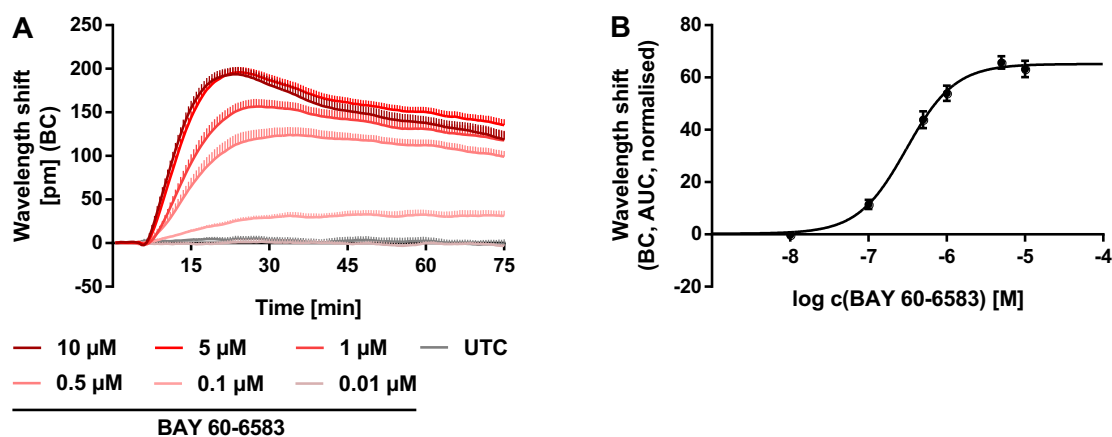


Figure 4: Dose-response curve of BAY 60-6583 in the DMR measurements. After 5 min of baseline recording, stimulation with 0.01–10 μM BAY 60-6583 was performed. The HEK GloSensor™ cells reacted dose-dependently with a positive wavelength shift mediated by dynamic mass redistribution of intracellular particles. The maximum effect was already reached at a concentration of 5 μM . The EC_{50} value was determined to be 0.306 μM , with the 95 % confidence interval ranging from 0.233 μM to 0.401 μM . Data are shown as the baseline-corrected (BC) wavelength shift in pm (A) and the corresponding dose-response curve of the AUC normalised to untreated control cells (UTC) (B). Results represent the mean and SEM ($n = 1$ experiment performed at least in triplicate).

The influence of EA 575® on the wavelength shift induced by 0.5 μM BAY 60-6583 was investigated, as already published [1]. The stimulation concentration was chosen as it is close to the previously determined EC_{50} value, and therefore shifts in either direction should be detectable.

The cellular reaction of HEK GloSensor™ cells to the agonist was significantly and dose-dependently inhibited up to 46.0 ± 12.4 % by the treatment with 160–240 $\mu\text{g/ml}$ EA 575® for 16 h, compared to stimulated control cells not treated with EA 575® (Figure 5A).

Subsequently, pre-incubation of HEK GloSensor™ cells with EA 575® was conducted for 1 and 16 h in order to assess whether the observed effect resulted from direct inhibition of the receptor. The reduction of wavelength shifts was observed solely after the pre-incubation period of 16 h, whereas the shorter incubation period of 1 h did not change the wavelength shifts mediated by BAY 60-6583 (Figure 5B).

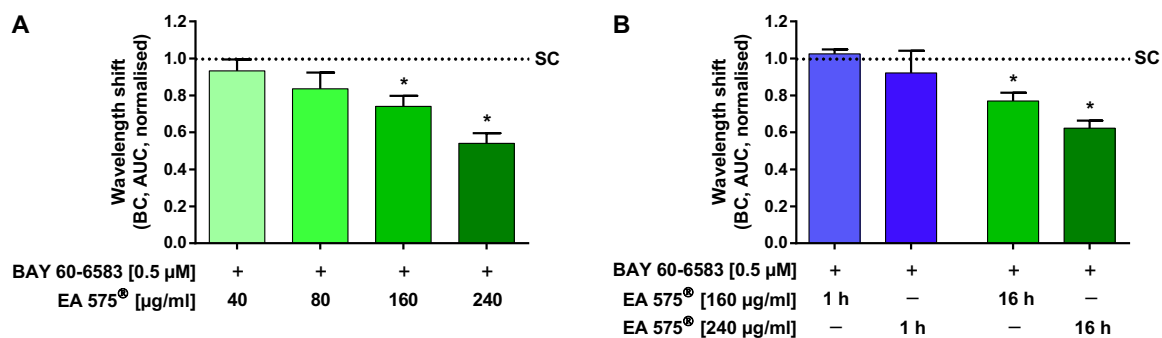


Figure 5: Influence of EA 575[®] (A) and different incubation periods thereof (B) on the cellular reaction of HEK GloSensor[™] cells evoked by stimulation of A_{2B}AR. HEK GloSensor[™] cells were pre-incubated with different concentrations of EA 575[®] for 16 h (A) and 1 or 16 h (B), prior to stimulation with 0.5 µM BAY 60-6583. Compared to stimulated control cells that were not treated with EA 575[®] (SC), the treatment with 160–240 µg/ml EA 575[®] for 16 h significantly and dose-dependently inhibited the positive wavelength shift mediated by dynamic mass redistribution of intracellular particles (A). No reduction in BAY 60-6583-mediated wavelength shift was measured after a pre-incubation time of 1 h (B). Data are shown as baseline-corrected (BC) AUC normalised to stimulated control cells that were not treated with EA 575[®] (SC). Results represent the mean and SEM (A: $n = 5$ independent experiments performed at least in triplicate; B: $n = 1$ experiment performed with 4 replicates, * $p < 0.05$). This figure has already been published in Meurer et al. (2023) [1].

5.2 Influence of EA 575[®] on A_{2B}AR-mediated intracellular cAMP levels

In order to confirm the results obtained in the DMR experiments, measurements of the second messenger cAMP were conducted using the GloSensor™ technology by Promega. A firefly luciferase is fused to a cAMP binding domain. Binding of cAMP leads to a conformational shift in the biosensor, which causes large increases in luminescence activity proportional to the intracellular cAMP level (Figure 6). HEK cells stably expressing GloSensor™ were used for the experiments.

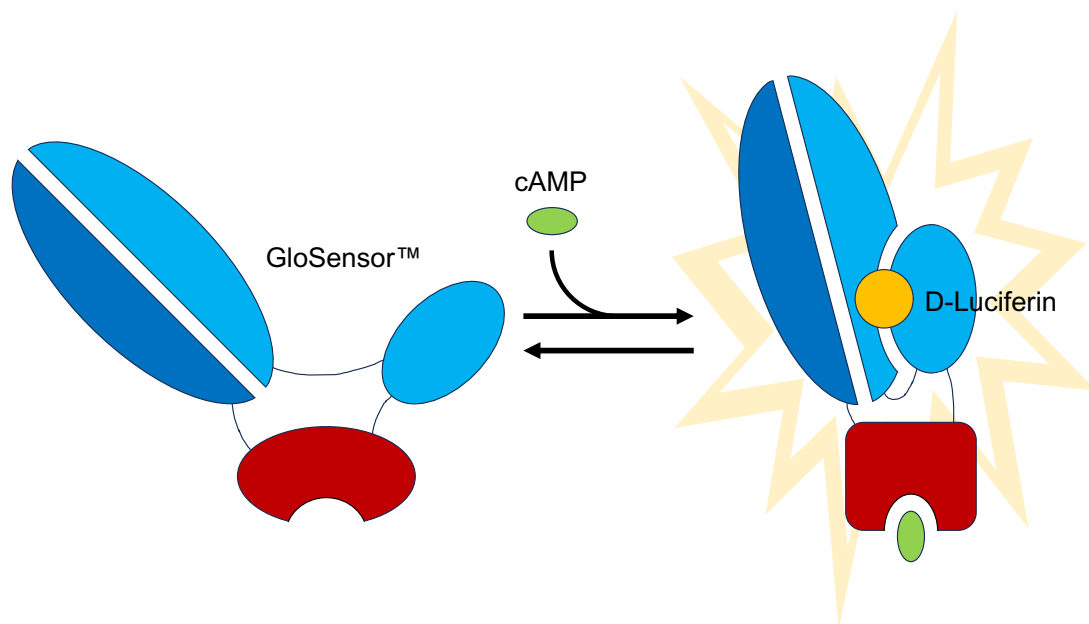


Figure 6: Principle of the GloSensor™ technology. Modified drawing according to <https://www.promega.de/products/cell-signaling/gpcr-signaling/glosensor-camp-cgmp-protease-biosensors/?catNum=E1290> (accessed 26 July, 2023).

A dose-response curve of the luminescence signal induced by stimulation with 0.1–10 μM BAY 60-6583 in combination with 1 μM forskolin was determined prior to the experiments with EA 575[®]. The EC_{50} was found to be 0.863 μM , with the 95 % confidence interval ranging from 0.774 μM to 0.964 μM . Stimulation with forskolin alone did not lead to an effect that seemed suitable for conducting the experiments with EA 575[®], as it was very small (Figure 7).

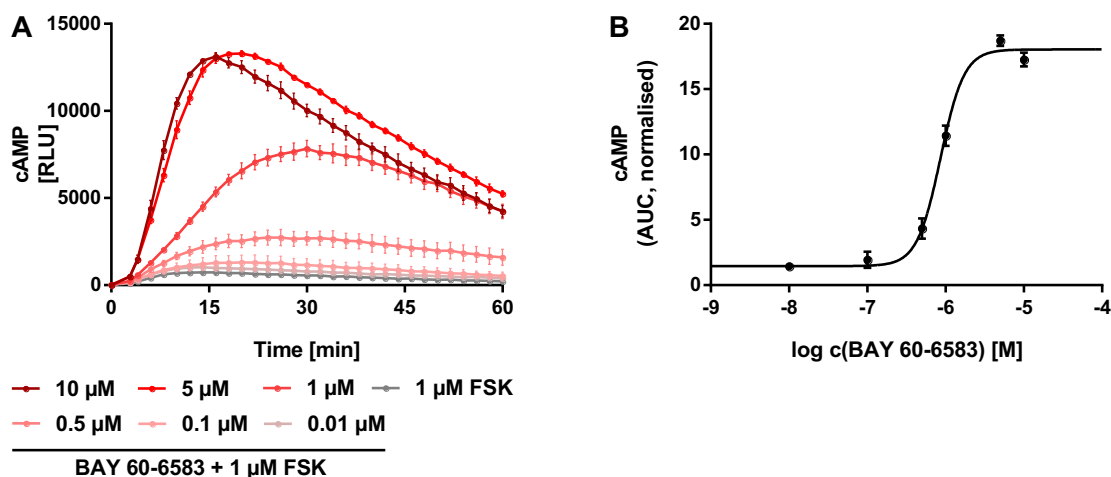


Figure 7: Dose-response curve of BAY 60-6583 in the cAMP level measurements. Stimulation of HEK GloSensor™ cells with 0.01–10 μ M BAY 60-6583 was conducted with simultaneous administration of 1 μ M forskolin (FSK). The resulting release of cAMP led to a dose-dependent increase in luminescence signal recorded in relative light units (RLU). The maximum effect was already reached at a concentration of 5 μ M. An EC_{50} value of 0.863 μ M was determined, with the 95 % confidence interval ranging from 0.774 μ M to 0.964 μ M. Data are presented as the generated luminescence in RLU (**A**) and the corresponding dose-response curve of the AUC normalised to control cells stimulated only with 1 μ M forskolin (**B**). Results represent the mean and SEM ($n = 1$ experiment performed in triplicate).

The influence of EA 575® on the intracellular cAMP level elevation mediated by stimulation of $A_{2B}AR$ was examined, as already published [1]. Although inhibition could be expected according to the DMR measurements, the agonist concentration was chosen to match the EC_{50} value, enabling the detection of both increases and decreases. Elevation in cAMP was therefore elicited by simultaneous stimulation with 1 μ M BAY 60-6583 and 1 μ M forskolin.

The treatment with 160–240 μ g/ml EA 575® for 16 h led to a significant and dose-dependent reduction in cAMP levels by up to 39.0 ± 9.92 %, compared to stimulated control cells not treated with EA 575® (Figure 8A).

The pre-incubation time required for this effect was defined more precisely in order to determine whether it was mediated by direct inhibition of the receptor. Thus, different pre-incubation periods were tested and it was found that at least 8 h were necessary to observe a significant decrease in cAMP levels (Figure 8B).

Results

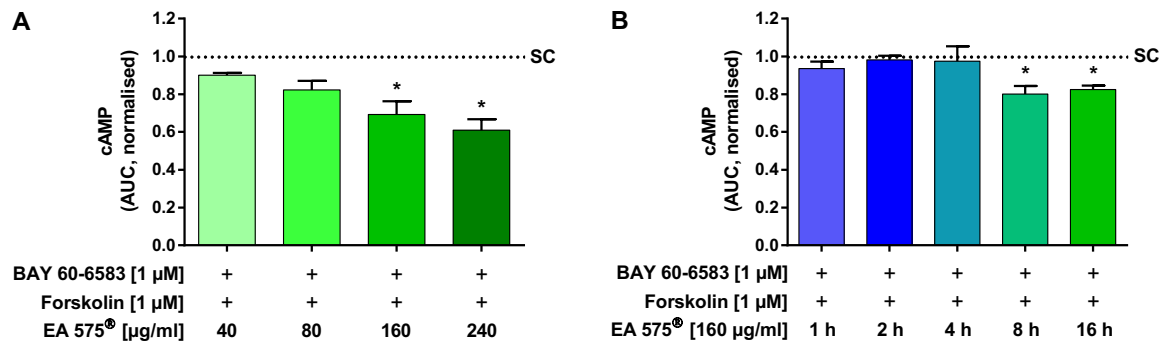


Figure 8: Influence of EA 575[®] (A) and different incubation periods thereof (B) on the intracellular cAMP levels in HEK GloSensor[™] cells elicited by stimulation of A_{2B}AR. Co-stimulation with 1 µM BAY 60-6583 and 1 µM forskolin was performed after pre-incubation with different concentrations of EA 575[®] for 16 h (A) and for 1–16 h with 160 µg/ml EA 575[®] (B). The cAMP increase mediated by stimulation of A_{2B}AR was significantly and dose-dependently inhibited by 160–240 µg/ml EA 575[®], compared to stimulated control cells that were not treated with EA 575[®] (SC) (A). Pre-incubation for at least 8 h was required to cause a significant decrease in cAMP levels (B). Data are presented as AUC normalised to stimulated control cells that were not treated with EA 575[®] (SC). Results represent the mean and SEM (*n* = 3 independent experiments performed in triplicate, * *p* < 0.05). This figure has also been included in Meurer et al. (2023) [1].

5.3 Influence of EA 575[®] on β -arrestin 2 recruitment to A_{2B}AR

In order to investigate another possible process involved in the inhibition of A_{2B}AR by EA 575[®], measurements of β -arrestin 2 recruitment were performed. For this purpose, NanoLuc[®] Binary Technology (NanoBiT™) was used. The smaller, low-affinity SmBiT with a mass of 1.3 kDa and the larger LgBiT with a mass of 17.6 kDa complement a functional NanoLuc[®] luciferase when in close proximity. HEK cells transiently expressing A_{2B}AR tagged with LgBiT and β -arrestin 2 tagged with SmBiT were employed. When β -arrestin 2 is recruited to the receptor, LgBiT and SmBiT fuse reversibly to form the complete NanoLuc[®] luciferase. In combination with the substrate coelenterazine h, luminescence is generated that is proportional to the recruitment of β -arrestin 2 to A_{2B}AR.

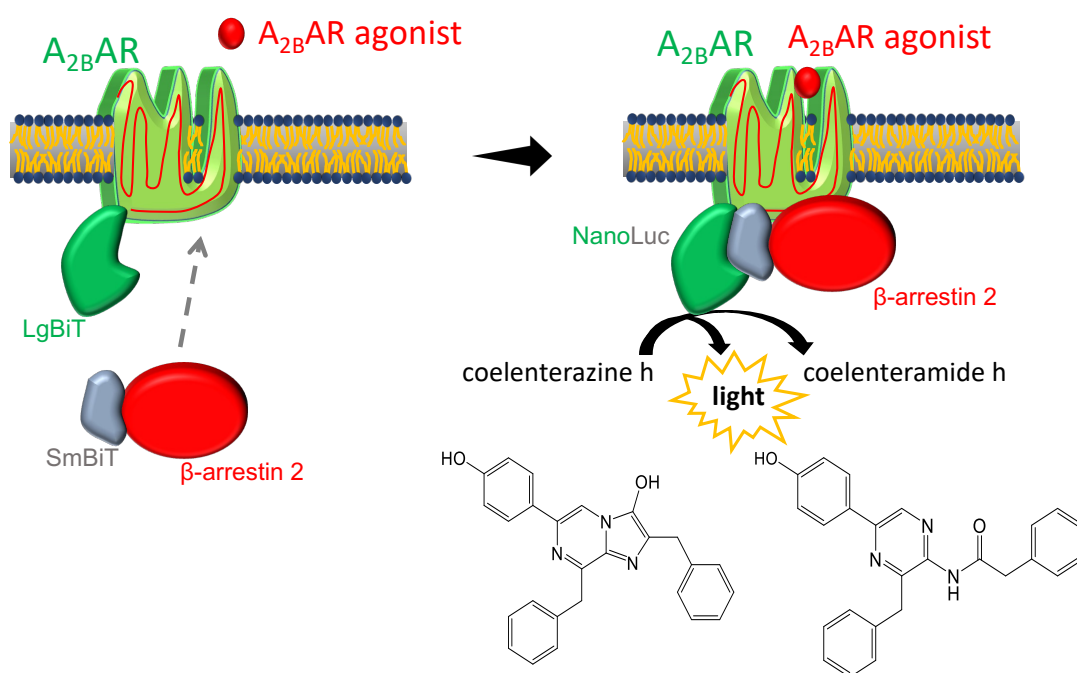


Figure 9: Principle of the measurements of β -arrestin 2 recruitment. Illustration taken and slightly modified from Saecker et al. (2023) [63].

Results

The impact of EA 575[®] on the β -arrestin 2 recruitment to A_{2B}AR following stimulation with the non-specific adenosine receptor agonist NECA, or BAY 60-6583, was investigated. As already published, the treatment with 160 μ g/ml EA 575[®] for 16 h led to a significant inhibition of both NECA- and BAY 60-6583-mediated β -arrestin 2 recruitment to A_{2B}AR by 16.9 ± 4.69 % and 9.31 ± 4.82 %, respectively (Figure 10) [1].

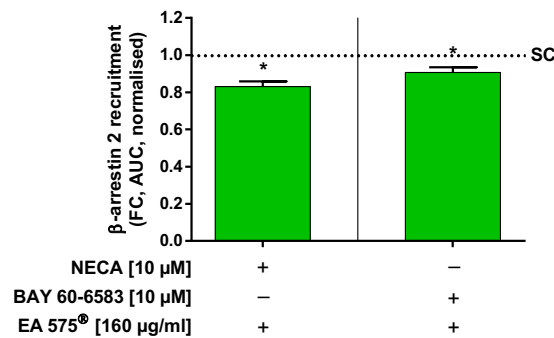


Figure 10: Influence of EA 575[®] on the recruitment of β -arrestin 2 to A_{2B}AR in transiently transfected HEK cells following stimulation with NECA or BAY 60-6583. Prior to the stimulation with 10 μ M NECA or 10 μ M BAY 60-6583, the cells were treated with 160 μ g/ml EA 575[®] for 16 h. The extract was able to significantly inhibit the recruitment of β -arrestin 2 to the A_{2B}AR mediated by either of the agonists. Data are shown as AUC of the fold change (FC) after stimulation normalised to equally stimulated control cells that were not treated with EA 575[®] (SC). Results represent the mean and SEM ($n = 3$ independent experiments performed in triplicate, * $p < 0.05$). This figure can also be found in Meurer et al. (2023) [1].

5.4 Influence of EA 575[®] on CRE activation and determination of the responsible receptor subtype

The influence of EA 575[®] on cAMP response elements (CRE) was investigated using HEK cells transiently expressing a destabilised NanoLuc[®] luciferase (NanoLuc[®]-PEST) under control of a promoter with CRE, as already published [1]. Activation of CRE promotes the expression of NanoLuc[®]-PEST, which displays the transcriptional activity induced by the CRE promoter region. The PEST sequence destabilises the reporter protein, resulting in a higher responsiveness to intracellular changes. The Vivazine[™] substrate was used to generate luminescence proportional to the transcriptional changes over a longer period of time.

The effect of EA 575[®] on adenosine-mediated CRE activation was examined first. The treatment with 80–240 µg/ml EA 575[®] for 16 h caused a significant reduction in CRE activation mediated by stimulation with 100 µM adenosine by a maximum of 24.2 ± 9.38 %, compared to stimulated control cells that were not treated with EA 575[®] (Figure 11A). The specifically A_{2B}AR-mediated CRE activation by 10 µM BAY 60-6583 was also inhibited by the treatment with EA 575[®] in a dose-dependent manner by up to 20.2 ± 2.67 %, being significant at 80–240 µg/ml (Figure 11B).

Since adenosine is a non-specific agonist that binds to all adenosine receptor subtypes, identification of the subtype accountable for the observed effect was addressed next. The A_{2B}AR-specific antagonist PSB-603 and the A_{2A}AR-specific antagonist SCH 442416 were used for this purpose. The cells were treated with the antagonists for 2 h before stimulation with 100 µM adenosine. PSB-603 significantly reduced the adenosine-mediated CRE activation by 33.3 ± 6.63 % at a concentration of 1 µM, while SCH 442416 was able to significantly inhibit the CRE activation by 54.1 ± 7.90 % at a concentration of 10 µM. Neither antagonist showed a significant decrease in the signal at lower concentrations. In contrast, 0.1 µM SCH 442416 significantly increased the CRE activation by 34.6 ± 12.3 % (Figure 11C).

Stimulation with 10 µM of the A_{2A}AR agonist CGS 21680 also mediated CRE activation, resulting in a significant 3.10 ± 0.24 -fold increase in the luminescence signal, compared to completely untreated control cells. Nevertheless, the effect elicited by A_{2A}AR stimulation was smaller than that evoked by 10 µM BAY 60-6583, which

Results

showed a 5.14 ± 0.93 -fold elevation, and 100 μM adenosine, for which the signal was highest with a 7.06 ± 1.09 -fold increase (Figure 11D).

These results indicate that both receptors influence CRE activation. Although an inhibition of the $A_{2B}\text{AR}$ -mediated CRE activation by EA 575[®] was shown, these data alone do not clearly identify the responsible receptor subtype.

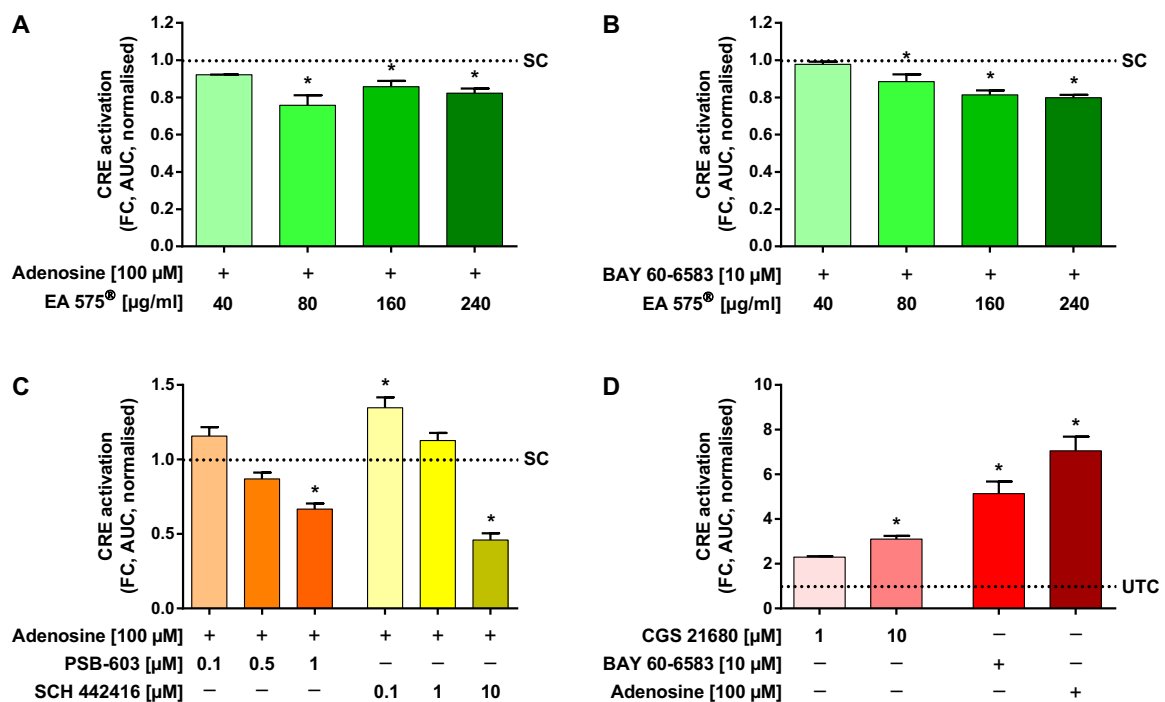


Figure 11: Influence of EA 575[®] (A,B) or the antagonists PSB-603 and SCH 442416 (C) on the CRE activation in transiently transfected HEK cells mediated by stimulation with adenosine (A,C,D), BAY 60-6583 (B,D) or CGS 21680 (D). Pre-incubation with 40–240 $\mu\text{g/ml}$ EA 575[®] was performed for 16 h (A,B) or with 0.1–10 μM of the antagonists for 2 h (C) prior to the addition of 100 μM adenosine (A,C) or 10 μM BAY 60-6583 (B). The treatment with 80–240 $\mu\text{g/ml}$ EA 575[®] (A) or 1 μM PSB-603 (C) significantly inhibited the non-specifically-mediated CRE activation, compared to stimulated control cells that were not pre-treated (SC). The CRE activation was also significantly reduced by 10 μM SCH 442416, whereas this effect could not be observed at lower concentrations of either antagonist. Instead, 0.1 μM SCH 442416 increased the CRE activation (C). The inhibition of the specifically $A_{2B}\text{AR}$ -mediated CRE activation was achieved by the treatment with 80–240 $\mu\text{g/ml}$ EA 575[®] (B). Influence of the $A_{2A}\text{AR}$ agonist CGS 21680 and, in comparison, BAY 60-6583 and adenosine on the CRE activation in transiently transfected HEK cells (D). The cells were stimulated with 1–10 μM CGS 21680, 10 μM BAY 60-6583 or 100 μM adenosine. The CRE activation mediated by 10 μM CGS 21680 via $A_{2A}\text{AR}$ was significantly increased compared with completely untreated control cells (UTC), but to a lesser extent than that mediated by BAY 60-6583 via $A_{2B}\text{AR}$ or non-specifically using adenosine (D). Data are shown as AUC of the fold change (FC) after stimulation normalised to stimulated control cells that were not pre-treated (SC) (A–C) or completely untreated control cells (UTC) (D). Results represent the mean and SEM ($n = 3$ independent experiments performed in triplicate, * $p < 0.05$). This figure was published [1].

5.5 Influence of EA 575[®] on IL-6 release and determination of the responsible receptor subtype

IL-6 release of Calu-3 cells was measured using the Lumit[™] IL-6 (Human) Immunoassay. Primary antibodies that specifically target IL-6 are added to the cell medium. These antibodies are labelled with SmBiT or LgBiT. When IL-6 is released, the antibodies bind to it, leading to the assembly of SmBiT and LgBiT, resulting in the formation of the active NanoLuc[®] luciferase. Together with the substrate, luminescence proportional to the IL-6 concentration is generated.

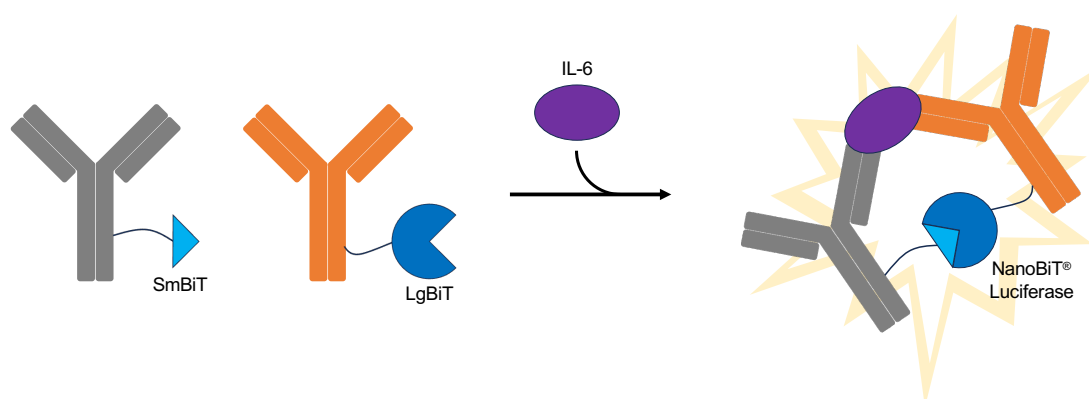


Figure 12: Principle of the Lumit[™] IL-6 (Human) Immunoassay. Modified drawing according to <https://www.promega.de/products/cell-health-assays/inflammation-assay/lumit-il-6-human-immunoassay/?catNum=W6030#protocols> (accessed 28 July, 2023).

Adenosine and BAY 60-6583 were tested for their ability to provoke IL-6 release in Calu-3 cells. TNF α was used as a positive control, resulting in a significant 5.19 ± 0.39 -fold IL-6 release compared to untreated control cells. Stimulation with adenosine led to a smaller but dose-dependent IL-6 release, being significant only for 100 μ M with a 1.63 ± 0.27 -fold increase. Higher IL-6 concentrations were detected upon A_{2B}AR-specific stimulation using BAY 60-6583, which elicited a significant 2.50 ± 0.27 -fold release (Figure 13).

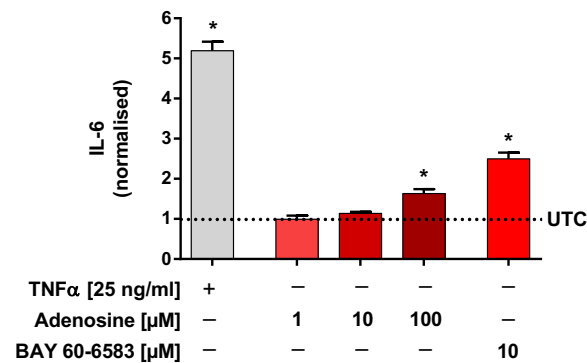


Figure 13: Influence of adenosine, BAY 60-6583, and TNF α on the IL-6 release in Calu-3 cells. Stimulation of Calu-3 cells was performed for 24 h using TNF α as a positive control, adenosine, or BAY 60-6583. Compared to untreated control cells (UTC), 25 ng/ml TNF α led to a significant IL-6 release. Adenosine showed a dose-dependent effect, that was significant only at 100 μ M. A significant IL-6 release was also elicited by 10 μ M BAY 60-6583. Results represent the mean normalised to untreated control cells (UTC) and SEM ($n = 1$ experiment performed at least in triplicate, * $p < 0.05$).

As already published, the influence of EA 575[®] on the adenosine-mediated IL-6 release and the adenosine receptor subtype responsible for this effect were examined [1].

The influence of EA 575[®] on the non-specifically mediated IL-6 release by 100 μ M adenosine was investigated first. The treatment with 80–240 μ g/ml EA 575[®] for 16 h caused a significant and dose-dependent decrease in adenosine-mediated IL-6 release by up to 33.7 ± 10.8 %, compared to stimulated control cells not treated with EA 575[®] (Figure 14A). Similarly, BAY 60-6583-mediated IL-6 release was significantly inhibited by the treatment with 40–240 μ g/ml EA 575[®] in a dose-dependent manner, reducing it up to 36.4 ± 2.16 % (Figure 14B).

In order to identify the specific receptor subtype responsible for the IL-6 release mediated by adenosine, the receptor-specific antagonists PSB-603 and SCH 442416 were tested. PSB-603 significantly inhibited the adenosine-mediated IL-6 release by 22.6 ± 8.19 % at a concentration of 1 μ M, whereas SCH 442416 increased the concentration of IL-6 even further by up to 25.0 ± 9.57 % (Figure 14C).

An alternative approach to this question was comparing different agonists. Stimulation with CGS 21680 had no significant effect, showing a maximal 1.33 ± 0.20 -fold IL-6 increase, whereas 10 μ M BAY 60-6583 caused a 2.91 ± 0.35 -fold increase in IL-6 release, compared to completely untreated control cells (Figure 14D).

These data indicate that adenosine mediates IL-6 release via $A_{2B}AR$, which is inhibited by EA 575[®].

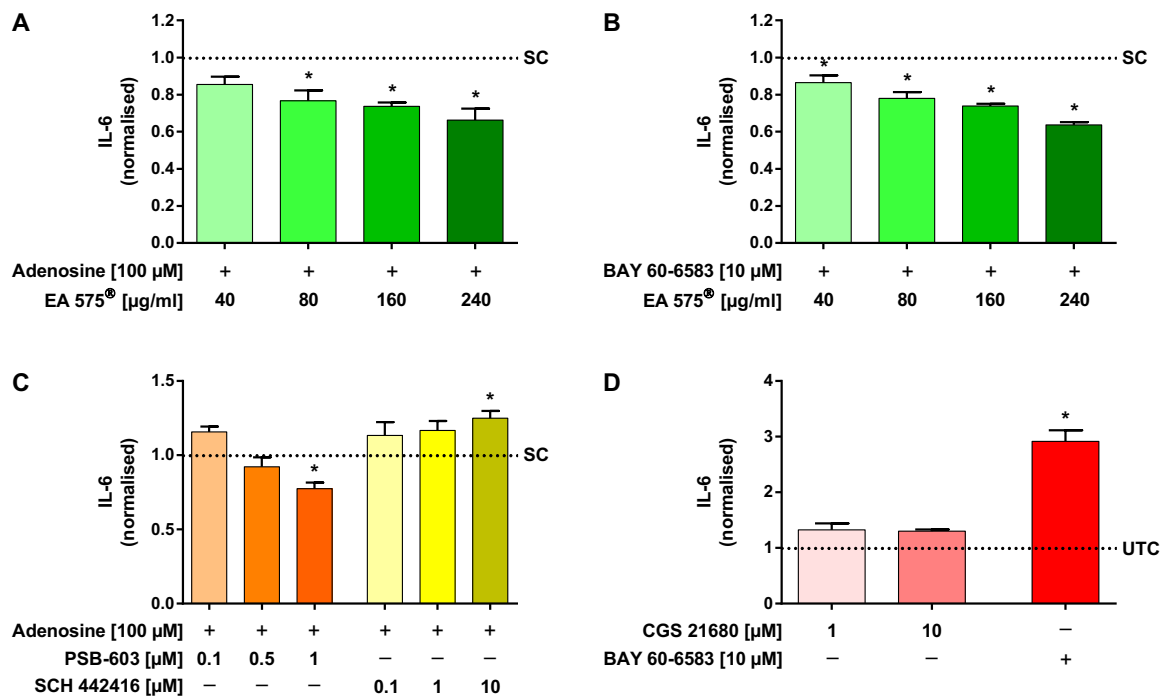


Figure 14: Influence of EA 575[®] (A,B) or the antagonists PSB-603 and SCH 442416 (C) on the IL-6 release of Calu-3 cells mediated by stimulation with adenosine (A,C), BAY 60-6583 (B,D) or CGS 21680 (D). Pre-incubation with 40–240 μ g/ml EA 575[®] was performed for 16 h (A,B) or with 0.1–10 μ M of the antagonists for 1 h (C) prior to the stimulation with 100 μ M adenosine (A,C) or 10 μ M BAY 60-6583 (B) for another 24 h. Compared to stimulated control cells that were not pre-treated (SC), the adenosine-mediated IL-6 release was significantly and dose-dependently inhibited by the treatment with 80–240 μ g/ml EA 575[®] (A) or 1 μ M PSB-603 (C). In contrast, SCH 442416 led to a further increase in IL-6. (C). The inhibition of the specifically $A_{2B}AR$ -mediated IL-6 release was observed after the treatment with 40–240 μ g/ml EA 575[®] (B). Influence of the $A_{2A}AR$ agonist CGS 21680 and, in comparison, BAY 60-6583 on the IL-6 release of Calu-3 cells (D). Stimulation of the cells was conducted using 1–10 μ M CGS 21680 or 10 μ M BAY 60-6583 for 24 h. The $A_{2A}AR$ -mediated IL-6 release showed a slight increase compared to completely untreated control cells (UTC), but it was neither significant nor dose-dependent (D). Results represent the mean normalised to stimulated control cells that were not pre-treated (SC) (A–C) or completely untreated control cells (UTC) (D) and SEM ($n = 3$ independent experiments performed in triplicate, * $p < 0.05$). This figure has already been incorporated in Meurer et al. (2023) [1].

5.6 Influence of adenosine receptor signalling on NFκB transcriptional activity

As already published, different adenosine receptor agonists were tested for their effects on NFκB transcriptional activity to evaluate whether the observed adenosine receptor-mediated IL-6 release in Calu-3 cells was NFκB-dependent [1]. For this purpose, Calu-3 cells stably expressing a secreted NanoLuc[®] luciferase under control of an NFκB response element were employed. The principle of the measurement is the same as described in 5.4 for the CRE activation measurements, with the difference that it is a secreted NanoLuc[®] luciferase under control of an NFκB promoter element in this case.

The reaction of the cellular system, showing a 1.62 ± 0.11 -fold increase in luminescence signal to the stimulation with 25 ng/ml TNFα for 3 h, served as a positive control. However, neither 10–100 μM adenosine, nor 1–10 μM NECA, nor 1–10 μM BAY 60-6583 showed any effect on NFκB transcriptional activity, indicating that adenosine receptor signalling does not influence NFκB transcriptional activity (Figure 15).

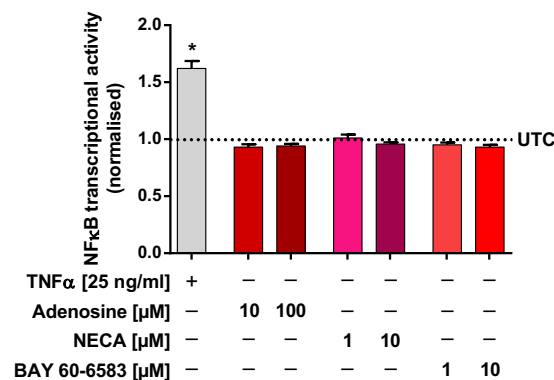


Figure 15: Influence of different adenosine receptor agonists on the NFκB transcriptional activity. Calu-3 cells stably expressing a secreted NanoLuc[®] luciferase under control of an NFκB binding sequence were stimulated for 3 h. TNFα at a concentration of 25 ng/ml was used as a positive control, resulting in a significant increase of the luminescence signal. In contrast, 10–100 μM adenosine, 1–10 μM NECA, or 1–10 μM BAY 60-6583 all did not affect NFκB transcriptional activity. Results represent the mean normalised to completely untreated control cells (UTC) and SEM ($n = 3$ independent experiments performed in triplicate, * $p < 0.05$). This figure has also been shown in Meurer et al. (2023) [1].

5.7 Identification of active constituents contained in EA 575[®]

In order to identify the constituents that are involved in the newly discovered effect of EA 575[®] on A_{2B}AR signalling, several different approaches were applied.

In a first approach, compounds previously identified in EA 575[®] were screened for their pharmacological activity. These compounds comprised the flavonoids rutin and nicotiflorin, the saponins α -hederin and hederacosides B, C, and D, as well as the dicaffeoylquinic acids 3,4-DQA, 3,5-DQA, and 4,5-DQA. The compounds were identified and quantified via HPLC analysis by comparison with the chromatograms of reference substances (Figure 16 & Table 9).

Solutions of the single substances were combined to represent the full extract or just parts of it according to their substance classes, as described in 4.9.3. These solutions are referred to as compound combinations (see Figure 1). To ensure equivalence of the prepared solutions to the extract itself, the peak areas of the substances in compound combination 1, which contained all of the substances, were compared to those in EA 575[®]. It was shown to be similar to the total extract, with all compounds within $\pm 20\%$ of the concentration determined in EA 575[®], except for nicotiflorin at 169% and hederacoside B at 261% (Figure 17 & Table 9).

Results

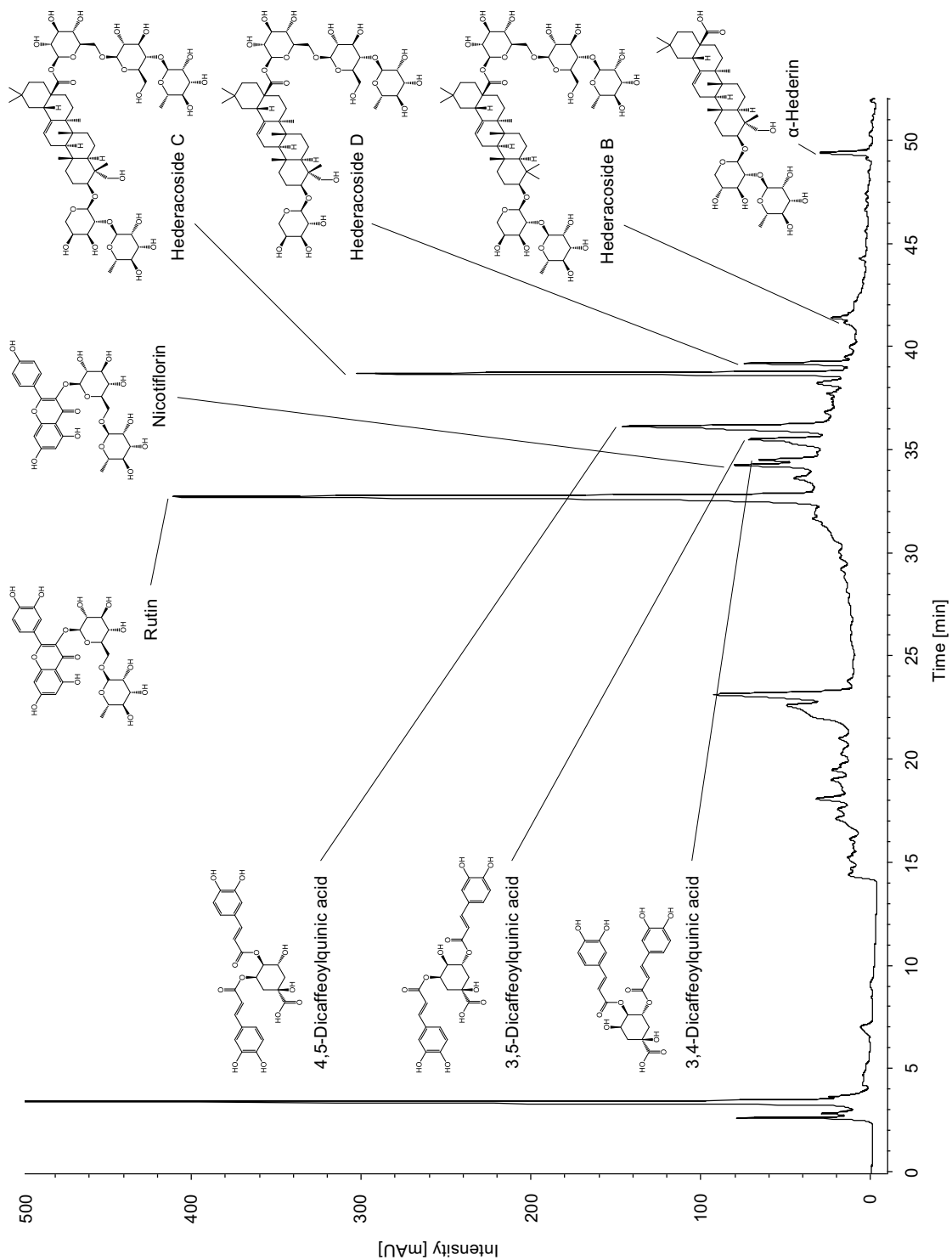


Figure 16: HPLC chromatogram of EA 575[®] at 205 nm with structural formulae of the main components

Table 9: Identification and quantification of the compounds in EA 575[®] and analysis of compound combination 1. Data of the reference substances and compound combination 1 represent the means of 2 HPLC runs. Data determined in the chromatograms of EA 575[®] were calculated as the mean of 9 runs.

Compound	Retention time of the reference substance [min]	Retention time in EA 575[®] [min]	Peak area/injected amount of reference [mAU*s/μg]	Peak area in the injected 80 μg EA 575[®] [mAU*s]	Peak area in compound combination 1 [mAU*s]	Percentage content in compound combination 1 in relation to EA 575[®] [%]
Rutin	32.6	32.6	2547	4828	5265	109
Nicotiflorin	34.1	34.2	2390	655	1106	169
3,4-DQA	34.3	34.4	2149	583	480	82
3,5-DQA	35.3	35.4	2193	990	1020	103
4,5-DQA	36.0	36.1	2200	2046	2245	110
Hederacoside C	38.7	38.6	225	2325	2100	90
Hederacoside D	39.2	39.0	247	546	630	115
Hederacoside B	41.4	41.2	162	71	186	261
α-Hederin	49.4	49.2	409	302	291	96

Results

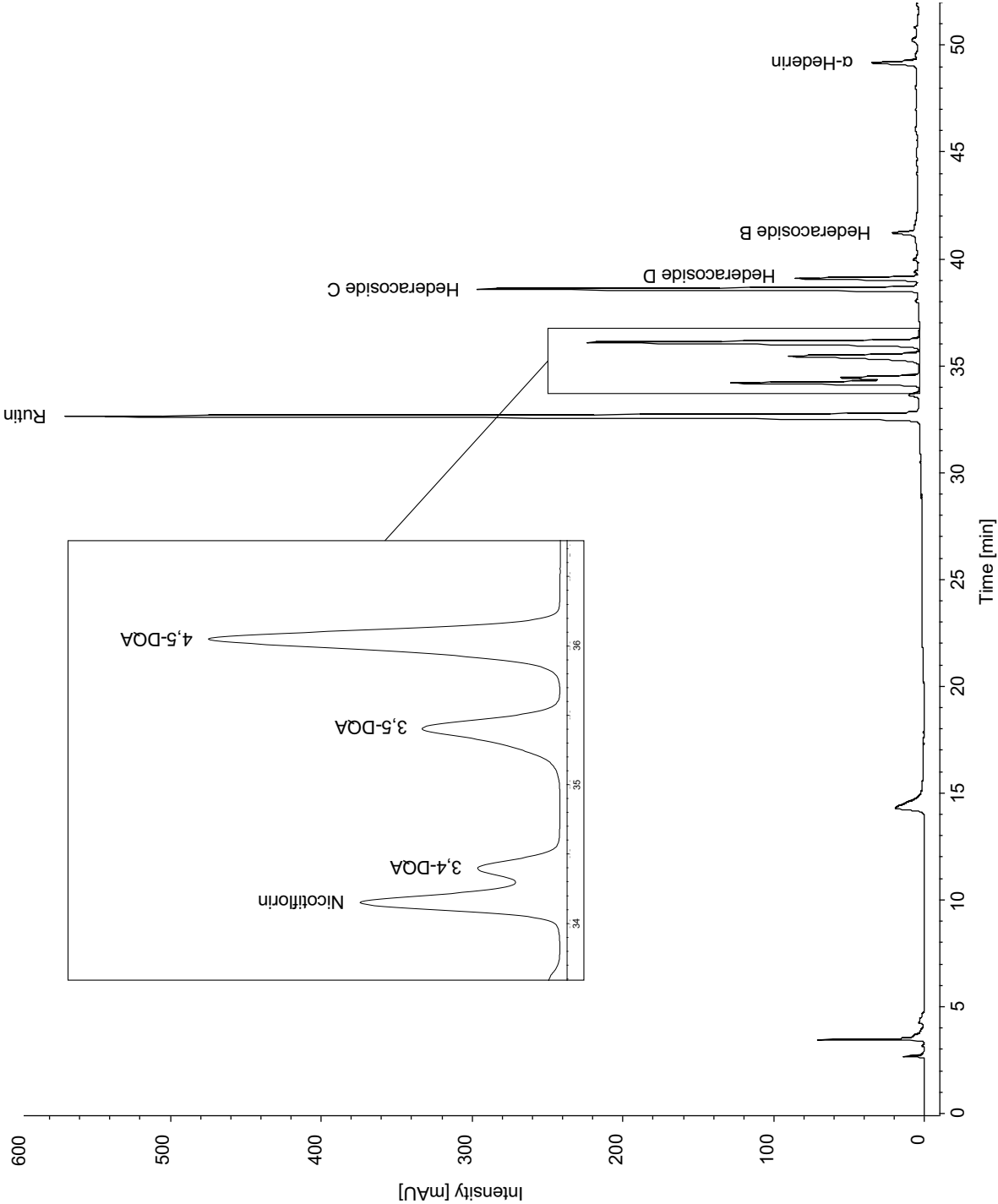


Figure 17: HPLC chromatogram of compound combination 1 at 205 nm

Then, these compound combinations were tested for their activity using the GloSensor™ cAMP assay. The solutions were used at a concentration equivalent to 160 µg/ml EA 575®. The experiment was conducted in the same manner as for EA 575®, with a pre-incubation of 16 h and co-stimulation with 1 µM BAY 60-6583 and 1 µM forskolin. However, none of the tested compound combinations was able to elicit any effect on the cAMP level increase mediated by stimulation of A_{2B}AR (Figure 18). The inhibition observed for the total extract could not be substantiated by these substances.

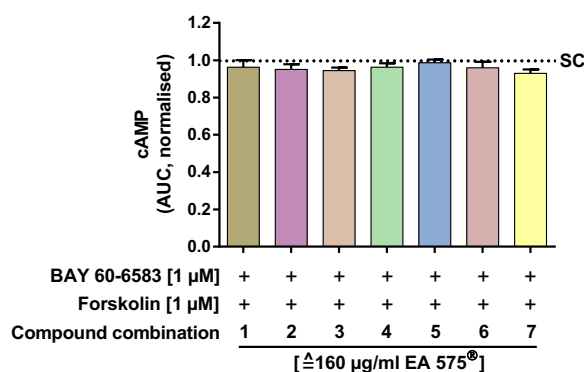


Figure 18: Influence of the compound combinations on the intracellular cAMP levels in HEK GloSensor™ cells elicited by stimulation of A_{2B}AR. Pre-incubation with the compound combinations at concentrations corresponding to 160 µg/ml EA 575® was conducted for 16 h before the cells were co-stimulated with 1 µM BAY 60-6583 and 1 µM forskolin. The cAMP level increase mediated by stimulation of A_{2B}AR was not significantly affected by any of the compound combinations. Data are shown as AUC normalised to stimulated control cells that were not pre-incubated with any compound (SC). Results represent the mean and SEM ($n = 3$ independent experiments performed with at least 5 replicates, * $p < 0.05$).

5.8 Bioassay-guided fractionation of EA 575[®]

The second approach to identify active constituents contained in EA 575[®] with an influence on A_{2B}AR signalling was bioassay-guided fractionation of the extract. Therefore, EA 575[®] was split into 6 fractions via HPLC, applying the method without phosphoric acid, as described in 4.10.1. Using the peak areas of 4,5-DQA, rutin, and hederacoside C in the chromatograms as references, fraction solutions corresponding to the concentration of the EA 575[®] stock solution were prepared (Figure S 14).

Then, the GloSensor™ cAMP assay was employed for the identification of pharmacologically active fractions. The treatment with the fractions equivalent to 160 µg/ml EA 575[®] was performed for 16 h prior to co-stimulation with 1 µM BAY 60-6583 and 1 µM forskolin. Fraction I led to a significant 23.9 ± 6.91 % reduction in cAMP levels, whereas the other fractions did not show a significant effect (Figure 19A).

Subsequently, a concentration series of fraction I was tested in order to determine whether the observed effect was dose-dependent. Fraction I was able to dose-dependently inhibit the A_{2B}AR-mediated cAMP level increase, with a significant reduction of 29.7 ± 4.59 % at a concentration equivalent to 240 µg/ml EA 575[®] (Figure 19B).

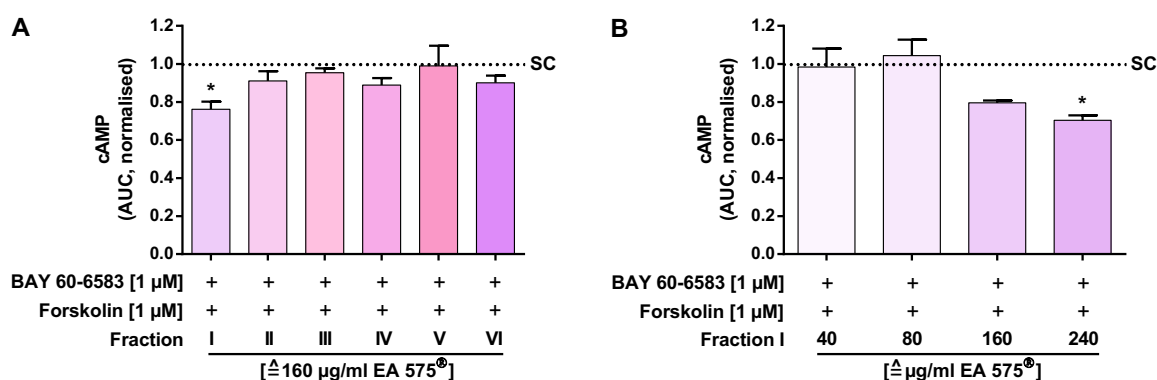


Figure 19: Influence of the fractions (A) and different concentrations of fraction I (B) on the intracellular cAMP levels in HEK GloSensor™ cells elicited by stimulation of A_{2B}AR. Prior to co-stimulation with 1 µM BAY 60-6583 and 1 µM forskolin, the cells were treated for 16 h with the fractions at concentrations equivalent to 160 µg/ml EA 575[®] (A) or with different concentrations of fraction I (B). A significant and dose-dependent inhibition of the A_{2B}AR-mediated cAMP level increase was caused by fraction I (A,B). The other fractions did not lead to a significant effect (A). Data are shown as AUC normalised to stimulated control cells that were not treated with any

fraction (SC). Results represent the mean and SEM ($n = 3$ independent experiments performed at least in triplicate, * $p < 0.05$).

In order to further narrow down potential A_{2B}AR-affecting constituents, fraction I was separated into five sub-fractions using HPLC, as described in 4.10.2. By comparing the areas of three representative reference peaks in the chromatograms of the sub-fractions with the chromatogram of fraction I, sub-fraction solutions equivalent to the stock solution of EA 575[®] were prepared (Figure 20–22 & Figure S 15).

Results

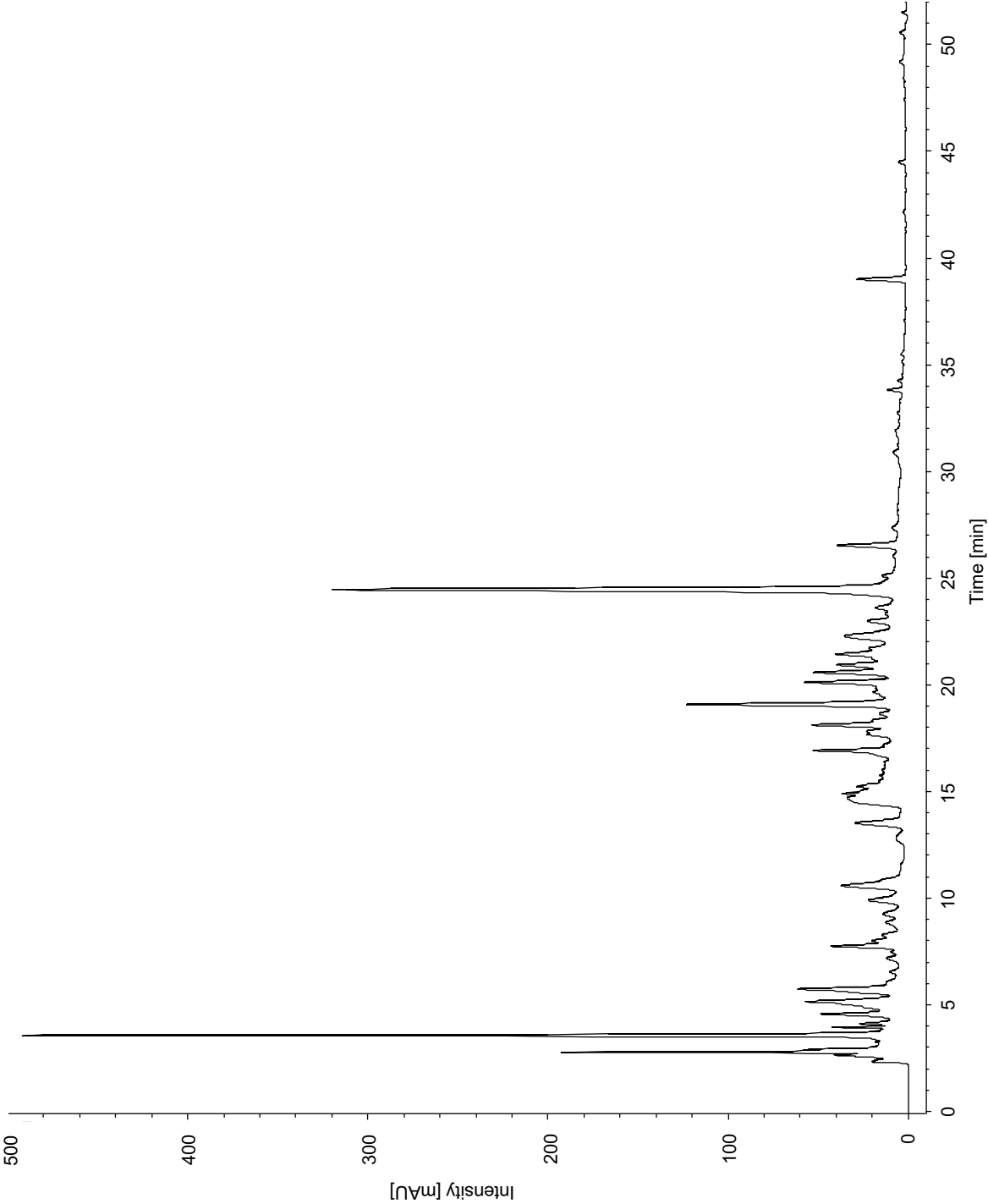


Figure 20: HPLC chromatogram of fraction I at 205 nm. The fractionation of EA 575[®] was successful. As expected, fraction I contained rather hydrophilic substances. All of the main components of this fraction eluted within approximately 25 min.

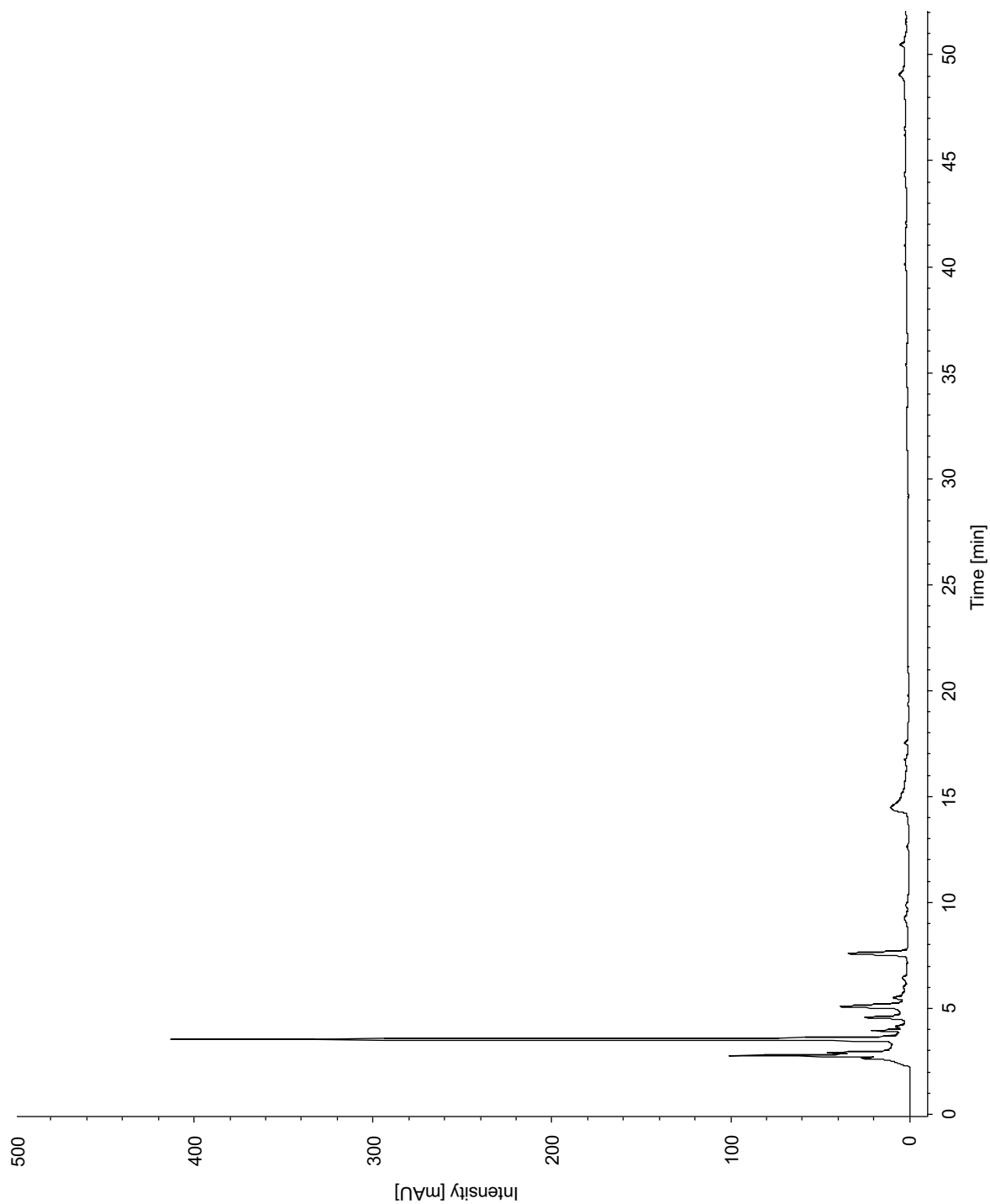


Figure 21: HPLC chromatogram of sub-fraction I-2 at 205 nm. The sub-fractionation of fraction I was also successful. The second of the five sub-fractions contained only highly hydrophilic substances, all of which eluted within 8 min.

Results

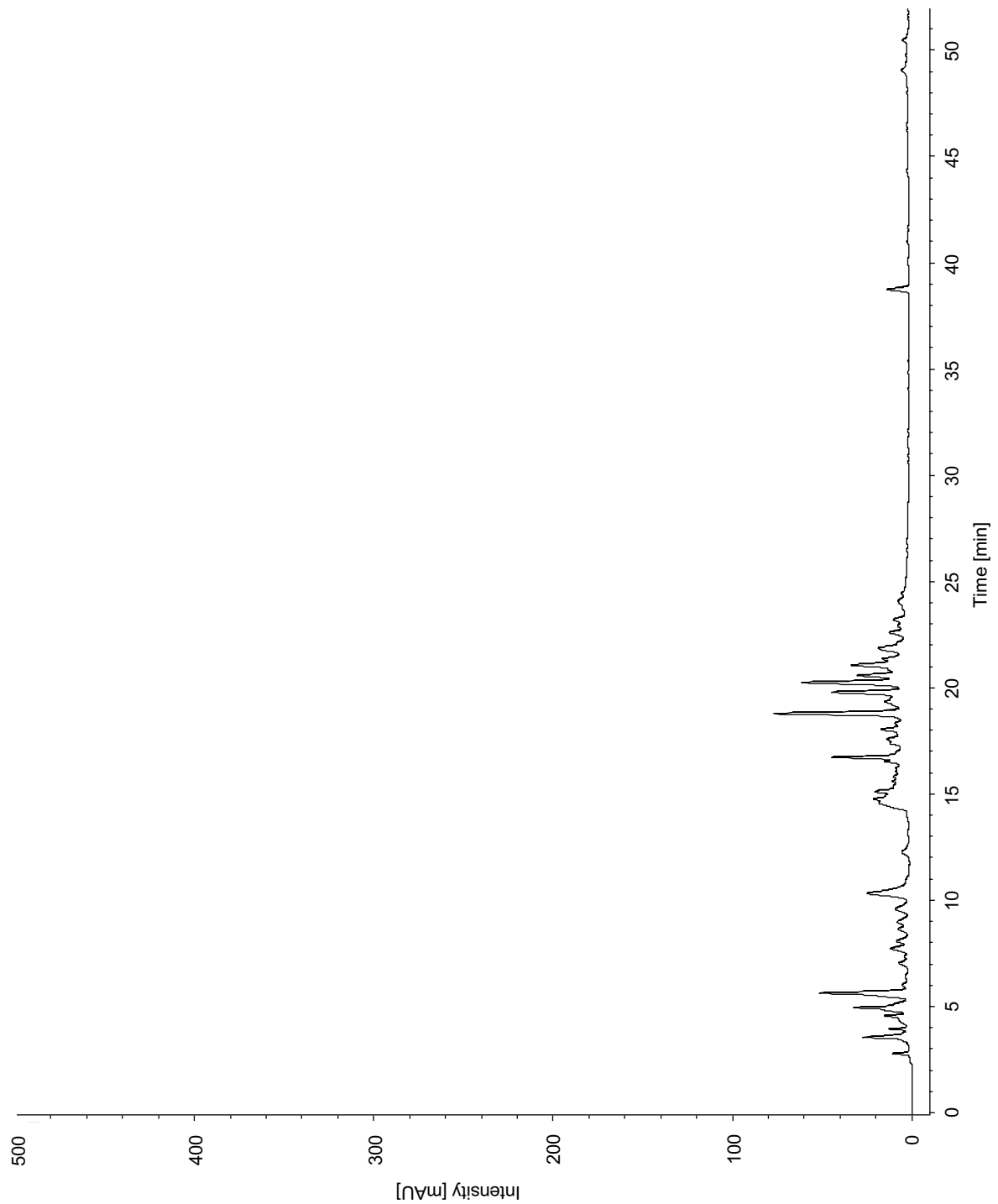


Figure 22: HPLC chromatogram of sub-fraction I-3 at 205 nm. The third of the five sub-fractions contained fewer highly hydrophilic substances, but more substances that eluted later. The main components of sub-fraction I-3 eluted between 14–24 min. Some substances that appeared at the beginning of this chromatogram could also be contained in sub-fraction I-2.

Then, the sub-fractions were tested using the GloSensor™ cAMP assay. Prior to co-stimulation with 1 μ M BAY 60-6583 and 1 μ M forskolin, pre-incubation for 16 h was performed with the sub-fractions at a concentration corresponding to 240 μ g/ml EA 575®. A significant reduction of 21.1 ± 4.17 % and 19.9 ± 8.42 % in cAMP levels was observed for sub-fractions I-2 and I-3, respectively. The other sub-fractions did not elicit a significant effect (Figure 23A).

Since the effects of the individual sub-fractions were rather small and it seemed that active constituents were distributed across two specific fractions, combinations of the sub-fractions were tested next to investigate whether the combined mixture would produce more significant results. The assay was carried out as described above for the individual sub-fractions, with each sub-fraction in the combination having a concentration corresponding to 240 μ g/ml EA 575®. All combinations with either sub-fraction I-2 or sub-fraction I-3 showed a significant effect. The combination of sub-fractions I-2 and I-3 elicited a slightly but not significantly stronger effect, reducing the cAMP levels by 23.3 ± 13.8 % (Figure 23B).

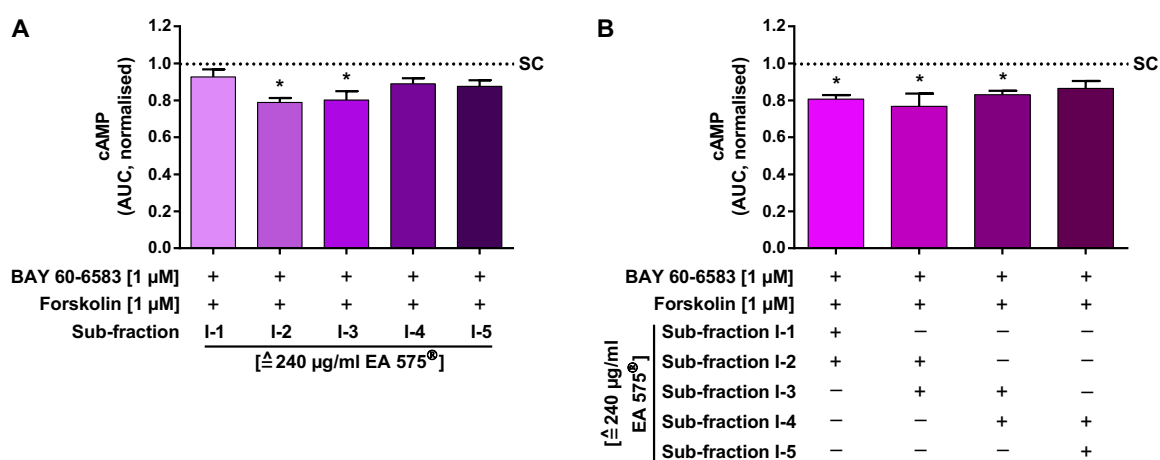


Figure 23: Influence of the sub-fractions (A) and combinations thereof (B) on the intracellular cAMP levels in HEK GloSensor™ cells elicited by stimulation of A_{2B}AR. The cells were treated with the sub-fractions at concentrations corresponding to 240 μ g/ml EA 575® for 16 h. Stimulation was conducted with 1 μ M BAY 60-6583 and 1 μ M forskolin simultaneously. Sub-fractions I-2 and I-3 significantly inhibited the A_{2B}AR-mediated cAMP level increase, whereas the other sub-fractions showed no effect (A). When combining several sub-fractions, a significant effect was observed for combinations containing either sub-fraction I-2 or sub-fraction I-3, and the slightly but not significantly strongest effect was elicited by the combination of sub-fractions I-2 and I-3 (B). Data are shown as AUC normalised to stimulated control cells that were not treated with any sub-fraction (SC). Results represent the mean and SEM (A: $n = 3$ independent experiments performed at least in triplicate; B: $n = 4$ independent experiments performed at least in triplicate, * $p < 0.05$).

Results

The cAMP experiments suggest that the constituents responsible for the influence of EA 575[®] on A_{2B}AR signalling are contained in sub-fractions I-2 and I-3. Since many peaks were detected in the chromatograms of these sub-fractions, further investigation was necessary. However, narrowing down the substances by another fractionation using the same method was not an option, as there were already two pharmacologically active sub-fractions. Therefore, mass spectrometry of sub-fractions I-2 and I-3 was performed in order to identify specific substances or substance classes characterising these sub-fractions.

Detailed lists of the presumed substances identified in sub-fractions I-2 and I-3 are provided in the supplemental material (Table S 2–5). Only measured masses that could be identified by comparison of their MS² spectra with literature data are listed there. More masses were present, but could not be clearly assigned to a substance. Therefore, these lists do not represent all compounds that can be found in the two sub-fractions.

Compounds from different substance classes were found to be contained in sub-fractions I-2 and I-3. Mainly, these compounds can be described as rather hydrophilic, and it is noticeable that many of the identified substances have carboxyl groups. Regarding these substance classes, no major differences between both sub-fractions could be observed.

In summary, several amino acids such as proline, valine, iso-/leucine, and tyrosine were identified. As mentioned above, carboxylic acids were the most prominent group. Furthermore, dicarboxylic acids, such as maleic acid or fumaric acid, succinic acid, and malic acid, as well as tricarboxylic acids, such as citric acid, were found.

As expected for a plant extract, secondary metabolites were present in the sub-fractions. Some of the identified structures, such as protocatechuic acid, caffeic acid, quinic acid have already been published as compounds of EA 575[®]. A specific molecular mass of the esters of quinic acid and caffeic acid was also found, but the isomers chlorogenic acid, neochlorogenic acid, and cryptochlorogenic acid could not be distinguished from each other. All of these were previously identified in EA 575[®]. Other secondary metabolites not previously reported for ivy comprised shikimic acid, salicylic acid, and vanillin.

Another common group contained in the sub-fractions was sugars and derivatives thereof. The identified structures included disaccharides, hexonic acids and isomers of glucaric acid, and sugar alcohols (e.g., mannitol or sorbitol).

Remarkably, the nucleobases guanine and adenine, and their corresponding nucleosides guanosine and adenosine were identified. In addition, the nucleotide uridine monophosphate was present.

Moreover, molecular masses of structures were found that could be presumed to be combinations of the substances described here, such as glycosylated amino acids or dipeptides. Additionally, there could be alkylated variants or sulfates of some substances mentioned above. Also, there were molecular masses which matched molecular formulae for iridoid glycosides. As none of these structures could be confirmed with certainty, they are not listed by name in this work.

Since a connection to adenosine receptors has been reported for chlorogenic acid [66], further research regarding chlorogenic acid and its isomers neochlorogenic acid and cryptochlorogenic acid was conducted. In a first step, the abundances of the three isomers in the HPLC chromatograms of sub-fractions I-2 and I-3 were investigated.

For this purpose, reference substances were analysed via HPLC, and the corresponding peaks in the sub-fractions were identified by comparing retention times and UV spectra. It was found that neochlorogenic acid eluted earlier than the other isomers, both of which eluted at the same time. Therefore, they likely eluted as one overlaying peak in the extract and sub-fraction chromatograms.

As can be seen in Figure S 15, none of the isomers were detectable in sub-fraction I-2, whereas a significant amount of neochlorogenic acid was found in sub-fraction I-3. However, only very small amounts of chlorogenic acid or cryptochlorogenic acid were detected in sub-fraction I-3, whereas higher levels were detected in sub-fractions I-4 and I-5.

Based on these findings, the influence of neochlorogenic acid and chlorogenic acid on $A_{2B}AR$ -mediated cAMP levels was investigated using the GloSensor™ cAMP assay. The cells were pre-incubated with different concentrations of the substances for 16 h, followed by co-stimulation with 1 μ M BAY 60-6583 and 1 μ M forskolin. None of the tested concentrations of either compound or a combination thereof was able to affect

Results

the cAMP level increase by stimulation of A_{2B}AR (Figure 24). The effect of EA 575[®] could therefore also not be substantiated by these substances.

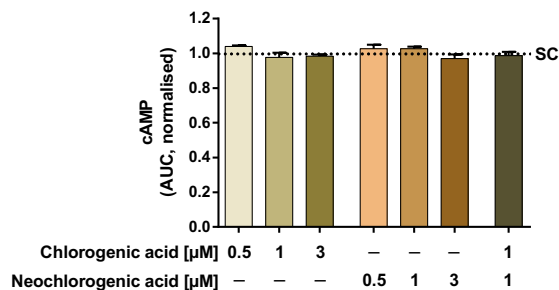


Figure 24: Influence of chlorogenic acid, neochlorogenic acid, and a combination thereof on the intracellular cAMP levels in HEK GloSensor™ cells elicited by stimulation of A_{2B}AR.

The cells were pre-incubated with different concentrations of chlorogenic acid, neochlorogenic acid, or a combination thereof, prior to simultaneous stimulation with 1 μM BAY 60-6583 and 1 μM forskolin. The cAMP level increase mediated by stimulation of A_{2B}AR was not significantly affected by any of the tested conditions. Data are shown as AUC normalised to stimulated control cells that were not pre-incubated with any compound (SC). Results represent the mean and SEM ($n = 1$ experiment performed in triplicate, * $p < 0.05$).

5.9 Generation and investigation of a HEK HiBiT-A_{2B}AR cell line using CRISPR/Cas9-mediated HDR

The CRISPR/Cas9 technology with DNA knock-in via homology-directed repair (HDR) was applied for the generation of a HEK HiBiT-A_{2B}AR cell line that expresses a HiBiT-tagged A_{2B}AR at an endogenous expression level. HiBiT is a small protein tag that generates luminescence upon binding to its complementation partner, LgBiT, as described in 5.3, with the difference that HiBiT exhibits much higher affinity for LgBiT than SmBiT.

For the use of this technology, CRISPR RNA (crRNA) and transactivating crRNA (tracrRNA) are annealed to form crRNA:tracrRNA duplexes, which are called guide RNA (gRNA). Both crRNA and tracrRNA are short, synthetically generated oligonucleotides of 36 nt and 67 nt, respectively, which are partially complementary to each other to allow binding. The crRNA is designed to specifically bind to a protospacer region localised on the gene of interest, whereas the tracrRNA is constant. The combined gRNA interacts with the Cas9 endonuclease to form a ribonucleoprotein (RNP).

The RNP was transfected into the cell along with the donor DNA by lipofection. Due to the crRNA being complementary to the protospacer on the gene of interest, the RNP is guided to the targeted cleavage site. The Cas9 endonuclease recognises a protospacer adjacent motif (PAM) site in close proximity on the complementary strand, which leads to a double-stranded DNA break.

One of the main pathways by which cells repair such DNA lesions is homology-directed repair. Since genetic information from a related sequence is used as a template for this pathway, HDR can be utilised to insert a short sequence into the gene of interest via a specific donor DNA. The desired insert sequence is flanked by homology arms that are complementary to the sequence into which the insert is to be introduced. Because of these homology arms, the donor DNA is recognised as an appropriate template and the insert sequence is integrated.

In the present work, the donor DNA was a 200 nt single-stranded oligodeoxynucleotide. The left homology arm consisted of the sequence up to the start codon of ADORA2B. The insert was the genetic information for HiBiT (33 nt) and a subsequent spacer (39 nt). The right homology arm was the beginning of the

Results

ADORA2B sequence. This led to the insertion of a sequence coding for HiBiT in front of the ADORA2B sequence, resulting in the expression of HiBiT-tagged A_{2B}AR.

By the use of an HDR enhancer, which is a low-molecular-weight compound that inhibits the other main repair pathway, homology-directed repair is favoured by the cell.

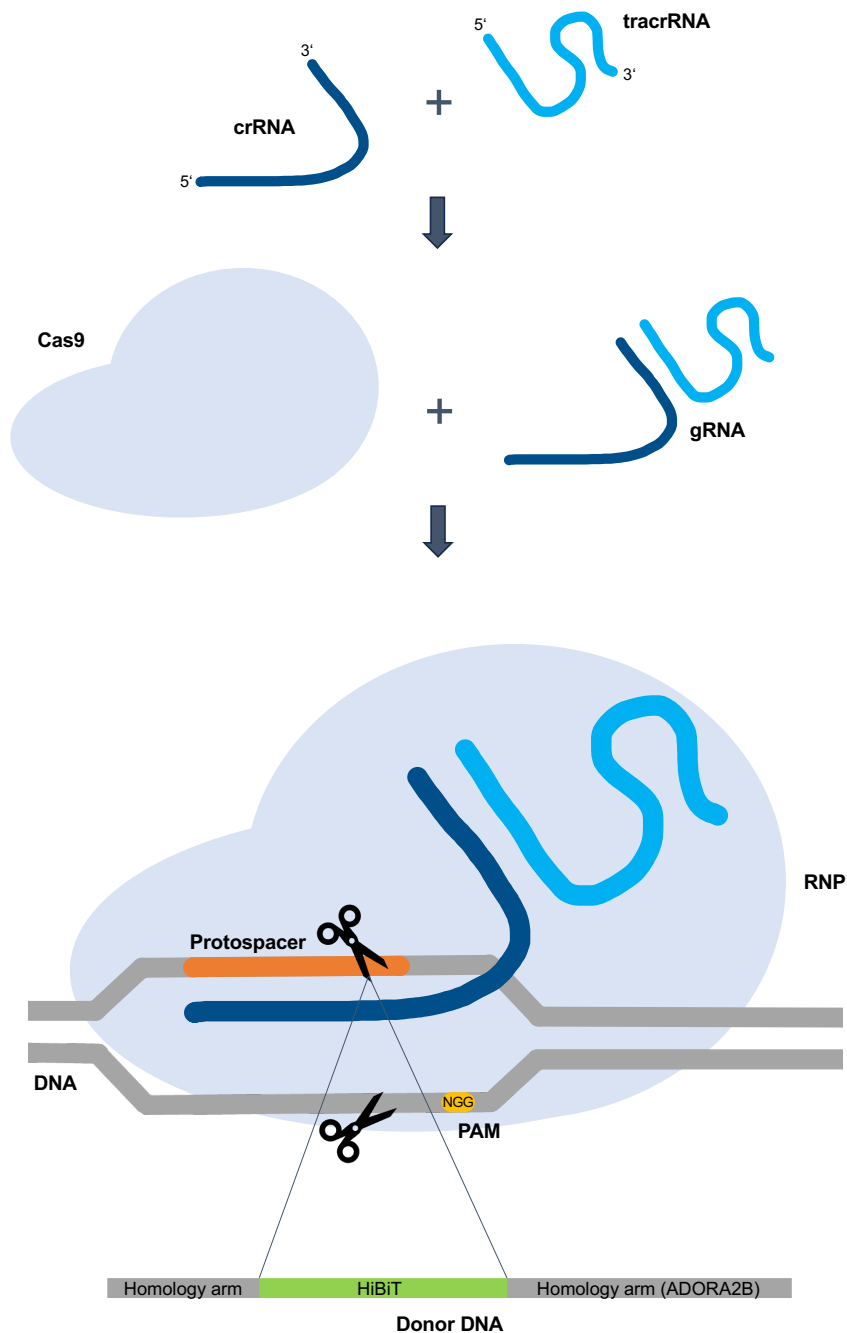


Figure 25: Principle of the CRISPR/Cas9-mediated HDR DNA knock-in. Modified drawing according to www.idtdna.com/crispr-cas9 (accessed 28 August, 2023).

After PCR screening for genome-edited clones that were genetically modified successfully and subsequent single-cell dilution, a single-cell clone called HEK CRISPR HiBiT-A_{2B}AR was obtained. This cell line was tested using different methods to determine whether it has HiBiT-tagged ADORA2B in its genome and whether it expresses HiBiT-tagged A_{2B}AR.

In a first step, the genome was investigated by PCR and subsequent DNA sequencing of the insert locus. It was shown that the DNA of this clone yielded PCR products for all specific primer combinations, indicating that HiBiT-tagged ADORA2B was present in the genome (Figure 26A). However, contemplating the PCR product of primer combination 2 after a longer electrophoresis time, it was observed that wild-type ADORA2B DNA was also present in the genome (Figure 26B). Sequencing was conducted using the PCR products of primer combinations 3 and 4 and the same primers, and it was found that the HiBiT and Spacer sequences were inserted correctly upstream of ADORA2B.

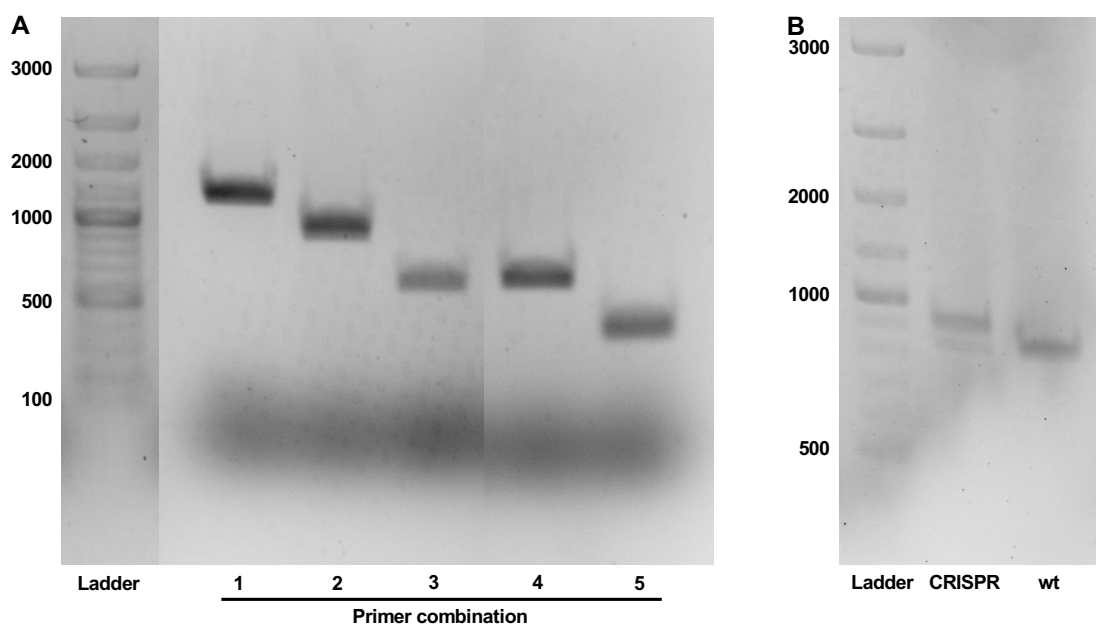


Figure 26: Agarose gel electrophoresis of HEK CRISPR HiBiT-A_{2B}AR DNA. Agarose gel electrophoresis was conducted on a 1 % agarose gel at 100 V for 45 min (A) and 75 min (B). All five primer combinations yielded the correct PCR products (A). After a longer electrophoresis time with the PCR product of primer combination 2, two bands were visible, one for the HiBiT-tagged ADORA2B sequence and one for the wild-type ADORA2B sequence (B). In contrast, HEK wild-type (wt) DNA yielded only the wild-type ADORA2B PCR product, as indicated by the corresponding band (B). The ladder was GeneRuler 100 bp Plus DNA Ladder.

Results

In order to assess whether the modified HiBiT-ADORA2B gene is expressed in the modified cell line, the mRNA was investigated. For this purpose, total RNA was extracted from the cells and converted to cDNA in order to perform PCR analyses. A specific PCR followed by agarose gel electrophoresis showed that cDNA encoding HiBiT-tagged A_{2B}AR was present in the HEK CRISPR HiBiT-A_{2B}AR cell line. Again, wild-type ADORA2B cDNA was also visible on the gel (Figure 27). Additionally, DNA sequencing was performed with the PCR products and the same primers used for the initial PCR. The sequence showed the correctly inserted genetic code for HiBiT and Spacer upstream of ADORA2B.

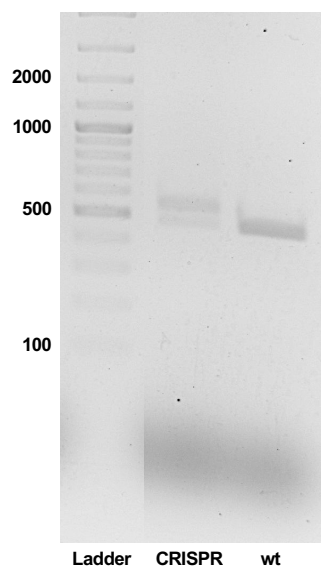


Figure 27: Agarose gel electrophoresis of HEK CRISPR HiBiT-A_{2B}AR cDNA. Agarose gel electrophoresis was performed on a 2 % agarose gel at 120 V for 60 min. The HEK CRISPR HiBiT-A_{2B}AR cDNA yielded two PCR products with the expected sizes, represented by two bands, one for the HiBiT-tagged ADORA2B sequence and one for the wild-type ADORA2B sequence. In comparison, the cDNA of HEK wild-type (wt) cells showed only the wild-type ADORA2B band. The ladder was GeneRuler 100 bp Plus DNA Ladder.

Next, investigations were carried out at the protein level. To determine the expression of HiBiT-tagged A_{2B}AR on the cell surface, HEK CRISPR HiBiT-A_{2B}AR cells were tested using Nano-Glo[®] HiBiT Extracellular Detection System. This method is suited to specifically quantitate receptors that are tagged with HiBiT on the extracellular side of the cell membrane. The complementary LgBiT is added to the medium, which then complements with the HiBiT tag of the receptor to form a functional NanoLuc[®] luciferase and, in combination with a substrate, produces luminescence proportional to the amount of HiBiT-tagged A_{2B}AR on the cell surface.

HEK CRISPR HiBiT-A_{2B}AR cells elicited a very small but significant 2.43 ± 0.46 -fold increase in luminescence signal compared to HEK wild-type cells (Figure 28A).

Since the signal was unusually small compared to overexpressing cells for example, the total amount of expressed HiBiT-A_{2B}AR in HEK CRISPR HiBiT-A_{2B}AR cells was examined. For this purpose, Nano-Glo[®] HiBiT Lytic Detection System was applied. The principle of this method is the same as that of the extracellular system, with the difference that the cells are lysed. Therefore, luminescence is generated proportional to the amount of HiBiT-tagged A_{2B}AR in the total cell lysate and not only to that on the cell surface.

The 1.28 ± 0.01 -fold increase in luminescence signal by HEK CRISPR HiBiT-A_{2B}AR cells in comparison to HEK wild-type cells was even lower than that observed using the extracellular assay (Figure 28B).

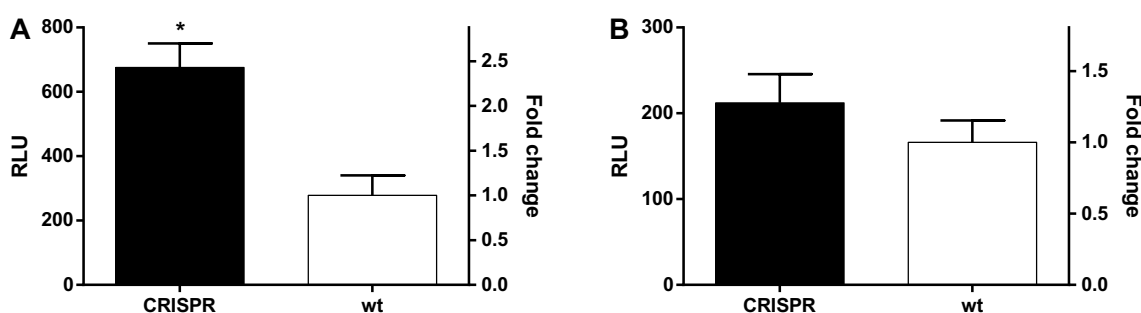


Figure 28: Quantification of HiBiT-tagged A_{2B}AR on the cell surface (A) and in the cell lysate (B) of HEK CRISPR HiBiT-A_{2B}AR cells. The luminescence signal of HEK CRISPR HiBiT-A_{2B}AR cells in comparison to HEK wild-type (wt) cells was measured 10 min after adding the LgBiT-substrate mixture in extracellular (A) or lytic buffer (B). HEK CRISPR HiBiT-A_{2B}AR cells produced higher luminescence than HEK wild-type cells in both assays, being significant in the extracellular assay. Data are presented as the generated luminescence in RLU (left y-axis) and the fold change relative to HEK wild-type (wt) cells (right y-axis). Results represent the mean and SEM (A: $n = 3$ independent experiments performed in triplicate; B: $n = 2$ independent experiments performed in triplicate, * $p < 0.05$)

5.10 Generation and investigation of an overexpressing HEK HiBiT-A_{2B}AR cell line

For a better comparison of the obtained HEK CRISPR HiBiT-A_{2B}AR cells with an overexpressing cell line, HEK cells were transfected with an analogous construct under control of a CMV promoter, and a single-cell clone was generated. In order to compare the expression rates of HiBiT-tagged A_{2B}AR in this cell line with the CRISPR cell line, the overexpressing cells were tested in comparison to HEK wild-type cells using Nano-Glo® HiBiT Extracellular Detection System.

It can be seen that the overexpressing HEK HiBiT-A_{2B}AR cells produced a luminescence signal of ~100,000 RLU, which corresponds to a 162 ± 3.88 -fold increase compared to HEK wild-type cells (Figure 29).

Compared to the HEK CRISPR HiBiT-A_{2B}AR cells, the increase in luminescence generated by the overexpressing HEK HiBiT-A_{2B}AR cells was 66.5-fold higher (compare Figure 28 above).

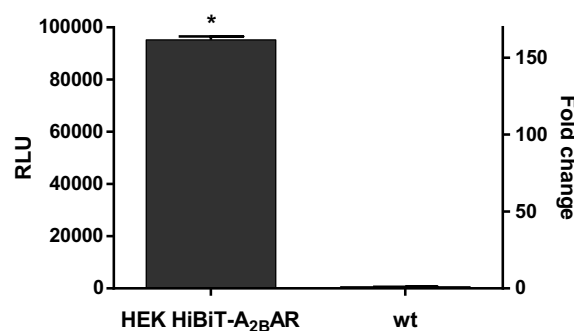


Figure 29: Quantification of HiBiT-tagged A_{2B}AR on the cell surface of HEK HiBiT-A_{2B}AR cells. The luminescence signal of HEK HiBiT-A_{2B}AR cells in comparison to HEK wild-type (wt) cells was measured 10 min after adding the LgBiT-substrate mixture in extracellular buffer. HEK HiBiT-A_{2B}AR cells produced a significantly higher luminescence than HEK wild-type cells. Data are presented as the generated luminescence in RLU (left y-axis) and the fold change relative to HEK wild-type (wt) cells (right y-axis). Results represent the mean and SEM ($n = 1$ experiment performed in triplicate, * $p < 0.05$)

6 Discussion*

In the present study, the mechanism of action of the ivy leaf dry extract EA 575[®] was further explored to explain its positive effects on inflammatory airway diseases [3–5]. Since adenosine receptor A_{2B} (A_{2B}AR) plays an essential role in the pathogenesis of chronic inflammatory airway diseases such as asthma, COPD, and pulmonary fibrosis [18–21], a possible effect of EA 575[®] on this receptor was investigated, as already published and discussed in Meurer et al. (2023) [1].

First, the potential impact of EA 575[®] on the cellular response of HEK cells to stimulation of A_{2B}AR was examined using DMR measurements. This label-free technology is well-suited for an initial investigation of the general influence of ligands on GPCR signalling due to its capability to provide a holistic overview of the complex cellular response [65]. EA 575[®] exhibited a dose-dependent inhibition of the cellular reaction to A_{2B}AR stimulation. This effect was observed after 16 h of pre-incubation, while no impact was seen after a short incubation time of 1 h, indicating no immediate but possibly indirect inhibition of A_{2B}AR.

In order to further specify the influenced cellular response observed in the DMR experiments, the second messenger cAMP was assessed. In alignment with the DMR results, a corresponding decrease in cAMP levels was observed after treatment with EA 575[®] under A_{2B}AR stimulatory conditions. A similar effect was shown for the highly selective A_{2B}AR antagonist PSB-603 using the same cAMP biosensor technology [67]. Next, the required minimum incubation period was challenged, and it was found that at least 8 h of EA 575[®] pre-incubation was necessary to mediate a reduction in cAMP levels. Such long incubation periods are unlikely to be in accordance with a direct mode of action, as these ligands typically compete for receptor-binding sites within minutes. PSB-603, for example, required a pre-incubation period of only 30 min in this assay [67]. These findings confirm that EA 575[®] is able to inhibit the A_{2B}AR signalling pathway and that this may be explained by an indirect mechanism of action. Since adenosine receptors are ubiquitously expressed in humans, this could be advantageous over

* Parts of this study, in particular the cellular assays investigating the influence of EA 575[®] on A_{2B}AR signalling, have been published recently within the scope of my doctoral studies [1]. For the sake of completeness and readability, these parts were incorporated into this work. This chapter therefore contains text passages from the referenced publication, which were revised and supplemented where necessary. This particularly concerns the pages 65–69. Further information can be found in 10.4.

orthosteric antagonism in terms of adverse effects [68]. To my knowledge, the findings presented here are the first to show the influence of an ivy extract on adenosine receptor A_{2B}.

To further investigate the mode of action of EA 575[®] on A_{2B}AR and to determine whether it also influences other downstream signalling pathways, the recruitment of β -arrestin 2 to A_{2B}AR was examined. For this purpose, a slightly modified assay system recently described by Saecker et al. (2023) was used [63]. Stimulation was performed using the non-specific adenosine receptor agonist NECA, as well as the specific A_{2B}AR agonist BAY 60-6583. Since A_{2B}AR is the only receptor tagged with LgBiT in this system, the effects detected after stimulation with NECA can also be considered specific for this receptor in this case. EA 575[®] caused a reduction in β -arrestin 2 recruitment to A_{2B}AR and thus affected the receptor signalling in an inhibitory manner in several ways. This is remarkable, as under β_2 -AR stimulatory conditions, EA 575[®] inhibits β -arrestin 2 recruitment while enhancing G protein/cAMP signalling [12].

In the downstream signalling cascade of G_s protein-coupled receptors, such as A_{2B}AR, cAMP causes phosphorylation of cAMP response element-binding protein via PKA, PKC, and ERK, and can thereby activate cAMP response elements (CRE) located in promoter regions, thus affecting the transcriptional activity of genes [69–72]. Since EA 575[®] reduced cAMP levels under A_{2B}AR stimulatory conditions, subsequent inhibition of CRE activation was expected. Indeed, EA 575[®] decreased CRE activation mediated both non-specifically by adenosine as well as A_{2B}AR-specifically by BAY 60-6583. A similar result was found for a specific A_{2B}AR antagonist, which reduced the NECA-mediated phosphorylation of CRE-binding protein [73].

One of the genes regulated by CRE codes for IL-6, which plays a crucial role in several inflammatory and airway diseases, such as asthma and COPD [40]. The IL-6 promoter region contains several elements that activate IL-6 expression, one of which is a CRE [74–78]. The release of IL-6 and other inflammatory and chemotactic mediators, in turn, can be mediated by adenosine via the A_{2B}AR signalling pathway, and CRE might be at least one important factor in this signalling cascade [79,80]. Since EA 575[®] inhibits both A_{2B}AR signalling and CRE activation, an effect on IL-6 release seemed plausible. Therefore, the potential effect of EA 575[®] on the adenosine-mediated IL-6 release in Calu-3 cells was tested. It was found that EA 575[®], in fact, reduced the adenosine-mediated release of IL-6, indicating a possible reduction in IL-6-mediated

airway inflammation and fibrosis. This inhibition of A_{2B} AR-mediated IL-6 release could also be reproduced with the specific agonist BAY 60-6583.

This is a new finding that complements the previously published decrease in IL-6 release by EA 575[®] via inhibition of NF κ B [12,16,17]. In the present study, it was demonstrated that neither adenosine, NECA, nor BAY 60-6583 influenced NF κ B transcriptional activity in Calu-3 cells. Although the IL-6 promoter region contains an NF κ B-binding element [81,82], the release of IL-6 via adenosine receptors is not mediated by this promoter element. This is in line with the results published by Sitaraman et al. (2001), who showed that the NF κ B-binding site, in contrast to the CRE-binding site, is not important for adenosine-mediated IL-6 release [80]. Similarly, Zhong et al. (2004) found that NECA does not affect NF κ B-mediated transcription but rather affects CRE-mediated transcription [79]. Therefore, in this case, EA 575[®] affects IL-6 release via another mechanism, which could be the inhibition of CRE.

Additionally, this study aimed to specify which adenosine receptor subtype is responsible for the observed effects in the IL-6 and CRE activation assays. Therefore, the inhibition of the adenosine-mediated CRE activation and IL-6 release with the A_{2A} AR antagonist SCH 442416 or the A_{2B} AR antagonist PSB-603 was investigated, as these are the predominantly expressed adenosine receptor subtypes in the cell types used [83–85]. Only PSB-603 reduced both CRE activation and IL-6 release after stimulation with adenosine. In contrast, SCH 442416 caused the inhibition of CRE activation but simultaneously led to a slight increase in IL-6 release. In addition, CGS 21680, a specific A_{2A} AR agonist, was shown to increase CRE activation in a dose-dependent manner but had no effect on IL-6 release. These data suggest that A_{2A} AR signalling activates CRE but does not result in an increase in IL-6. This might be because IL-6 is regulated not only by the cAMP response element but also by several other elements, as mentioned above. Instead, these findings indicate that adenosine mediates IL-6 release through CRE activation via A_{2B} AR.

Furthermore, adenosine mediates IL-6 release only in concentrations as high as 10–100 μ M, as shown in this study and others [72,79,80,86]. Considering the affinities of adenosine to the different receptor subtypes (EC_{50} : A_1 = 0.31 μ M, A_{2A} = 0.73 μ M, A_{2B} = 23.5 μ M, A_3 = 0.29 μ M) [87], this also suggests mediation via A_{2B} AR. Taken together, the published receptor-affinity data and the present results indicate that adenosine-induced IL-6 release is mediated through the A_{2B} AR signalling pathway.

These findings disagree with those of Sun et al. (2008), who stated that $A_{2A}AR$, but not $A_{2B}AR$, is responsible for adenosine-mediated IL-6 release [72], but are consistent with data from Sitaraman et al. (2001) and Zhong et al. (2004 & 2005), who both identified $A_{2B}AR$ as being responsible for adenosine-mediated IL-6 release [79,80,86]. Although not particularly distinguishing between the two receptors, several other studies have provided additional evidence for the $A_{2B}AR$ -mediated inhibition of IL-6 release. Elevated IL-6 levels in ADA-deficient and bleomycin-treated mice were reduced by the administration of a specific $A_{2B}AR$ antagonist [37,39]. Additionally, a NECA-mediated increase in IL-6 was reduced by antagonists of $A_{2B}AR$ in these models [39,56]. A reduction in NECA-mediated IL-6 elevation by $A_{2B}AR$ antagonists was also shown in macrophages [30,58]. Secretion of IL-6 after treating pulmonary arterial smooth muscle cells of PAH patients with BAY 60-6583 under hypoxic conditions was also reduced by a specific antagonist of $A_{2B}AR$ [31].

Moreover, $A_{2A}AR$ signalling is described as anti-inflammatory and lung-protective, which basically matches the results of the present study, suggesting that this receptor does not contribute to IL-6 release, but rather attenuates it [18–20]. Nevertheless, the findings of other studies in terms of the influence of $A_{2A}AR$ on IL-6 are controversial. There have been reports of both increases [88] as well as reductions [89–92] by the stimulation of $A_{2A}AR$ with CGS 21680. In alignment with the results presented here, other researchers found no effect [93,94]. On the other hand, the genetic knockout of $A_{2A}AR$ in mice led to higher expression of IL-6 in one study [95], but did not affect IL-6 in another study examining an ADA/ $A_{2A}AR$ double knockout [96]. Antagonism of $A_{2A}AR$ caused elevation of IL-6 levels, matching the present findings [90,91,93].

Several factors may account for these controversial findings. First, the effect of adenosine may depend on its concentration and the stage of the disease. At low levels, adenosine activates high-affinity receptors such as $A_{2A}AR$, triggering anti-inflammatory pathways. In highly inflammatory environments and chronic disease states such as asthma or COPD, higher levels of adenosine are released. Adenosine concentrations have been estimated to reach approximately 200 μM in the lungs of asthmatics [22]. At such high concentrations, low-affinity $A_{2B}AR$ is activated, which may lead to further exacerbation of airway inflammation [21]. Inhibition of $A_{2B}AR$ is therefore considered beneficial in chronic inflammatory airway diseases [18–20]. In a guinea pig model of asthma, antagonism of $A_{2B}AR$ ameliorated the changes provoked by an allergen

challenge, whereas A_{2A}AR antagonism deteriorated them [97]. A_{2B}AR antagonism also proved beneficial in mouse models of chronic lung diseases, as it attenuated bronchoconstriction, airway inflammation, pulmonary fibrosis, and airspace enlargement [32,37,39,98].

Taken together, this offers a possible explanation for the initial positive clinical effects of EA 575[®] in adjuvant asthma therapy by means of a possible reduction in adenosine-mediated inflammation and bronchoconstriction [10]. Still, further research regarding which constituents play a role in the observed effects was deemed necessary to fully understand the mechanisms of action of this versatile extract. Therefore, the present work approached to identify the compounds that are involved in the newly discovered effect of EA 575[®] on A_{2B}AR signalling.

It has been shown that fractions of an ivy leaf extract enriched in phenolics and flavonoids exhibited anti-inflammatory properties, but the specific substances responsible for these effects have not been identified [99,100]. The present investigation initially focused on the most abundant flavonoids, dicaffeoylquinic acids and saponins that were previously identified [13]. In this regard, seven compound combinations were prepared from these substances, with concentrations corresponding as closely as possible to the amounts determined in the full extract. The aim was to find the substance class or combinations thereof responsible for the inhibition of A_{2B}AR signalling.

The concentrations of the substances in the compound combinations were determined to be within $\pm 20\%$ of those found in the extract, and were therefore considered equivalent. They were tested at a concentration corresponding to 160 $\mu\text{g/ml}$ EA 575[®], the concentration at which significant effects were consistently observed in all assays conducted in the present study. Two substances diverged further. The concentration of nicotiflorin was 169 % of that in the extract. However, since the applied concentration was theoretically equivalent to 160 $\mu\text{g/ml}$, this in turn corresponds to ~ 240 $\mu\text{g/ml}$ EA 575[®], for which consistently significant effects have also been shown. Hederacoside B had an even higher divergence, with 261 % of the concentration in the extract. The overestimation might be due to the relatively small peak in the extract chromatogram at a time point at which multiple substances co-elute. Their peaks are not baseline-separated, which could have falsified the calculated peak area. In addition, hederacoside B is a compound with a rather low concentration in the extract.

Discussion

Furthermore, a concentration of 400 µg/ml EA 575[®] has been previously used without issues, which approximately corresponds to the concentration of hederacoside B in this solution [16]. The higher concentrations of the two substances were therefore not considered a concern.

The compound combinations were tested via cAMP level measurements under A_{2B}AR stimulatory conditions, a method that proved suitable in the present study to detect the effect of EA 575[®] on A_{2B}AR signalling. Furthermore, this assay was selected because it represents the earliest downstream event in the signalling cascade of A_{2B}AR among the techniques used in this study. However, the approach was not successful, as none of the tested substances showed an effect. The inhibition of A_{2B}AR signalling by EA 575[®] could therefore not be substantiated by these constituents and another approach to find active compounds had to be considered.

Bioassay-guided fractionation of EA 575[®] was performed next. This is a commonly used technique to isolate and identify pharmacologically active molecules from complex mixtures, such as plant extracts, with numerous reports of success [101,102]. It usually involves chromatographic fractionation, followed by bioassay screening of the resulting fractions. Subsequently, the molecules are isolated from the bioactive fractions, identified, and their bioactivity is assessed [103]. In the case of this work, EA 575[®] was separated into six fractions by HPLC, and each fraction was tested via measurements of the cAMP levels following A_{2B}AR stimulation to determine which fractions still showed the desired bioactivity.

In contrast to the analytical HPLC method, a mobile phase without phosphoric acid was used for the fractionation. This allowed the removal of the solvent from the fractions without an excessive acid concentration, as the phosphoric acid would not have evaporated with the solvent, which could have resulted in decomposition of constituents. Furthermore, it was necessary in order to use the fractions in the following cell-based assays, as the acid could have negatively affected the physiologic pH in the cell culture media.

On the other hand, omitting the phosphoric acid from the eluent resulted in a different HPLC chromatogram since some of the constituents eluted differently at the higher pH value (compare Figure 16 & Figure S 13). The eluent of the analytical HPLC with phosphoric acid had a pH of 2, while the eluent of the preparative HPLC without acid

was nearly neutral. If RP-HPLC is employed, as in this study, the higher pH has the following impacts on the retention times. Substances that are uncharged at pH 2, such as carboxylic acids, are deprotonated at pH 7 and thus charged negatively, resulting in earlier elution. Conversely, substances with basic chemical moieties that are protonated and charged at pH 2 may be uncharged at pH 7, resulting in later elution.

This, in turn, led to the presence of usually later eluting compounds in some fractions, which would not be expected from examining the chromatogram of the method with phosphoric acid in the mobile phase. For instance, although only the initial 10 minutes were collected as fraction I, the chromatogram of the analytical HPLC method with phosphoric acid reveals the elution of substances with retention times exceeding 10 minutes (Figure 20). Furthermore, the DQAs are contained in fraction III, whereas the flavonoids are contained in fraction IV, despite the flavonoids eluting prior to the DQAs when an eluent with acid was utilised. As explained above, this may be due to a charge of the DQAs caused by deprotonation of the carboxylic acid groups. Nonetheless, the fractionation process was successful as evidenced by the observable separation of the extract when assessing all fraction chromatograms (Figure S 14).

The concentrations of the fractions were calculated relative to the total extract, based on specific peaks of known substances that were most abundant in the particular fractions. Subsequently, solutions equivalent to the EA 575[®] stock solution were prepared. Some of the fractions did not contain any of the substances identified in the previous analyses and could therefore not be quantified by the reference substances. To ensure a bioactive level of these fractions, their solutions were prepared in the same manner as the fraction with the lowest calculated concentration. Then, the fractions were tested at a concentration equivalent to 160 µg/ml EA 575[®].

A dose-dependent effect was found for fraction I, indicating that the constituents responsible for the inhibition of A_{2B}AR by EA 575[®] were contained in this fraction. Since this fraction was the first to elute, the contained compounds were likely to be rather hydrophilic, but as stated above, there were also more lipophilic substances than might be expected in the first 10 minutes of elution.

Since there were still numerous peaks in the chromatogram of this fraction, further refinement was required to narrow down potential bioactive compounds. Consequently, fraction I was fractionated further into five sub-fractions. The

Discussion

sub-fractions were collected in the same elution period as fraction I, but each comprised only 2 minutes of elution time. This sub-fractionation was successful, as further separation could be observed in the chromatograms. Still, there were some peaks present in more than one sub-fraction, indicating that some constituents were distributed over two or more sub-fractions (Figure S 15). This may be attributed to substances with broader peaks, which eluted precisely during the change of the collection vessel, spanning the elution time of two sub-fractions. Alternatively, it may be due to substances in different ionisation states, as described above, resulting in a longer elution period or elution at two distinct times in two different sub-fractions.

The calculation of the concentration relative to fraction I was conducted similarly to the calculation of the fraction concentrations before. Since none of the substances identified in the previous analyses was contained, three of the most prominent peaks were chosen as reference peaks. These peaks were not further specified than their elution time and peak areas in order to compare them to the same peaks in the total fraction I. Two of the reference peaks were found in two sub-fractions each and none of them were contained in the first of the sub-fractions. The sub-fraction solutions were prepared so that the sum of the peak areas of each of the three peaks in the sub-fractions corresponded to those in fraction I, which in turn was concentration-equivalent to the total extract and for which a dose-dependent effect was demonstrated. Therefore, the concentration of the sub-fraction solutions was considered equivalent to the stock solution of EA 575[®].

The sub-fractions were tested at a concentration corresponding to 240 µg/ml EA 575[®] by measuring the effect on the A_{2B}AR-mediated cAMP level increase. The higher concentration was chosen in this case to ensure the presence of a bioactive level. Given the possibility that the compounds responsible for the effect might be distributed over multiple sub-fractions, the use of a higher concentration should compensate for possible lower concentrations of these split substances. Moreover, this higher extract concentration consistently showed significant effects across all assays conducted in this study. On the other hand, the risk of overdosing was considered to be rather low, as the concentration is well below the 400 µg/ml used previously [16].

Significant reductions in cAMP levels mediated by sub-fractions I-2 and I-3 were found, indicating that the pharmacologically active compounds are contained in these sub-fractions. The assumption, that the constituents being searched for could be found

in multiple sub-fractions, was thus confirmed. Furthermore, each of the two sub-fractions showed a comparatively small effect. Therefore, combinations of adjacent sub-fractions were tested to determine whether this resulted in a stronger effect. The sub-fractions were mixed so that each one corresponded to a concentration of 240 µg/ml EA 575[®]. Assuming that individual substances occur in two fractions, the quantity should then correspond correctly to that in the total extract. If the bioactive substances were contained in sub-fractions I-2 and I-3, the combination of both should have elicited a stronger effect than either alone or when combined with another sub-fraction. Only combinations containing either one of the two sub-fractions showed a significant effect, thus confirming that both sub-fractions contain bioactive constituents. A slightly but not significantly stronger effect was observed for the combination of sub-fractions I-2 and I-3, therefore the hypothesis could not be confirmed with certainty.

Given the chromatograms of sub-fractions I-2 and I-3, there were still numerous substances that might be responsible for the effect. Especially in the first 10 min of elution, there were peaks detected in either sub-fraction, which may indicate the presence of common substances. Further fractionation using the same method was not considered useful to narrow down the constituents of the two pharmacologically active sub-fractions. There were already two bioactive sub-fractions, and further separation would probably only have resulted in additional sub-fractions having an effect, rather than isolating the active constituents. Therefore, sub-fractions I-2 and I-3 were analysed by LC-MS/MS and subsequent comparison with spectral data in the PubChem database to identify contained substances. This procedure is one of the most common and reliable methods for the identification of small molecules in complex natural products [104,105]. It has also been employed to identify the major components of EA 575[®] before [13].

Within each sub-fraction individually, 17 substances were identified. Notably, 8 of these compounds were common to both sub-fractions. Furthermore, both sub-fractions contained compounds of the same or similar substance classes. In general, the compounds can be described as small and hydrophilic, with many of them having carboxylic acid groups. This observation is in agreement with what was expected from the early elution and fractionation at a neutral pH, as described above. There were

Discussion

amino acids, mono-, di-, and tricarboxylic acids, sugars, disaccharides, and secondary metabolites detected in both sub-fractions.

However, small differences can be observed. The smaller amino acids proline and valine were identified in sub-fraction I-2, whereas iso-/leucine and tyrosine were discovered in sub-fraction I-3. Also, very hydrophilic amino sugars, sugar alcohols and hexonic acids were exclusively found in sub-fraction I-2. While a nucleotide was detected in sub-fraction I-2, nucleosides were identified in sub-fraction I-3. Since RP-HPLC was used, these differences are chromatographically reasonable. Sub-fraction I-2 contains the more hydrophilic substances, while substances with slightly higher lipophily appear in sub-fraction I-3.

More peaks were present in the LC-MS/MS chromatograms of the two sub-fractions, but only assumptions about possible compounds could be made for the corresponding molecular masses. These included mainly structural derivatives of the substance classes named above, such as glycosylated amino acids in sub-fraction I-2, as well as dipeptides, alkylated variants, or sulfates in sub-fraction I-3. Remarkably, the analysis also led to the suggestion of iridoid glycosides contained in sub-fraction I-3. However, these structures could not be confirmed with certainty within the scope of this study. One of the limitations of the method is that it often fails to explain all detected peaks, as the size of spectral libraries is limited and does not contain data for every chemical substance [104,105].

Another reason may be the size of the substances. The more complex the molecule is, the more options there are for possible molecular formulae. For example, Kerber et al. (2004) calculated that there are 32 possible molecular formulae for a mass of only 146 Da, with each of them having over a thousand to millions of potential structural formulae. Just $C_8H_6N_2O$ alone yields over 109 million possible structures, while the current PubChem library search produces only 773 results, not to mention spectral data availability [106]. Although plant compounds may be more likely to be known and listed in databases, and modern mass spectrometry may be able to more accurately narrow down possible molecular formulae, identification still remains difficult for some substances, especially for complex molecules.

To the best of my knowledge, most of the substances identified here, have not previously been reported for EA 575[®] before. A possible reason for this might be that

these substances are not major compounds in the total extract, but are enriched in these smaller fractions. However, it is not surprising that amino acids or nucleic acid components were identified in the sub-fractions of EA 575[®], as these are found in all living organisms. Succinic acid, malic acid, fumaric acid, and citric acid are part of the citric acid cycle and can therefore also be expected to be found in a plant extract. The occurrence of shikimic acid, vanillin, and salicylic acid can be explained by the shikimate pathway and subsequent phenylpropanoid biosynthesis [107]. While these substances may not be relevant to the extract's activity, their identification validates the functionality of the method.

The detection of adenosine may be remarkable in the search for a substance responsible for the effect of EA 575[®] on A_{2B}AR. Although adenosine itself cannot be the candidate under consideration due to its agonistic mode of action, it is possible that there might be derivatives of adenosine that exhibit inhibitory properties. Cytokinins for example, natural derivatives of adenine, have been discovered in various plant species, with the most prevalent naturally occurring cytokinin being zeatin [108]. Zeatin riboside, the corresponding adenosine derivative, has also been identified in *Hedera helix* [109]. Furthermore, this substance has been shown to activate A_{2A}AR signalling [110,111]. *In silico* analysis revealed that kinetin, another cytokinin, exhibits binding affinity to A_{2A}AR [112,113]. However, to my knowledge, there have been no reports of naturally occurring cytokinins that inhibit A_{2B}AR signalling so far. A potential effect of adenosine derivatives possibly present in EA 575[®] that might explain the inhibition of A_{2B}AR signalling could therefore be the subject of future studies.

Substances identified in the two sub-fractions that have previously been described for EA 575[®] or *Hedera helix* comprised protocatechuic acid, caffeic acid, quinic acid, and the structural isomers of chlorogenic acid [13,100]. Remarkably, there have been reports of A_{2A}AR receptor activation by chlorogenic acid and the compatibility to the receptor's active site [66]. Chlorogenic acid and its isomers neochlorogenic acid and cryptochlorogenic acid could not be differentiated reliably with the LC-MS/MS method used. While there are already published mass spectrometry-based techniques for the specific distinction of chlorogenic acid isomers [114], the present study utilised the HPLC method described in 4.9 to investigate the abundance of the three structural isomers. This method was chosen for its suitability in characterising constituents of EA 575[®] and the availability of data for the fractions and the total extract.

Discussion

By comparison with the elution times and UV spectra of reference substances, it was found that only in sub-fraction I-3 a significant amount of neochlorogenic acid and very small amounts of chlorogenic or cryptochlorogenic acid were detectable. The latter were found mainly in the later eluting sub-fractions. Therefore, a possible effect of neochlorogenic acid and also chlorogenic acid on the $A_{2B}AR$ -mediated increase in cAMP was tested. Although not abundant in both bioactive sub-fractions, chlorogenic acid was included because the activity was described specifically for this isomer [66]. The concentrations were selected to match the levels in the tested concentrations of EA 575[®], as determined from their HPLC chromatograms. However, none of them elicited an effect, and they could not be attributed for the effect of EA 575[®]. Nevertheless, this outcome could be expected considering that the majority of these substances were found in sub-fractions that did not demonstrate an effect. Although the specific compounds that are responsible for the observed effect of EA 575[®] on $A_{2B}AR$ signalling could not be identified, the present work allows a further reduction of potential candidates.

Another part of the present work was the generation of a cell line that expresses HiBiT-tagged $A_{2B}AR$ at an endogenous expression level to conduct further studies on the receptor's behaviour. Traditionally, tags are applied to receptors using techniques such as transfections with genetically modified plasmids, leading to transient or stable overexpression of these tagged receptors. Overexpression of specific receptors can perturb the cellular equilibrium by resource overload, stoichiometric imbalance, promiscuous interactions, and pathway modulation [115]. This can result in artificial results that do not accurately reflect the natural behaviour of the receptor.

A method to overcome these disadvantages and display the natural biology of receptors is genome editing via CRISPR/Cas9-mediated HDR. This technique offers the possibility to precisely label receptors with tags while maintaining the endogenous promotion, and therefore, expression levels [116]. For this purpose, the site-specific cleaving abilities of CRISPR/Cas9 in combination with the native cellular DNA repair mechanism of homology-directed repair are utilised [117].

Schwinn and colleagues (2018 & 2020) successfully used the technique to integrate HiBiT into the genome as a reporter tag at multiple sites, including three that encode GPCRs [117,118]. Boursier et al. (2020) applied the method to endogenously label β -adrenergic receptors [119]. Furthermore, CRISPR/Cas9-mediated genome editing

was used by White et al. (2019) to fuse NanoLuc[®] luciferase to A_{2B}AR in HEK cells [120]. To the best of my knowledge, insertion of HiBiT into the genomic sequence coding for A_{2B}AR via CRISPR/Cas9-mediated homology-directed repair has not been previously shown.

While Schwinn et al. (2018 & 2020) attached HiBiT to the C-terminus of the receptors [117,118], this study aimed for an N-terminal integration, which was already demonstrated by Boursier and colleagues (2020) [119], for the ability to conduct internalisation measurements and single-particle tracking experiments. In contrast to the studies of White et al. (2019), A_{2B}AR was tagged only with HiBiT instead of the complete NanoLuc[®] luciferase [120]. The smaller 1.3 kDa tag was preferred over the whole 19.1 kDa enzyme, as it was considered easier to integrate via homology-directed repair, and should less likely influence the receptor's natural behaviour, although no functional impact of the complete NanoLuc[®] luciferase was found previously [120]. However, the complete NanoLuc[®] luciferase was shown to exhibit higher background luminescence, which is disadvantageous especially for low-abundance receptors such as A_{2B}AR [119]. Additionally, it was demonstrated that HiBiT did not influence the activity of β_2 -AR [119]. Therefore, HiBiT was inserted at the endogenous N-terminus of the ADORA2B sequence.

The genetic information coding for a short 13 amino acid spacer was integrated between the HiBiT and the ADORA2B sequence to increase the accessibility of the tag. For this purpose, small, polar, and uncharged amino acids such as glycine, serine, alanine, and threonine were chosen, providing a flexible linker between the receptor and the tag [121]. The use of this spacer proved advantageous in experiments with overexpressing cells in terms of luminescence intensity (data not shown). Boursier et al. (2020) also used a short 8 amino acid glycine-serine-spacer for their experiments with HiBiT at β -ARs [119].

Unlike plasmid transfections that usually involve resistance genes for selection of successfully modified cells, clonal isolation had to be achieved without antibiotics due to the lack of resistance. Although the possibility of a resistance knock-in via CRISPR/Cas9 has been shown before [122], this approach is not commonly used and was not conducted in this study in order to keep the genetic modifications to a minimum. Instead, pools of 10 cells were screened by PCR for successful modification to increase the hit probability. Out of this pre-selection, successfully genome-edited

Discussion

clones were isolated by limiting dilution and a single-cell clone was obtained. This procedure is similar to the limiting dilution or cell sorting via a flow cytometry method, and subsequent luminescence screening for genome-edited cells performed in other studies [117–119]. Due to very small luminescence signals of the obtained clones in this study, screening via this method was not successful, whereas the applied PCR screening proved to be a reliable technique to identify genome-edited clones.

PCR analyses and sequencing of the clone's genomic DNA revealed that in addition to the desired HiBiT-ADORA2B sequence, wild-type DNA was also present, indicating heterozygosity. The mRNA analysis discussed below showed the same. According to the supplier, DSMZ, the HEK cells used in this study have a near-triploid karyotype with 6 % polyploidy of 69 chromosomes. This aligns with other reports of a non-diploid karyotype in HEK cells [123]. Considering this, it seems difficult to obtain homozygous HEK cell clones, which was also stated by other authors [120,124]. However, White and colleagues (2019) obtained HEK cells with a functional genome-edited A_{2B}AR, which were also heterozygous for the insert [120].

In order to examine the expression of HiBiT-A_{2B}AR under endogenous promotion in the obtained cell line, mRNA analysis was carried out. It was demonstrated that RNA encoding HiBiT-tagged A_{2B}AR was present in the cell line. This indicates that the correctly modified HiBiT-ADORA2B gene is translated into mRNA, which in turn indicates its expression. While it has been shown that mRNA expression can predict signaling and functional response of some GPCRs, this correlation does not extend universally to all proteins, particularly low-abundance and membrane proteins [125,126]. Therefore, experiments at the protein level were conducted next.

To investigate the expression of the HiBiT-tagged A_{2B}AR on the cell surface, Nano-Glo[®] HiBiT Extracellular Detection System was employed. Very similar live-cell methods have been successfully used by other researchers to quantitate HiBiT-tagged receptors that were modified by CRISPR/Cas9-mediated HDR [117–119]. Compared to HEK wild-type cells, a significantly 2.43-fold increased luminescence signal was detected, but the absolute RLU values with a mean of 676 were very small. In relation to overexpressing cell lines, which demonstrated RLU values exceeding 1,000,000 in this assay, the observed luminescence was extraordinarily low. For example, the overexpressing HiBiT-β₂-AR cell line used by Bussmann et al. (2020) exhibited up to 4,000,000 RLU [14]. However, smaller luminescence signals could be expected since

the tagged receptors in this cell line are expressed under endogenous regulation, as opposed to the highly active CMV promoter used in these overexpressing cells.

A possible explanation for the relatively low extracellular luminescence of the obtained HEK CRISPR HiBiT-A_{2B}AR cell line could be that the genetic modification has caused a malfunction, preventing the receptors from being embedded in the cell membrane, resulting in their intracellular retention. To address this, Nano-Glo® HiBiT Lytic Detection System was used, with which all HiBiT-tagged receptors in the cell are detected. Other researchers have also employed this method to quantitate HiBiT-tagged receptors that underwent modification via CRISPR/Cas9-mediated HDR [117,118,122]. However, the very small increase in luminescence signal compared to HEK wild-type cells was even lower than that observed in the extracellular assays. This suggests that receptor membrane transportation is functioning properly and receptors are not trapped intracellular but are instead located on the cell surface. The lower signal and fold change in this assay may result from a lower signal-to-noise ratio caused by lysis of the cells. Schwinn and colleagues (2018) compared the lytic assay to a live-cell method similar to the extracellular assay used in the present study and found that the detection of HiBiT from lysates yielded lower luminescence [117].

Other researchers also observed very low RLU values for some HiBiT-tagged receptors under endogenous promotion. In the study by Schwinn et al. (2020), the tested HiBiT-tagged GPCRs yielded comparatively low luminescence, which was varying in different cell types [118]. In contrast, Boursier et al. (2020) demonstrated a relatively high luminescence by HiBiT-tagged β_2 -AR [119]. This suggests that the luminescence signal levels of these genetically modified receptors depend on the levels of their endogenous expression in the respective cell type.

The endogenous expression level of ADORA2B in HEK cells has previously been determined to be relatively low [85,127]. This aligns with the luminescence signal of a NanoLuc®-tagged A_{2B}AR in HEK cells being small compared to that of overexpressed, as well as other endogenously expressed GPCRs in the same cell line [120]. Still, the absolute RLU values of the receptor were higher than those exhibited by the cell line in the present study. However, RLU values are influenced by several factors, such as the luminescence reader used or the seeded cell count, which, in fact, was higher in the study by White and colleagues (2019) [120]. Another reason for the higher luminescence signal might be the use of the complete NanoLuc® luciferase, which

Discussion

could possibly be advantageous in combination with this receptor. It has been observed that CRISPR/Cas9-mediated genome editing can alter expression levels, resulting in increases, decreases, or no differences, depending on the gene and the tag [124,128]. Furthermore, it has been shown that the complete NanoLuc[®] luciferase tag exhibited slightly stronger luminescence than the HiBiT tag incubated with saturating LgBiT [117].

In order to facilitate a clearer understanding and comparison of the results obtained, an overexpressing HEK HiBiT-A_{2B}AR cell line was generated. The plasmid, under control of a CMV promoter, was designed to match the CRISPR/Cas9-modified HiBiT-ADORA2B gene. To compare the luminescence produced by this overexpressing cell line with that of the HEK CRISPR HiBiT-A_{2B}AR cells, it was tested analogously using Nano-Glo[®] HiBiT Extracellular Detection System.

The overexpressing cells elicited a significant 162-fold increase in luminescence signal compared to HEK wild-type cells. This luminescence increase was 66.5-fold higher than the 2.43-fold increase generated by the HEK CRISPR HiBiT-A_{2B}AR cells, indicating a 66.5-fold higher expression of HiBiT-tagged A_{2B}AR on the cell surface. In the study by White et al. (2019), HEK cells overexpressing NanoLuc-A_{2B}AR showed an ~100-fold higher luminescence signal than their genome-edited cells counterparts [120]. Another study demonstrated an ~60–75-fold higher expression of a NanoLuc[®]-tagged GPCR in an overexpressing system compared to the receptor genetically modified by CRISPR/Cas9-mediated HDR [124], which is comparable to the results of the present study.

The results of this study demonstrate a successful genetic modification of the ADORA2B gene in HEK cells by CRISPR/Cas9-mediated HDR. However, the small signal elicited by the generated cells is not suitable for the intended purposes. The dynamic range does not permit the measurement of internalisation, and the low luminescence does not enable the use in single-particle tracking experiments.

7 Conclusion and Outlook

The present study demonstrates the inhibitory effect of EA 575[®] on A_{2B}AR signalling, implying a potential reduction in adenosine-mediated inflammation and bronchoconstriction in chronic airway diseases. Thus, a novel mode of action was revealed that sheds light on the initial positive clinical outcomes associated with the extract in adjuvant asthma therapy [10].

Initially, the effect of EA 575[®] on the cellular reaction following A_{2B}AR stimulation was tested and an inhibition in dynamic mass redistribution was found. These findings were confirmed by the investigation of A_{2B}AR-mediated second messenger cAMP release and the recruitment of β -arrestin 2 to A_{2B}AR, which were also inhibited by EA 575[®]. Additionally, the data indicated an indirect mechanism of action.

Next, the inhibition of CRE activation and the subsequent IL-6 release by EA 575[®] was demonstrated. It was specified that this effect was mediated via the A_{2B}AR signalling pathway. Furthermore, the mechanism was shown to be NF κ B-independent, which distinguishes it from the previously published inhibition of NF κ B by EA 575[®]. This way, EA 575[®] inhibits the A_{2B}AR signalling cascade, leading to a decrease in IL-6 release (Figure 30). The results presented here provide a rationale for additional studies in animals or human subjects to prove further effects regarding chronic airway diseases such as asthma or COPD.

Future research could investigate the influence of EA 575[®] on additional signalling pathways associated with adenosine and chronic airway diseases, such as the hypoxic adenosine axis. Hypoxia promotes inflammation and tissue injury in chronic lung diseases [18]. Via hypoxia-inducible factors in the promoter regions, A_{2B}AR, as well as CD73 and CD39, are upregulated [30,129–131]. At the same time, ADA activity is downregulated [30,132]. This results in elevated adenosine levels, correlating with disease severity [133,134]. Interestingly, a CRE has been reported in the CD73 promoter region, with A_{2B}AR playing a predominant role in its activation [131,135,136].

Another potential research topic could be the examination of mast cells and histamine release. Bronchoconstriction in asthma and COPD is mediated via the activation of A_{2B}AR on mast cells, leading to their degranulation and subsequent histamine release,

as evidenced by elevated histamine levels in asthmatics [22,137]. The inhibition of A_{2B}AR signalling by EA 575[®] could also impact this pathway.

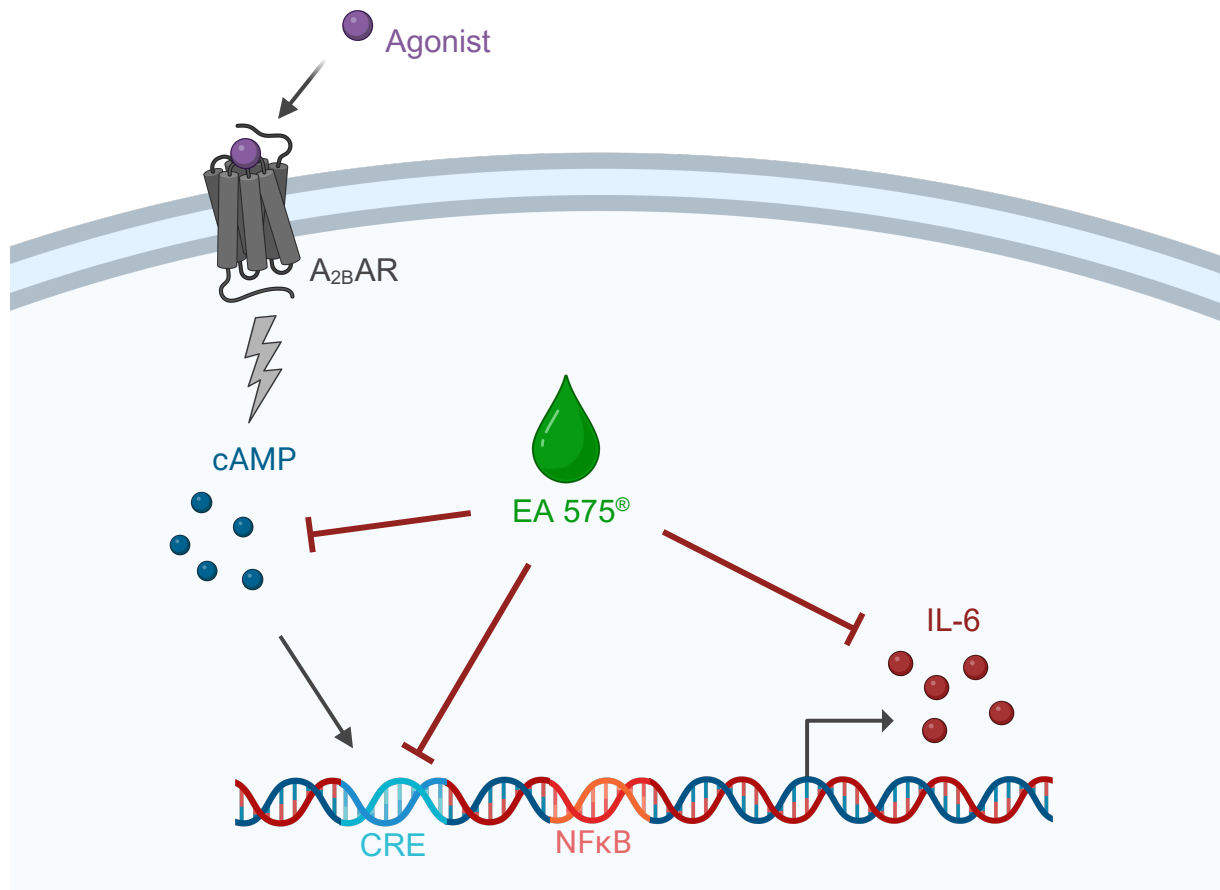


Figure 30: Schematic illustration of the proposed mode of action of EA 575[®] on A_{2B}AR signalling. Created with [BioRender.com](https://www.biorender.com).

This study also aimed to identify the constituents of EA 575[®] responsible for the newly discovered mechanism of action. Bioassay-guided fractionation resulted in two sub-fractions that elicited effects similar to the total extract. These sub-fractions were characterised by HPLC and LC-MS/MS to contain predominantly hydrophilic substances. Single substances accountable for the effect could not be identified. However, the analysis ruled out most of the major components of EA 575[®] as the sought-after constituents. Furthermore, the present study allows the reduction of potential candidates. The active compounds have to be contained in the two sub-fractions and are therefore likely hydrophilic. This provides a rationale for investigating an ivy leaf dry extract enriched in hydrophilic substances.

Future research could focus on identifying adenosine derivatives potentially present in EA 575[®], since adenosine has been identified in this study. Novel mass spectrometry-based approaches, such as molDiscovery, or other analytical technologies in combination with computational tools, could be valuable in this search [104,105].

Moreover, additional bioassay-guided fractionation of the obtained bioactive sub-fractions using other separation methods could be performed. Utilising HPLC columns with different selectivities, for example RP columns with a shorter chain length, phenyl columns, or cyano columns, might be a possibility to further narrow down the substances affecting A_{2B}AR signalling. In the best case, this could yield a fraction that contains the desired substances without many other ineffective compounds, facilitating clear identification.

Another part of this work was the generation of HEK cells expressing HiBiT-tagged A_{2B}AR at an endogenous expression level. CRISPR/Cas9-mediated HDR was used to introduce the genetic information encoding HiBiT into the genome of HEK cells. Analyses of genomic DNA and RNA revealed the correct insertion upstream of the ADORA2B gene, indicating the expression of HiBiT-tagged A_{2B}AR. This was confirmed at the protein level by a significant signal increase in a luminescence assay. In conclusion, the generation of a HEK cell line expressing HiBiT-tagged A_{2B}AR under endogenous promotion was successful, but the obtained signals were insufficient for the desired applications.

For a better comparison and understanding of these cells, a HEK cell line overexpressing HiBiT-A_{2B}AR was additionally generated. While not the focus of this study, and despite the previously mentioned disadvantages, this cell line could serve for future research. If the generation of a genome-edited cell line succeeds in the future, the properties of both could be compared to gain further insights into the differences between physiologic and overexpressing conditions.

Given the general success of genome editing via CRISPR/Cas9-mediated HDR, it can be employed to generate another cell line expressing HiBiT-tagged A_{2B}AR at an endogenous expression level. To this end, it should be considered using a cell line with higher endogenous expression of A_{2B}AR, for example the human mast cell line HMC-1 [127]. Then, internalisation measurements or single-particle tracking experiments could be conducted, as intended with the cells in this work.

8 References

1. Meurer, F.; Häberlein, H.; Franken, S. Ivy Leaf Dry Extract EA 575® Has an Inhibitory Effect on the Signalling Cascade of Adenosine Receptor A2B. *International Journal of Molecular Sciences* **2023**, *Vol. 24*, Page 12373 **2023**, *24* (15), 12373. <https://doi.org/10.3390/IJMS241512373>.
2. Kardos, P.; Dinh, Q. T.; Fuchs, K. H.; Gillissen, A.; Klimek, L.; Koehler, M.; Sitter, H.; Worth, H. [Guidelines of the German Respiratory Society for Diagnosis and Treatment of Adults Suffering from Acute, Subacute and Chronic Cough]. *Pneumologie* **2019**, *73* (3), 143–180. <https://doi.org/10.1055/A-0808-7409>.
3. Lang, C.; Röttger-Lüer, P.; Staiger, C. A Valuable Option for the Treatment of Respiratory Diseases: Review on the Clinical Evidence of the Ivy Leaves Dry Extract EA 575®. *Planta Med* **2015**, *81* (12–13), 968–974. <https://doi.org/10.1055/S-0035-1545879>.
4. Schaefer, A.; Ludwig, F.; Giannetti, B. M.; Bulitta, M.; Wacker, A. Efficacy of Two Dosing Schemes of a Liquid Containing Ivy Leaves Dry Extract EA 575 versus Placebo in the Treatment of Acute Bronchitis in Adults. *ERJ Open Res* **2019**, *5* (4). <https://doi.org/10.1183/23120541.00019-2019>.
5. Schaefer, A.; Kehr, M. S.; Giannetti, B. M.; Bulitta, M.; Staiger, C. A Randomized, Controlled, Double-Blind, Multi-Center Trial to Evaluate the Efficacy and Safety of a Liquid Containing Ivy Leaves Dry Extract (EA 575®) vs. Placebo in the Treatment of Adults with Acute Cough. *Pharmazie* **2016**, *71* (9), 504–509. <https://doi.org/10.1691/PH.2016.6712>.
6. Völp, A.; Schmitz, J.; Bulitta, M.; Raskopf, E.; Acikel, C.; Mösges, R. Ivy Leaves Extract EA 575 in the Treatment of Cough during Acute Respiratory Tract Infections: Meta-Analysis of Double-Blind, Randomized, Placebo-Controlled Trials. *Sci Rep* **2022**, *12* (1). <https://doi.org/10.1038/S41598-022-24393-1>.
7. Seifert, G.; Upstone, L.; Watling, C. P.; Vogelberg, C. Ivy Leaf Dry Extract EA 575 for the Treatment of Acute and Chronic Cough in Pediatric Patients: Review and Expert Survey. *Curr Med Res Opin* **2023**, *39* (10), 1407–1417. <https://doi.org/10.1080/03007995.2023.2258777>.
8. Global Initiative for Asthma. Global Strategy for Asthma Management and Prevention. **2023**.
9. Global Initiative For Chronic Obstructive Lung Disease. Global Strategy for the Diagnosis, Management, and Prevention of Chronic Obstructive Pulmonary Disease (2024 Report). **2023**.
10. Zeil, S.; Schwanebeck, U.; Vogelberg, C. Tolerance and Effect of an Add-on Treatment with a Cough Medicine Containing Ivy Leaves Dry Extract on Lung Function in Children with Bronchial Asthma. *Phytomedicine* **2014**, *21* (10), 1216–1220. <https://doi.org/10.1016/J.PHYMED.2014.05.006>.
11. Schulte-Michels, J.; Wolf, A.; Aatz, S.; Engelhard, K.; Sieben, A.; Martinez-Osuna, M.; Häberlein, F.; Häberlein, H. α -Hederin Inhibits G Protein-Coupled Receptor Kinase 2-Mediated Phosphorylation of B2-Adrenergic Receptors. *Phytomedicine* **2016**, *23* (1), 52–57. <https://doi.org/10.1016/j.phymed.2015.12.001>.
12. Meurer, F.; Schulte-Michels, J.; Häberlein, H.; Franken, S. Ivy Leaves Dry Extract EA 575® Mediates Biased B2-Adrenergic Receptor Signaling.

- Phytomedicine* **2021**, *90* (June), 1–6.
<https://doi.org/10.1016/j.phymed.2021.153645>.
13. Greunke, C.; Hage-Hülsmann, A.; Sorkalla, T.; Keksel, N.; Häberlein, F.; Häberlein, H. A Systematic Study on the Influence of the Main Ingredients of an Ivy Leaves Dry Extract on the B2-Adrenergic Responsiveness of Human Airway Smooth Muscle Cells. *Pulm Pharmacol Ther* **2015**, *31*, 92–98.
<https://doi.org/10.1016/j.pupt.2014.09.002>.
 14. Bussmann, H.; Schulte-Michels, J.; Bingel, M.; Meurer, F.; Aatz, S.; Häberlein, F.; Franken, S.; Häberlein, H. A Comparative Study on the Influence of an Ivy Preparation and an Ivy/Thyme Combination on the B2-Adrenergic Signal Transduction. *Heliyon* **2020**, *6* (5).
<https://doi.org/10.1016/j.heliyon.2020.e03960>.
 15. Sieben, A.; Prenner, L.; Sorkalla, T.; Wolf, A.; Jakobs, D.; Runkel, F.; Häberlein, H. α -Hederin, but Not Hederacoside c and Hederagenin from *Hedera Helix*, Affects the Binding Behavior, Dynamics, and Regulation of B2- Adrenergic Receptors. *Biochemistry* **2009**, *48* (15), 3477–3482.
<https://doi.org/10.1021/bi802036b>.
 16. Schulte-Michels, J.; Runkel, F.; Gokorsch, S.; Häberlein, H. Ivy Leaves Dry Extract EA 575® Decreases LPS-Induced IL-6 Release from Murine Macrophages. *Pharmazie* **2016**, *71* (3), 158–161.
<https://doi.org/10.1691/ph.2016.5835>.
 17. Schulte-Michels, J.; Keksel, C.; Häberlein, H.; Franken, S. Anti-Inflammatory Effects of Ivy Leaves Dry Extract: Influence on Transcriptional Activity of NF κ B. *Inflammopharmacology* **2019**, *27* (2), 339–347. <https://doi.org/10.1007/S10787-018-0494-9>.
 18. Li, X.; Berg, N. K.; Mills, T.; Zhang, K.; Eltzschig, H. K.; Yuan, X. Adenosine at the Interphase of Hypoxia and Inflammation in Lung Injury. *Front Immunol* **2021**, *11*. <https://doi.org/10.3389/FIMMU.2020.604944>.
 19. Le, T. T. T.; Berg, N. K.; Harting, M. T.; Li, X.; Eltzschig, H. K.; Yuan, X. Purinergic Signaling in Pulmonary Inflammation. *Front Immunol* **2019**, *10* (JULY). <https://doi.org/10.3389/FIMMU.2019.01633>.
 20. Zhou, Y.; Schneider, D. J.; Blackburn, M. R. Adenosine Signaling and the Regulation of Chronic Lung Disease. *Pharmacology and Therapeutics*. *Pharmacol Ther* July 2009, pp 105–116.
<https://doi.org/10.1016/j.pharmthera.2009.04.003>.
 21. Blackburn, M. R. Too Much of a Good Thing: Adenosine Overload in Adenosine-Deaminase-Deficient Mice. *Trends Pharmacol Sci* **2003**, *24* (2), 66–70. [https://doi.org/10.1016/S0165-6147\(02\)00045-7](https://doi.org/10.1016/S0165-6147(02)00045-7).
 22. Driver, A. G.; Kukoly, C. A.; Ali, S.; Mustafa, S. J. Adenosine in Bronchoalveolar Lavage Fluid in Asthma. *American Review of Respiratory Disease* **1993**, *148* (1), 91–97. <https://doi.org/10.1164/ajrccm/148.1.91>.
 23. Huszár, É.; Vass, G.; Vizi, É.; Csoma, Z.; Barát, E.; Molnár-Világos, G.; Herjavec, I.; Horváth, I. Adenosine in Exhaled Breath Condensate in Healthy Volunteers and in Patients with Asthma. *Eur Respir J* **2002**, *20* (6), 1393–1398.
<https://doi.org/10.1183/09031936.02.00005002>.
 24. Esther, C. R.; Boysen, G.; Olsen, B. M.; Collins, L. B.; Ghio, A. J.; Swenberg, J. W.; Boucher, R. C. Mass Spectrometric Analysis of Biomarkers and Dilution Markers in Exhaled Breath Condensate Reveals Elevated Purines in Asthma and Cystic Fibrosis. *Am J Physiol Lung Cell Mol Physiol* **2009**, *296* (6), L987.
<https://doi.org/10.1152/ajplung.90512.2008>.

References

25. Esther, C. R.; Lazaar, A. L.; Bordonali, E.; Qaqish, B.; Boucher, R. C. Elevated Airway Purines in COPD. *Chest* **2011**, *140* (4), 954–960. <https://doi.org/10.1378/chest.10-2471>.
26. Vizi, É.; Huszár, É.; Csoma, Z.; Böszörményi-Nagy, G.; Barát, E.; Horváth, I.; Herjavec, I.; Kollai, M. Plasma Adenosine Concentration Increases during Exercise: A Possible Contributing Factor in Exercise-Induced Bronchoconstriction in Asthma. *Journal of Allergy and Clinical Immunology* **2002**, *109* (3), 446–448. <https://doi.org/10.1067/mai.2002.121955>.
27. Cushley, M.; Tattersfield, A.; Holgate, S. Inhaled Adenosine and Guanosine on Airway Resistance in Normal and Asthmatic Subjects. *Br J Clin Pharmacol* **1983**, *15* (2), 161–165. <https://doi.org/10.1111/j.1365-2125.1983.tb01481.x>.
28. Mann, J. S.; Holgate, S. T.; Renwick, A. G.; Cushley, M. J. Airway Effects of Purine Nucleosides and Nucleotides and Release with Bronchial Provocation in Asthma. *J Appl Physiol (1985)* **1986**, *61* (5), 1667–1676. <https://doi.org/10.1152/JAPPL.1986.61.5.1667>.
29. Oosterhoff, Y.; De Jong, J. W.; Jansen, M. A. M.; Koeter, G. H.; Postma, D. S. Airway Responsiveness to Adenosine 5'-Monophosphate in Chronic Obstructive Pulmonary Disease Is Determined by Smoking. *American Review of Respiratory Disease* **1993**, *147* (3), 553–558. <https://doi.org/10.1164/ajrccm/147.3.553>.
30. Zhou, Y.; Murthy, J. N.; Zeng, D.; Belardinelli, L.; Blackburn, M. R. Alterations in Adenosine Metabolism and Signaling in Patients with Chronic Obstructive Pulmonary Disease and Idiopathic Pulmonary Fibrosis. *PLoS One* **2010**, *5* (2). <https://doi.org/10.1371/JOURNAL.PONE.0009224>.
31. Mertens, T. C. J.; Hanmandlu, A.; Tu, L.; Phan, C.; Collum, S. D.; Chen, N. Y.; Weng, T.; Davies, J.; Liu, C.; Eltzhig, H. K.; Jyothula, S. S. K.; Rajagopal, K.; Xia, Y.; Guha, A.; Bruckner, B. A.; Blackburn, M. R.; Guignabert, C.; Karmouty-Quintana, H. Switching-Off Adora2b in Vascular Smooth Muscle Cells Halts the Development of Pulmonary Hypertension. *Front Physiol* **2018**, *9* (JUN). <https://doi.org/10.3389/FPHYS.2018.00555>.
32. Karmouty-Quintana, H.; Weng, T.; Garcia-Morales, L. J.; Chen, N. Y.; Pedroza, M.; Zhong, H.; Molina, J. G.; Bunge, R.; Bruckner, B. A.; Xia, Y.; Johnston, R. A.; Loebe, M.; Zeng, D.; Seethamraju, H.; Belardinelli, L.; Blackburn, M. R. Adenosine A2B Receptor and Hyaluronan Modulate Pulmonary Hypertension Associated with Chronic Obstructive Pulmonary Disease. *Am J Respir Cell Mol Biol* **2013**, *49* (6), 1038–1047. <https://doi.org/10.1165/RCMB.2013-0089OC>.
33. Blackburn, M. R.; Datta, S. K.; Kellems, R. E. Adenosine Deaminase-Deficient Mice Generated Using a Two-Stage Genetic Engineering Strategy Exhibit a Combined Immunodeficiency. *J Biol Chem* **1998**, *273* (9), 5093–5100. <https://doi.org/10.1074/jbc.273.9.5093>.
34. Chunn, J. L.; Young, H. W. J.; Banerjee, S. K.; Colasurdo, G. N.; Blackburn, M. R. Adenosine-Dependent Airway Inflammation and Hyperresponsiveness in Partially Adenosine Deaminase-Deficient Mice. *J Immunol* **2001**, *167* (8), 4676–4685. <https://doi.org/10.4049/JIMMUNOL.167.8.4676>.
35. Blackburn, M. R.; Volmer, J. B.; Thrasher, J. L.; Zhong, H.; Crosby, J. R.; Lee, J. J.; Kellems, R. E. Metabolic Consequences of Adenosine Deaminase Deficiency in Mice Are Associated with Defects in Alveogenesis, Pulmonary Inflammation, and Airway Obstruction. *J Exp Med* **2000**, *192* (2), 159–170. <https://doi.org/10.1084/JEM.192.2.159>.

36. Chunn, J. L.; Molina, J. G.; Mi, T.; Xia, Y.; Kellems, R. E.; Blackburn, M. R. Adenosine-Dependent Pulmonary Fibrosis in Adenosine Deaminase-Deficient Mice. *J Immunol* **2005**, *175* (3), 1937–1946. <https://doi.org/10.4049/JIMMUNOL.175.3.1937>.
37. Sun, C.-X.; Zhong, H.; Mohsenin, A.; Morschl, E.; Chunn, J. L.; Molina, J. G.; Belardinelli, L.; Zeng, D.; Blackburn, M. R. Role of A2B Adenosine Receptor Signaling in Adenosine-Dependent Pulmonary Inflammation and Injury. *J Clin Invest* **2006**, *116* (8), 2173–2182. <https://doi.org/10.1172/JCI27303>.
38. Chunn, J. L.; Mohsenin, A.; Young, H. W. J.; Lee, C. G.; Elias, J. A.; Kellems, R. E.; Blackburn, M. R. Partially Adenosine Deaminase-Deficient Mice Develop Pulmonary Fibrosis in Association with Adenosine Elevations. *Am J Physiol Lung Cell Mol Physiol* **2006**, *290* (3). <https://doi.org/10.1152/AJPLUNG.00258.2005>.
39. Karmouty-Quintana, H.; Zhong, H.; Acero, L.; Weng, T.; Melicoff, E.; West, J. D.; Hemnes, A.; Grenz, A.; Eltzschig, H. K.; Blackwell, T. S.; Xia, Y.; Johnston, R. A.; Zeng, D.; Belardinelli, L.; Blackburn, M. R. The A 2B Adenosine Receptor Modulates Pulmonary Hypertension Associated with Interstitial Lung Disease . *The FASEB Journal* **2012**, *26* (6), 2546–2557. <https://doi.org/10.1096/FJ.11-200907>.
40. Rincon, M.; Irvin, C. G. Role of IL-6 in Asthma and Other Inflammatory Pulmonary Diseases. *Int J Biol Sci* **2012**, *8* (9), 1281–1290. <https://doi.org/10.7150/IJBS.4874>.
41. Marini, M.; Vittori, E.; Hollemborg, J.; Mattoli, S. Expression of the Potent Inflammatory Cytokines, Granulocyte-Macrophage-Colony-Stimulating Factor and Interleukin-6 and Interleukin-8, in Bronchial Epithelial Cells of Patients with Asthma. *J Allergy Clin Immunol* **1992**, *89* (5), 1001–1009. [https://doi.org/10.1016/0091-6749\(92\)90223-O](https://doi.org/10.1016/0091-6749(92)90223-O).
42. Mattoli, S.; Mattoso, V. L.; Soloperto, M.; Allegra, L.; Fasoli, A. Cellular and Biochemical Characteristics of Bronchoalveolar Lavage Fluid in Symptomatic Nonallergic Asthma. *J Allergy Clin Immunol* **1991**, *87* (4), 794–802. [https://doi.org/10.1016/0091-6749\(91\)90125-8](https://doi.org/10.1016/0091-6749(91)90125-8).
43. Neveu, W. A.; Allard, J. L.; Raymond, D. M.; Bourassa, L. M.; Burns, S. M.; Bunn, J. Y.; Irvin, C. G.; Kaminsky, D. A.; Rincon, M. Elevation of IL-6 in the Allergic Asthmatic Airway Is Independent of Inflammation but Associates with Loss of Central Airway Function. *Respir Res* **2010**, *11* (1). <https://doi.org/10.1186/1465-9921-11-28>.
44. Konno, S. I.; Gonokami, Y.; Kurokawa, M.; Kawazu, K.; Asano, K.; Okamoto, K. I.; Adachi, M. Cytokine Concentrations in Sputum of Asthmatic Patients. *Int Arch Allergy Immunol* **1996**, *109* (1), 73–78. <https://doi.org/10.1159/000237234>.
45. Broide, D. H.; Lotz, M.; Cuomo, A. J.; Coburn, D. A.; Federman, E. C.; Wasserman, S. I. Cytokines in Symptomatic Asthma Airways. *J Allergy Clin Immunol* **1992**, *89* (5), 958–967. [https://doi.org/10.1016/0091-6749\(92\)90218-Q](https://doi.org/10.1016/0091-6749(92)90218-Q).
46. Yokoyama, A.; Kohno, N.; Fujino, S.; Hamada, H.; Inoue, Y.; Fujioka, S.; Ishida, S.; Hiwada, K. Circulating Interleukin-6 Levels in Patients with Bronchial Asthma. *Am J Respir Crit Care Med* **1995**, *151* (5), 1354–1358. <https://doi.org/10.1164/AJRCCM.151.5.7735584>.
47. Tillie-Leblond, I.; Pugin, J.; Marquette, C. H.; Lamblin, C.; Saulnier, F.; Brichet, A.; Wallaert, B.; Tonnel, A. B.; Gosset, P. Balance between Proinflammatory Cytokines and Their Inhibitors in Bronchial Lavage from Patients with Status

References

- Asthmaticus. *Am J Respir Crit Care Med* **1999**, *159* (2), 487–494.
<https://doi.org/10.1164/AJRCCM.159.2.9805115>.
48. Dixon, A. E.; Raymond, D. M.; Suratt, B. T.; Bourassa, L. M.; Irvin, C. G. Lower Airway Disease in Asthmatics with and without Rhinitis. *Lung* **2008**, *186* (6), 361–368. <https://doi.org/10.1007/S00408-008-9119-1>.
49. Morjaria, J. B.; Babu, K. S.; Vijayanand, P.; Chauhan, A. J.; Davies, D. E.; Holgate, S. T. Sputum IL-6 Concentrations in Severe Asthma and Its Relationship with FEV1. *Thorax* **2011**, *66* (6), 537.
<https://doi.org/10.1136/THX.2010.136523>.
50. Attaran, D.; Lari, S. M.; Towhidi, M.; Marallu, H. G.; Ayatollahi, H.; Khajehdaluae, M.; Ghanei, M.; Basiri, R. Interleukin-6 and Airflow Limitation in Chemical Warfare Patients with Chronic Obstructive Pulmonary Disease. *Int J Chron Obstruct Pulmon Dis* **2010**, *5*, 335–340.
<https://doi.org/10.2147/COPD.S12545>.
51. Eickmeier, O.; Huebner, M.; Herrmann, E.; Zissler, U.; Rosewich, M.; Baer, P. C.; Buhl, R.; Schmitt-Grohé, S.; Zielen, S.; Schubert, R. Sputum Biomarker Profiles in Cystic Fibrosis (CF) and Chronic Obstructive Pulmonary Disease (COPD) and Association between Pulmonary Function. *Cytokine* **2010**, *50* (2), 152–157. <https://doi.org/10.1016/J.CYTO.2010.02.004>.
52. Donaldson, G. C.; Seemungal, T. A. R.; Patel, I. S.; Bhowmik, A.; Wilkinon, T. M. A.; Hurst, J. R.; MacCallum, P. K.; Wedzicha, J. A. Airway and Systemic Inflammation and Decline in Lung Function in Patients with COPD. *Chest* **2005**, *128* (4), 1995–2004. <https://doi.org/10.1378/CHEST.128.4.1995>.
53. Hacievliyagil, S. S.; Gunen, H.; Mutlu, L. C.; Karabulut, A. B.; Temel, I. Association between Cytokines in Induced Sputum and Severity of Chronic Obstructive Pulmonary Disease. *Respir Med* **2006**, *100* (5), 846–854.
<https://doi.org/10.1016/J.RMED.2005.08.022>.
54. Celli, B. R.; Locantore, N.; Yates, J.; Tal-Singer, R.; Miller, B. E.; Bakke, P.; Calverley, P.; Coxson, H.; Crim, C.; Edwards, L. D.; Lomas, D. A.; Duvoix, A.; MacNee, W.; Rennard, S.; Silverman, E.; Vestbo, J.; Wouters, E.; Agustí, A. Inflammatory Biomarkers Improve Clinical Prediction of Mortality in Chronic Obstructive Pulmonary Disease. *Am J Respir Crit Care Med* **2012**, *185* (10), 1065–1072. <https://doi.org/10.1164/RCCM.201110-1792OC>.
55. Saito, F.; Tasaka, S.; Inoue, K. I.; Miyamoto, K.; Nakano, Y.; Ogawa, Y.; Yamada, W.; Shiraishi, Y.; Hasegawa, N.; Fujishima, S.; Takano, H.; Ishizaka, A. Role of Interleukin-6 in Bleomycin-Induced Lung Inflammatory Changes in Mice. *Am J Respir Cell Mol Biol* **2008**, *38* (5), 566–571.
<https://doi.org/10.1165/RCMB.2007-0299OC>.
56. Pedroza, M.; Schneider, D. J.; Karmouty-Quintana, H.; Coote, J.; Shaw, S.; Corrigan, R.; Molina, J. G.; Alcorn, J. L.; Galas, D.; Gelinas, R.; Blackburn, M. R. Interleukin-6 Contributes to Inflammation and Remodeling in a Model of Adenosine Mediated Lung Injury. *PLoS One* **2011**, *6* (7).
<https://doi.org/10.1371/JOURNAL.PONE.0022667>.
57. Ryzhov, S.; Zaynagetdinov, R.; Goldstein, A. E.; Novitskiy, S. V.; Blackburn, M. R.; Biaggioni, I.; Feoktistov, I. Effect of A2B Adenosine Receptor Gene Ablation on Adenosine-Dependent Regulation of Proinflammatory Cytokines. *J Pharmacol Exp Ther* **2008**, *324* (2), 694–700.
<https://doi.org/10.1124/JPET.107.131540>.
58. Philip, K.; Mills, T. W.; Davies, J.; Chen, N. Y.; Karmouty-Quintana, H.; Luo, F.; Molina, J. G.; Amione-Guerra, J.; Sinha, N.; Guha, A.; Eltzschig, H. K.;

- Blackburn, M. R. HIF1A Up-Regulates the ADORA2B Receptor on Alternatively Activated Macrophages and Contributes to Pulmonary Fibrosis. *FASEB J* **2017**, *31* (11), 4745–4758. <https://doi.org/10.1096/FJ.201700219R>.
59. Karmouty-Quintana, H.; Philip, K.; Acero, L. F.; Chen, N. Y.; Weng, T.; Molina, J. G.; Luo, F.; Davies, J.; Le, N. B.; Bunge, I.; Volcik, K. A.; Le, T. T. T.; Johnston, R. A.; Xia, Y.; Eltzschig, H. K.; Blackburn, M. R. Deletion of ADORA2B from Myeloid Cells Dampens Lung Fibrosis and Pulmonary Hypertension. *FASEB J* **2015**, *29* (1), 50–60. <https://doi.org/10.1096/FJ.14-260182>.
60. Charette, S. J.; Cosson, P. Preparation of Genomic DNA from Dictyostelium Discoideum for PCR Analysis. *Biotechniques* **2004**, *36* (4), 574–575. <https://doi.org/10.2144/04364BM01>.
61. Uphoff, C. C.; Drexler, H. G. Detecting Mycoplasma Contamination in Cell Cultures by Polymerase Chain Reaction. *Methods Mol Biol* **2011**, *731*, 93–103. https://doi.org/10.1007/978-1-61779-080-5_8.
62. Uphoff, C. C.; Drexler, H. G. Comparative PCR Analysis for Detection of Mycoplasma Infections in Continuous Cell Lines. *In Vitro Cell Dev Biol Anim* **2002**, *38*, 79–85. <https://doi.org/10.00+0.00>.
63. Saecker, L.; Häberlein, H.; Franken, S. Investigation of Adenosine A1 Receptor-Mediated β -Arrestin 2 Recruitment Using a Split-Luciferase Assay. *Front Pharmacol* **2023**, *14*. <https://doi.org/10.3389/FPHAR.2023.1172551>.
64. Watson, M. J.; Worthington, E. N.; Clunes, L. A.; Rasmussen, J. E.; Jones, L.; Tarran, R. Defective Adenosine-Stimulated cAMP Production in Cystic Fibrosis Airway Epithelia: A Novel Role for CFTR in Cell Signaling. *FASEB J* **2011**, *25* (9), 2996–3003. <https://doi.org/10.1096/FJ.11-186080>.
65. Schröder, R.; Janssen, N.; Schmidt, J.; Kebig, A.; Merten, N.; Hennen, S.; Müller, A.; Blättermann, S.; Mohr-Andrä, M.; Zahn, S.; Wenzel, J.; Smith, N. J.; Gomeza, J.; Drewke, C.; Milligan, G.; Mohr, K.; Kostenis, E. Deconvolution of Complex G Protein–Coupled Receptor Signaling in Live Cells Using Dynamic Mass Redistribution Measurements. *Nature Biotechnology* **2010**, *28*:9 **2010**, *28* (9), 943–949. <https://doi.org/10.1038/nbt.1671>.
66. Fuentes, E.; Caballero, J.; Alarcón, M.; Rojas, A.; Palomo, I. Chlorogenic Acid Inhibits Human Platelet Activation and Thrombus Formation. *PLoS One* **2014**, *9* (3), 1–13. <https://doi.org/10.1371/journal.pone.0090699>.
67. Goulding, J.; May, L. T.; Hill, S. J. Characterisation of Endogenous A2A and A2B Receptor-Mediated Cyclic AMP Responses in HEK 293 Cells Using the GloSensor™ Biosensor: Evidence for an Allosteric Mechanism of Action for the A2B-Selective Antagonist PSB 603. *Biochem Pharmacol* **2018**, *147*, 55–66. <https://doi.org/10.1016/J.BCP.2017.10.013>.
68. Barresi, E.; Martini, C.; Da Settimo, F.; Greco, G.; Taliani, S.; Giacomelli, C.; Trincavelli, M. L. Allosterism vs. Orthosterism: Recent Findings and Future Perspectives on A2B AR Physio-Pathological Implications. *Front Pharmacol* **2021**, *12*. <https://doi.org/10.3389/FPHAR.2021.652121>.
69. Montminy, M. R.; Bilezikjian, L. M. Binding of a Nuclear Protein to the Cyclic-AMP Response Element of the Somatostatin Gene. *Nature* **1987**, *328* (6126), 175–178. <https://doi.org/10.1038/328175A0>.
70. Montminy, M. R.; Sevarino, K. A.; Wagner, J. A.; Mandel, G.; Goodman, R. H. Identification of a Cyclic-AMP-Responsive Element within the Rat Somatostatin Gene. *Proc Natl Acad Sci U S A* **1986**, *83* (18), 6682–6686. <https://doi.org/10.1073/PNAS.83.18.6682>.

References

71. Yamamoto, K. K.; Gonzalez, G. A.; Biggs, W. H.; Montminy, M. R. Phosphorylation-Induced Binding and Transcriptional Efficacy of Nuclear Factor CREB. *Nature* **1988**, *334* (6182), 494–498. <https://doi.org/10.1038/334494A0>.
72. Sun, Y.; Wu, F.; Sun, F.; Huang, P. Adenosine Promotes IL-6 Release in Airway Epithelia. *The Journal of Immunology* **2008**, *180* (6), 4173–4181. <https://doi.org/10.4049/jimmunol.180.6.4173>.
73. Du, X.; Ou, X.; Song, T.; Zhang, W.; Cong, F.; Zhang, S.; Xiong, Y. Adenosine A2B Receptor Stimulates Angiogenesis by Inducing VEGF and ENOS in Human Microvascular Endothelial Cells. *Exp Biol Med (Maywood)* **2015**, *240* (11), 1472–1479. <https://doi.org/10.1177/1535370215584939>.
74. Ray, A.; LaForge, K. S.; Sehgal, P. B. On the Mechanism for Efficient Repression of the Interleukin-6 Promoter by Glucocorticoids: Enhancer, TATA Box, and RNA Start Site (Inr Motif) Occlusion. *Mol Cell Biol* **1990**, *10* (11), 5736–5746. <https://doi.org/10.1128/mcb.10.11.5736-5746.1990>.
75. Ray, A.; Sassone-Corsi, P.; Sehgal, P. B. A Multiple Cytokine- and Second Messenger-Responsive Element in the Enhancer of the Human Interleukin-6 Gene: Similarities with c-Fos Gene Regulation. *Mol Cell Biol* **1989**, *9* (12), 5537–5547. <https://doi.org/10.1128/mcb.9.12.5537-5547.1989>.
76. Ray, A.; Tatter, S. B.; May, L. T.; Sehgal, P. B. Activation of the Human “Beta 2-Interferon/Hepatocyte-Stimulating Factor/Interleukin 6” Promoter by Cytokines, Viruses, and Second Messenger Agonists. *Proceedings of the National Academy of Sciences* **1988**, *85* (18), 6701–6705. <https://doi.org/10.1073/PNAS.85.18.6701>.
77. Krueger, J.; Ray, A.; Tamm, I.; Sehgal, P. B. Expression and Function of Interleukin-6 in Epithelial Cells. *J Cell Biochem* **1991**, *45* (4), 327–334. <https://doi.org/10.1002/jcb.240450404>.
78. Zhang, Y.; Lin, J. X.; Vilcek, J. Synthesis of Interleukin 6 (Interferon-B2/B Cell Stimulatory Factor 2) in Human Fibroblasts Is Triggered by an Increase in Intracellular Cyclic AMP. *Journal of Biological Chemistry* **1988**, *263* (13), 6177–6182. [https://doi.org/10.1016/s0021-9258\(18\)68768-x](https://doi.org/10.1016/s0021-9258(18)68768-x).
79. Zhong, H.; Belardinelli, L.; Maa, T.; Feoktistov, I.; Biaggioni, I.; Zeng, D. A2B Adenosine Receptors Increase Cytokine Release by Bronchial Smooth Muscle Cells. *Am J Respir Cell Mol Biol* **2004**, *30* (1), 118–125. <https://doi.org/10.1165/rcmb.2003-0118OC>.
80. Sitaraman, S. V.; Merlin, D.; Wang, L.; Wong, M.; Gewirtz, A. T.; Si-Tahar, M.; Madara, J. L. Neutrophil-Epithelial Crosstalk at the Intestinal Luminal Surface Mediated by Reciprocal Secretion of Adenosine and IL-6. *J Clin Invest* **2001**, *107* (7), 861–869. <https://doi.org/10.1172/JCI11783>.
81. Libermann, T. A.; Baltimore, D. Activation of Interleukin-6 Gene Expression through the NF-Kappa B Transcription Factor. *Mol Cell Biol* **1990**, *10* (5), 2327–2334. <https://doi.org/10.1128/mcb.10.5.2327-2334.1990>.
82. Shimizu, H.; Mitomo, K.; Watanabe, T.; Okamoto, S.; Yamamoto, K. Involvement of a NF-Kappa B-like Transcription Factor in the Activation of the Interleukin-6 Gene by Inflammatory Lymphokines. *Mol Cell Biol* **1990**, *10* (2), 561–568. <https://doi.org/10.1128/mcb.10.2.561-568.1990>.
83. Cobb, B. R.; Ruiz, F.; King, C. M.; Fortenberry, J.; Greer, H.; Kovacs, T.; Sorscher, E. J.; Clancy, J. P. A2 Adenosine Receptors Regulate CFTR through PKA and PLA2. *Am J Physiol Lung Cell Mol Physiol* **2002**, *282* (1 26-1), 12–25. <https://doi.org/10.1152/ajplung.2002.282.1.12>.

84. Szkotak, A. J.; Ng, A. M. L.; Man, S. F. P.; Baldwin, S. A.; Cass, C. E.; Young, J. D.; Duszyk, M. Coupling of CFTR-Mediated Anion Secretion to Nucleoside Transporters and Adenosine Homeostasis in Calu-3 Cells. *Journal of Membrane Biology* **2003**, *192* (3), 169–179. <https://doi.org/10.1007/s00232-002-1073-x>.
85. Atwood, B. K.; Lopez, J.; Wager-Miller, J.; Mackie, K.; Straiker, A. Expression of G Protein-Coupled Receptors and Related Proteins in HEK293, AtT20, BV2, and N18 Cell Lines as Revealed by Microarray Analysis. *BMC Genomics* **2011**, *12*. <https://doi.org/10.1186/1471-2164-12-14>.
86. Zhong, H.; Belardinelli, L.; Maa, T.; Zeng, D. Synergy between A2B Adenosine Receptors and Hypoxia in Activating Human Lung Fibroblasts. *Am J Respir Cell Mol Biol* **2005**, *32* (1), 2–8. <https://doi.org/10.1165/RCMB.2004-0103OC>.
87. Fredholm, B. B.; IJzerman, A. P.; Jacobson, K. A.; Linden, J.; Müller, C. E. International Union of Basic and Clinical Pharmacology. LXXXI. Nomenclature and Classification of Adenosine Receptors—an Update. *Pharmacol Rev* **2011**, *63* (1), 1–34. <https://doi.org/10.1124/PR.110.003285>.
88. Geraghty, N. J.; Adhikary, S. R.; Watson, D.; Sluyter, R. The A2A Receptor Agonist CGS 21680 Has Beneficial and Adverse Effects on Disease Development in a Humanised Mouse Model of Graft-versus-Host Disease. *Int Immunopharmacol* **2019**, *72*, 479–486. <https://doi.org/10.1016/J.INTIMP.2019.04.037>.
89. Pei, H.; Linden, J. Adenosine Influences Myeloid Cells to Inhibit Aeroallergen Sensitization. *Am J Physiol Lung Cell Mol Physiol* **2016**, *310* (10), L985–L992. <https://doi.org/10.1152/AJPLUNG.00330.2015>.
90. Zheng, X.; Wang, D. The Adenosine A2A Receptor Agonist Accelerates Bone Healing and Adjusts Treg/Th17 Cell Balance through Interleukin 6. *Biomed Res Int* **2020**, *2020*. <https://doi.org/10.1155/2020/2603873>.
91. Tang, L. M.; Wang, Y. P.; Wang, K.; Pu, L. Y.; Zhang, F.; Li, X. C.; Kong, L. B.; Sun, B. C.; Li, G. Q.; Wang, X. H. Protective Effect of Adenosine A2A Receptor Activation in Small-for-Size Liver Transplantation. *Transpl Int* **2007**, *20* (1), 93–101. <https://doi.org/10.1111/J.1432-2277.2006.00394.X>.
92. Rogachev, B.; Ziv, N. Y.; Mazar, J.; Nakav, S.; Chaimovitz, C.; Zlotnik, M.; Douvdevani, A. Adenosine Is Upregulated during Peritonitis and Is Involved in Downregulation of Inflammation. *Kidney Int* **2006**, *70* (4), 675–681. <https://doi.org/10.1038/SJ.KI.5001609>.
93. Zhang, L.; Franchini, M.; Wehrli Eser, M.; Dip, R. Enhanced IL-6 Transcriptional Response to Adenosine Receptor Ligands in Horses with Lower Airway Inflammation. *Equine Vet J* **2012**, *44* (1), 81–87. <https://doi.org/10.1111/J.2042-3306.2010.00350.X>.
94. Schwaninger, M.; Neher, M.; Viegas, E.; Schneider, A.; Spranger, M. Stimulation of Interleukin-6 Secretion and Gene Transcription in Primary Astrocytes by Adenosine. *J Neurochem* **1997**, *69* (3), 1145–1150. <https://doi.org/10.1046/J.1471-4159.1997.69031145.X>.
95. McColl, S. R.; St-Onge, M.; Dussault, A.-A.; Laflamme, C.; Bouchard, L.; Boulanger, J.; Pouliot, M. Immunomodulatory Impact of the A2A Adenosine Receptor on the Profile of Chemokines Produced by Neutrophils. *FASEB J* **2006**, *20* (1), 187. <https://doi.org/10.1096/FJ.05-4804FJE>.
96. Mohsenin, A.; Mi, T.; Xia, Y.; Kellems, R. E.; Chen, J. F.; Blackburn, M. R. Genetic Removal of the A2A Adenosine Receptor Enhances Pulmonary Inflammation, Mucin Production, and Angiogenesis in Adenosine Deaminase-

References

- Deficient Mice. *Am J Physiol Lung Cell Mol Physiol* **2007**, 293 (3).
<https://doi.org/10.1152/AJPLUNG.00187.2007>.
97. Pejman, L.; Omrani, H.; Mirzamohammadi, Z.; Shahbazfar, A. A.; Khalili, M.; Keyhanmanesh, R. The Effect of Adenosine A2A and A2B Antagonists on Tracheal Responsiveness, Serum Levels of Cytokines and Lung Inflammation in Guinea Pig Model of Asthma. *Adv Pharm Bull* **2014**, 4 (2), 131–138.
<https://doi.org/10.5681/apb.2014.020>.
98. Mustafa, S. J.; Nadeem, A.; Fan, M.; Zhong, H.; Belardinelli, L.; Zeng, D. Effect of a Specific and Selective A2B Adenosine Receptor Antagonist on Adenosine Agonist AMP and Allergen-Induced Airway Responsiveness and Cellular Influx in a Mouse Model of Asthma. *Journal of Pharmacology and Experimental Therapeutics* **2007**, 320 (3), 1246–1251.
<https://doi.org/10.1124/jpet.106.112250>.
99. Shokry, A. A.; El-Shiekh, R. A.; Kamel, G.; Bakr, A. F.; Ramadan, A. Bioactive Phenolics Fraction of Hedera Helix L. (Common Ivy Leaf) Standardized Extract Ameliorates LPS-Induced Acute Lung Injury in the Mouse Model through the Inhibition of Proinflammatory Cytokines and Oxidative Stress. *Heliyon* **2022**, 8 (5). <https://doi.org/10.1016/J.HELIYON.2022.E09477>.
100. Shokry, A. A.; El-Shiekh, R. A.; Kamel, G.; Bakr, A. F.; Sabry, D.; Ramadan, A. Anti-Arthritic Activity of the Flavonoids Fraction of Ivy Leaves (Hedera Helix L.) Standardized Extract in Adjuvant Induced Arthritis Model in Rats in Relation to Its Metabolite Profile Using LC/MS. *Biomedicine & Pharmacotherapy* **2022**, 145. <https://doi.org/10.1016/J.BIOPHA.2021.112456>.
101. Malviya, N.; Malviya, S. Bioassay Guided Fractionation-an Emerging Technique Influence the Isolation, Identification and Characterization of Lead Phytomolecules. *International Journal of Hospital Pharmacy* **2017**.
<https://doi.org/10.28933/ijhp-2017-07-0901>.
102. Mani, J.; Johnson, J.; Hosking, H.; Hoyos, B. E.; Walsh, K. B.; Neilsen, P.; Naiker, M. Bioassay Guided Fractionation Protocol for Determining Novel Active Compounds in Selected Australian Flora. *Plants (Basel)* **2022**, 11 (21).
<https://doi.org/10.3390/PLANTS11212886>.
103. Salac, E. L. O.; Alvarez, M. R.; Gaurana, R. S.; Grijaldo, S. J. B.; Serrano, L. M.; Juan, F. de; Abogado, R.; Padolina, I.; Deniega, F. M.; Delica, K.; Fernandez, K.; Lebrilla, C. B.; Manalo, M. N.; Heralde, F. M.; Completo, G. C. J.; Nacario, R. C. Biological Assay-Guided Fractionation and Mass Spectrometry-Based Metabolite Profiling of Annona Muricata L. Cytotoxic Compounds against Lung Cancer A549 Cell Line. *Plants (Basel)* **2022**, 11 (18).
<https://doi.org/10.3390/PLANTS11182380>.
104. Gaudêncio, S. P.; Pereira, F. Dereplication: Racing to Speed up the Natural Products Discovery Process. *Nat Prod Rep* **2015**, 32 (6), 779–810.
<https://doi.org/10.1039/C4NP00134F>.
105. Cao, L.; Guler, M.; Tagirdzhanov, A.; Lee, Y. Y.; Gurevich, A.; Mohimani, H. MolDiscovery: Learning Mass Spectrometry Fragmentation of Small Molecules. *Nat Commun* **2021**, 12 (1). <https://doi.org/10.1038/S41467-021-23986-0>.
106. Kerber, A.; Laue, R.; Meringer, M.; Ucker, C. R. ". Molecules in Silico: The Generation of Structural Formulae and Its Applications. *Journal of Computer Chemistry, Japan* **2004**, 3 (3), 85–96. <https://doi.org/10.2477/JCCJ.3.85>.
107. Vogt, T. Phenylpropanoid Biosynthesis. *Mol Plant* **2010**, 3 (1), 2–20.
<https://doi.org/10.1093/MP/SSP106>.

108. Mok, D. W. S.; Mok, M. C. CYTOKININ METABOLISM AND ACTION. *Annu Rev Plant Physiol Plant Mol Biol* **2001**, *52*, 89–118. <https://doi.org/10.1146/ANNUREV.ARPLANT.52.1.89>.
109. López-Carbonell, M.; Moret, A.; Nadal, M. Changes in Cell Ultrastructure and Zeatin Riboside Concentrations in *Hedera Helix*, *Pelargonium Zonale*, *Prunus Avium*, and *Rubus Ulmifolius* Leaves Infected by Fungi. *Plant Dis* **1998**, *82* (8), 914–918. <https://doi.org/10.1094/PDIS.1998.82.8.914>.
110. Lee, Y. C.; Yang, Y. C.; Huang, C. L.; Kuo, T. Y.; Lin, J. H.; Yang, D. M.; Huang, N. K. When Cytokinin, a Plant Hormone, Meets the Adenosine A_{2A} Receptor: A Novel Neuroprotectant and Lead for Treating Neurodegenerative Disorders? *PLoS One* **2012**, *7* (6). <https://doi.org/10.1371/JOURNAL.PONE.0038865>.
111. Lappas, C. M. The Plant Hormone Zeatin Riboside Inhibits T Lymphocyte Activity via Adenosine A_{2A} Receptor Activation. *Cell Mol Immunol* **2015**, *12* (1), 107–112. <https://doi.org/10.1038/CMI.2014.33>.
112. Naseem, M.; Othman, E. M.; Fathy, M.; Iqbal, J.; Howari, F. M.; AlRemeithi, F. A.; Kodandaraman, G.; Stopper, H.; Bencurova, E.; Vlachakis, D.; Dandekar, T. Integrated Structural and Functional Analysis of the Protective Effects of Kinetin against Oxidative Stress in Mammalian Cellular Systems. *Sci Rep* **2020**, *10* (1). <https://doi.org/10.1038/S41598-020-70253-1>.
113. Othman, E. M.; Fathy, M.; Bekhit, A. A.; Abdel-Razik, A. R. H.; Jamal, A.; Nazzal, Y.; Shams, S.; Dandekar, T.; Naseem, M. Modulatory and Toxicological Perspectives on the Effects of the Small Molecule Kinetin. *Molecules* **2021**, *26* (3). <https://doi.org/10.3390/MOLECULES26030670>.
114. Ramabulana, A. T.; Steenkamp, P.; Madala, N.; Dubery, I. A. Profiling of Chlorogenic Acids from *Bidens Pilosa* and Differentiation of Closely Related Positional Isomers with the Aid of UHPLC-QTOF-MS/MS-Based In-Source Collision-Induced Dissociation. *Metabolites* **2020**, *10* (5). <https://doi.org/10.3390/METABO10050178>.
115. Moriya, H. Quantitative Nature of Overexpression Experiments. *Mol Biol Cell* **2015**, *26* (22), 3932–3939. <https://doi.org/10.1091/MBE.E15-07-0512>.
116. Soave, M.; Stoddart, L. A.; White, C. W.; Kilpatrick, L. E.; Goulding, J.; Briddon, S. J.; Hill, S. J. Detection of Genome-Edited and Endogenously Expressed G Protein-Coupled Receptors. *FEBS J* **2021**, *288* (8), 2585–2601. <https://doi.org/10.1111/FEBS.15729>.
117. Schwinn, M. K.; Machleidt, T.; Zimmerman, K.; Eggers, C. T.; Dixon, A. S.; Hurst, R.; Hall, M. P.; Encell, L. P.; Binkowski, B. F.; Wood, K. V. CRISPR-Mediated Tagging of Endogenous Proteins with a Luminescent Peptide. *ACS Chem Biol* **2018**, *13* (2), 467–474. <https://doi.org/10.1021/acschembio.7b00549>.
118. Schwinn, M. K.; Steffen, L. S.; Zimmerman, K.; Wood, K. V.; Machleidt, T. A Simple and Scalable Strategy for Analysis of Endogenous Protein Dynamics. *Sci Rep* **2020**, *10* (1), 1–14. <https://doi.org/10.1038/s41598-020-65832-1>.
119. Boursier, M. E.; Levin, S.; Zimmerman, K.; Machleidt, T.; Hurst, R.; Butler, B. L.; Eggers, C. T.; Kirkland, T. A.; Wood, K. V.; Ohana, R. F. The Luminescent HiBiT Peptide Enables Selective Quantitation of G Protein-Coupled Receptor Ligand Engagement and Internalization in Living Cells. *J Biol Chem* **2020**, *295* (15), 5124–5135. <https://doi.org/10.1074/JBC.RA119.011952>.
120. White, C. W.; Johnstone, E. K. M.; See, H. B.; Pflieger, K. D. G. NanoBRET Ligand Binding at a GPCR under Endogenous Promotion Facilitated by

References

- CRISPR/Cas9 Genome Editing. *Cell Signal* **2019**, *54*, 27–34. <https://doi.org/10.1016/j.cellsig.2018.11.018>.
121. Chen, X.; Zaro, J. L.; Shen, W. C. Fusion Protein Linkers: Property, Design and Functionality. *Adv Drug Deliv Rev* **2013**, *65* (10), 1357–1369. <https://doi.org/10.1016/J.ADDR.2012.09.039>.
 122. Oh-hashii, K.; Furuta, E.; Fujimura, K.; Hirata, Y. Application of a Novel HiBiT Peptide Tag for Monitoring ATF4 Protein Expression in Neuro2a Cells. *Biochem Biophys Rep* **2017**, *12*, 40–45. <https://doi.org/10.1016/j.bbrep.2017.08.002>.
 123. Stepanenko, A. A.; Dmitrenko, V. V. HEK293 in Cell Biology and Cancer Research: Phenotype, Karyotype, Tumorigenicity, and Stress-Induced Genome-Phenotype Evolution. *Gene* **2015**, *569* (2), 182–190. <https://doi.org/10.1016/J.GENE.2015.05.065>.
 124. White, C. W.; Caspar, B.; Vanyai, H. K.; Pflieger, K. D. G.; Hill, S. J. CRISPR-Mediated Protein Tagging with Nanoluciferase to Investigate Native Chemokine Receptor Function and Conformational Changes. *Cell Chem Biol* **2020**, *27* (5), 499-510.e7. <https://doi.org/10.1016/J.CHEMBIOL.2020.01.010>.
 125. Jiang, L.; Wang, M.; Lin, S.; Jian, R.; Li, X.; Chan, J.; Dong, G.; Fang, H.; Robinson, A. E.; GTEx Consortium; Snyder, M. P. A Quantitative Proteome Map of the Human Body. *Cell* **2020**, *183* (1), 269-283.e19. <https://doi.org/10.1016/J.CELL.2020.08.036>.
 126. Sriram, K.; Wiley, S. Z.; Moyung, K.; Gorr, M. W.; Salmerón, C.; Marucut, J.; French, R. P.; Lowy, A. M.; Insel, P. A. Detection and Quantification of GPCR mRNA: An Assessment and Implications of Data from High-Content Methods. *ACS Omega* **2019**, *4* (16), 17048–17059. <https://doi.org/10.1021/ACSOMEGA.9B02811>.
 127. Thul, P. J.; Akesson, L.; Wiking, M.; Mahdessian, D.; Geladaki, A.; Ait Blal, H.; Alm, T.; Asplund, A.; Björk, L.; Breckels, L. M.; Bäckström, A.; Danielsson, F.; Fagerberg, L.; Fall, J.; Gatto, L.; Gnann, C.; Hober, S.; Hjelmare, M.; Johansson, F.; Lee, S.; Lindskog, C.; Mulder, J.; Mulvey, C. M.; Nilsson, P.; Oksvold, P.; Rockberg, J.; Schutten, R.; Schwenk, J. M.; Sivertsson, A.; Sjöstedt, E.; Skogs, M.; Stadler, C.; Sullivan, D. P.; Tegel, H.; Winsnes, C.; Zhang, C.; Zwahlen, M.; Mardinoglu, A.; Pontén, F.; Von Feilitzen, K.; Lilley, K. S.; Uhlén, M.; Lundberg, E. A Subcellular Map of the Human Proteome. *Science (1979)* **2017**, *356* (6340). <https://doi.org/10.1126/science.aal3321>.
 128. Khan, A. O.; White, C. W.; Pike, J. A.; Yule, J.; Slater, A.; Hill, S. J.; Poulter, N. S.; Thomas, S. G.; Morgan, N. V. Optimised Insert Design for Improved Single-Molecule Imaging and Quantification through CRISPR-Cas9 Mediated Knock-In. *Sci Rep* **2019**, *9* (1). <https://doi.org/10.1038/S41598-019-50733-9>.
 129. Kong, T.; Westerman, K. A.; Faigle, M.; Eltzschig, H. K.; Colgan, S. P. HIF-dependent Induction of Adenosine A2B Receptor in Hypoxia. *The FASEB Journal* **2006**, *20* (13), 2242–2250. <https://doi.org/10.1096/FJ.06-6419COM>.
 130. Eltzschig, H. K.; Ibla, J. C.; Furuta, G. T.; Leonard, M. O.; Jacobson, K. A.; Enjyoji, K.; Robson, S. C.; Colgan, S. R. Coordinated Adenine Nucleotide Phosphohydrolysis and Nucleoside Signaling in Posthypoxic Endothelium: Role of Ectonucleotidases and Adenosine A2B Receptors. *J Exp Med* **2003**, *198* (5), 783–796. <https://doi.org/10.1084/JEM.20030891>.
 131. Synnestvedt, K.; Furuta, G. T.; Comerford, K. M.; Louis, N.; Karhausen, J.; Eltzschig, H. K.; Hansen, K. R.; Thompson, L. F.; Colgan, S. P. Ecto-5'-Nucleotidase (CD73) Regulation by Hypoxia-Inducible Factor-1 Mediates

- Permeability Changes in Intestinal Epithelia. *J Clin Invest* **2002**, *110* (7), 993–1002. <https://doi.org/10.1172/JCI15337>.
132. Goodarzi, M. T.; Abdi, M.; Tavilani, H.; Nadi, E.; Rashidi, M. Adenosine Deaminase Activity in COPD Patients and Healthy Subjects. *Iran J Allergy Asthma Immunol* **2010**, *9* (1), 7–12.
133. Garcia-Morales, L. J.; Chen, N. Y.; Weng, T.; Luo, F.; Davies, J.; Philip, K.; Volcik, K. A.; Melicoff, E.; Amione-Guerra, J.; Bunge, R. R.; Bruckner, B. A.; Loebe, M.; Eltzschig, H. K.; Pandit, L. M.; Blackburn, M. R.; Karmouty-Quintana, H. Altered Hypoxic-Adenosine Axis and Metabolism in Group III Pulmonary Hypertension. *Am J Respir Cell Mol Biol* **2016**, *54* (4), 574–583. <https://doi.org/10.1165/RCMB.2015-0145OC>.
134. Singh Patidar, B.; Meena, A.; Kumar, M.; Menon, B.; Rohil, V.; Kumar Bansal, S. Adenosine Metabolism in COPD: A Study on Adenosine Levels, 5'-Nucleotidase, Adenosine Deaminase and Its Isoenzymes Activity in Serum, Lymphocytes and Erythrocytes. *COPD* **2018**, *15* (6), 559–571. <https://doi.org/10.1080/15412555.2018.1537365>.
135. Narravula, S.; Lennon, P. F.; Mueller, B. U.; Colgan, S. P. Regulation of Endothelial CD73 by Adenosine: Paracrine Pathway for Enhanced Endothelial Barrier Function. *J Immunol* **2000**, *165* (9), 5262–5268. <https://doi.org/10.4049/JIMMUNOL.165.9.5262>.
136. Hansen, K. R.; Resta, R.; Webb, C. F.; Thompson, L. F. Isolation and Characterization of the Promoter of the Human 5'-Nucleotidase (CD73)-Encoding Gene. *Gene* **1995**, *167* (1–2), 307–312. [https://doi.org/10.1016/0378-1119\(95\)00574-9](https://doi.org/10.1016/0378-1119(95)00574-9).
137. Polosa, R. Adenosine-Receptor Subtypes: Their Relevance to Adenosine-Mediated Responses in Asthma and Chronic Obstructive Pulmonary Disease. *European Respiratory Journal*. European Respiratory Society August 1, 2002, pp 488–496. <https://doi.org/10.1183/09031936.02.01132002>.

9 Supplemental Material

May 2023, Rev. 01



May 2023, Rev. 01



Protocol at a glance (Rev.17)

Plasmid DNA purification (NucleoBond® Xtra Midi / Maxi)

	Midi		Maxi	
1–3 Cultivation and harvest	4,500–6,000 x g 4 °C, 15 min			
4–5 Cell lysis <i>(Important: Check Buffer LYS for precipitated SDS)</i>	High-copy / low-copy 8 mL / 16 mL 8 mL / 16 mL Buffer RES Buffer LYS RT, 5 min		High-copy / low-copy 12 mL / 24 mL 12 mL / 24 mL Buffer RES Buffer LYS RT, 5 min	
6 Equilibration of the column and filter	12 mL Buffer EQU		25 mL Buffer EQU	
7 Neutralization	8 mL / 16 mL Buffer NEU Mix thoroughly until colorless		12 mL / 24 mL Buffer NEU Mix thoroughly until colorless	
8 Clarification and loading of the lysate	Invert the tube 3 times Load lysate on NucleoBond® Xtra Column Filter			
9 1st Wash	5 mL Buffer EQU		15 mL Buffer EQU	
10 Filter removal	Discard NucleoBond® Xtra Column Filter		Discard NucleoBond® Xtra Column Filter	
11 2nd Wash	8 mL Buffer WASH		25 mL Buffer WASH	
12 Elution	5 mL Buffer ELU		15 mL Buffer ELU	
13 Precipitation	NucleoBond® Xtra Midi	NucleoBond® Xtra Midi Plus	NucleoBond® Xtra Maxi	NucleoBond® Xtra Maxi Plus
	3.5 mL Isopropanol Vortex 4,5–15,000 x g 4 °C, 30 min	3.5 mL Isopropanol Vortex RT, 2 min Load NucleoBond® Finalizer	10.5 mL Isopropanol Vortex 4,5–15,000 x g 4 °C, 30 min	10.5 mL Isopropanol Vortex RT, 2 min Load NucleoBond® Finalizer Large
14 Washing and drying	2 mL 70 % ethanol 4,5–15,000 x g RT, 5 min 10–15 min	2 mL 70 % ethanol ≥ 6 x air until dry	4 mL 70 % ethanol 4,5–15,000 x g RT, 5 min 15–30 min	4 mL 70 % ethanol ≥ 6 x air until dry
15 Reconstitution	Appropriate volume of TE buffer	200–800 µL Buffer TRIS	Appropriate volume of TE buffer	400–1000 µL Buffer TRIS

Figure S 1: Protocol of the NucleoBond™ Xtra Midi kit by Macherey-Nagel. For more information visit <https://www.mn-net.com/de/nucleobond-xtra-midi-kit-for-transfection-grade-plasmid-dna-740410.50>

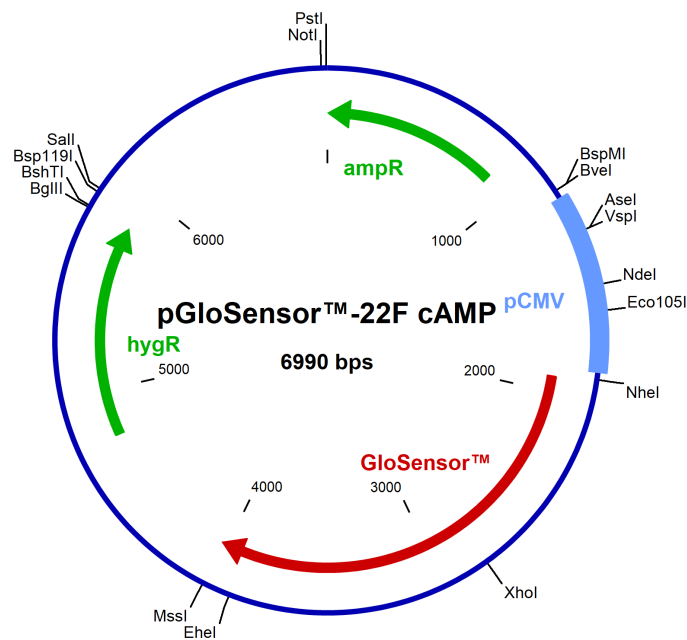


Figure S 2: Plasmid map of pGloSensor™-22F cAMP

2. Nucleofection®

One Nucleofection® Sample contains

1 x 10 ⁶ cells
1 – 5 µg plasmid DNA (in 1 – 5 µl H ₂ O or TE) or 2 µg pmaxGFP® Vector or 30 – 300nM siRNA (3 – 30 pmol/sample)
100 µl Cell Line Nucleofector® Solution V

- 2.1 Please make sure that the entire supplement is added to the Nucleofector® Solution
- 2.2 Prepare 6-well plates by filling appropriate number of wells with 1 ml of supplemented culture media and pre-incubate/equilibrate plates in a humidified 37°C/5% CO₂ incubator
- 2.3 Harvest the cells by trypsinization [please see 1.7 – 1.9]
- 2.4 Count an aliquot of the cells and determine cell density
- 2.5 Centrifuge the required number of cells [1 x 10⁶ cells per sample] at 200xg for 10 minutes at room temperature. Remove supernatant completely
- 2.6 Resuspend the cell pellet carefully in 100 µl room-temperature Nucleofector® Solution per sample

Note Avoid leaving the cells in Nucleofector® Solution for extended periods of time (longer than 15 minutes), as this may reduce cell viability and gene transfer efficiency

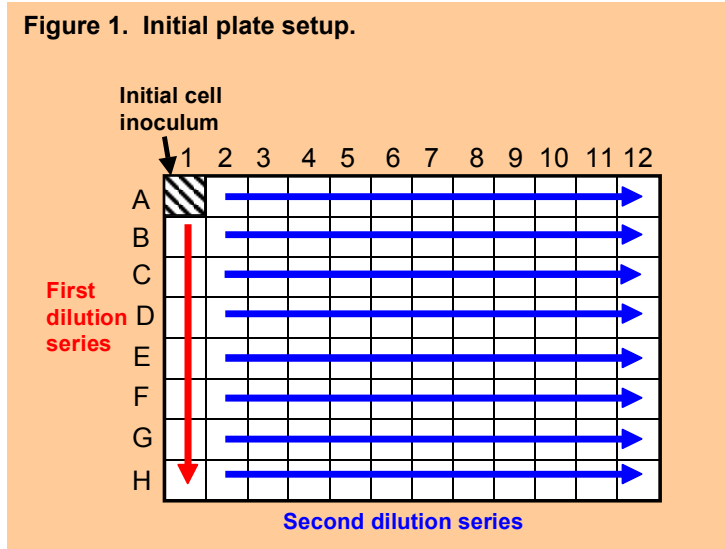
- 2.7 Combine 100 µl of cell suspension with 1 – 5 µg DNA, 2 µg pmaxGFP® Vector or 30 nM – 300 nM siRNA [3 – 30 pmol/sample] or other substrates
- 2.8 Transfer cell/DNA suspension into certified cuvette (sample must cover the bottom of the cuvette without air bubbles). Close the cuvette with the cap
- 2.9 Select the appropriate Nucleofector® Program **0-001** (0-01 for Nucleofector® I Device)
- 2.10 Insert the cuvette with cell/DNA suspension into the Nucleofector® Cuvette Holder and apply the selected program by pressing the X-button
- 2.11 Take the cuvette out of the holder once the program is finished
- 2.12 Immediately add ~500 µl of the pre-equilibrated culture medium to the cuvette and gently transfer the sample into the prepared 6-well plate (final volume 1.5 ml media per well). Use the supplied pipettes and avoid repeated aspiration of the sample

Figure S 3: Protocol for electroporation of HEK cells by Lonza. For more information visit <https://knowledge.lonza.com/cell?id=46>

Procedure

1. Fill the reagent dispensing tray with 12mL of the appropriate culture medium, then using an 8-channel micropipettor add 100µL medium to all the wells in the 96 well plate except well **A1** (see diagram below) which is left empty.

Figure 1. Initial plate setup.



Adding 4000 cells in well A1 (2×10^4 cells/mL) is a good starting cell concentration. Increase this concentration for more difficult to grow cell lines.

Transferring clones directly from a well in a 96 well plate into a T-25 flask is not recommended. The cells may be unable to grow due to their inability to condition the larger volume of medium in the flask. Using some conditioned medium when subculturing the cells for the first time will also help them survive and grow.

2. Add 200µL of the cell suspension to well **A1**. (See Figure 1.) Then using a single channel pipettor quickly transfer 100µL from the first well to well **B1** and mix by gently pipetting. Avoid bubbles. Using the same tip, repeat these 1:2 dilutions down the entire column, discarding 100µL from **H1** so that it ends up with the same volume as the wells above it.
3. With the 8-channel micropipettor add an additional 100µL of medium to each well in column 1 (giving a final volume of cells and medium of 200µL/well). Then using the same pipettor quickly transfer 100µL from the wells in the first column (**A1** through **H1**) to those in the second column (**A2** through **H2**) and mix by gently pipetting. **Avoid bubbles!**
4. Using the same tips, repeat these 1:2 dilutions across the entire plate, discarding 100µL from each of the wells in the last column (**A12** through **H12**) so that all the wells end up with 100µL of cell suspension.
5. Bring the final volume of all the wells to 200µL by adding 100µL medium to each well. Then label the plate with the date and cell type. Adding filtered conditioned medium (medium in which cells have been previously grown for 24 hours) to the wells can increase the success rate (cloning efficiency) for difficult to grow cells.
6. Incubate plate undisturbed at 37°C in a humidified CO₂ incubator.
7. Clones should be detectable by microscopy after 4 to 5 days and be ready to score after 7 to 10 days, depending on the growth rate of the cells. (See Figure 2 on page 3.) Check each well and mark all wells that contain just a single colony. These colonies can then be subcultured from the wells into

Figure S 4: Protocol for single-cell cloning by Corning. For more information visit https://www.corning.com/catalog/cls/documents/protocols/Single_cell_cloning_protocol.pdf

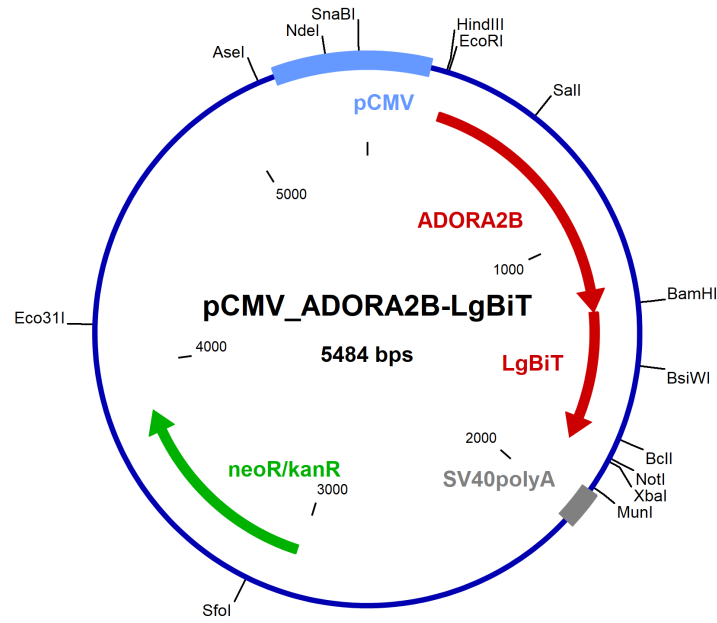


Figure S 5: Plasmid map of pCMV_ADORA2B-LgBiT

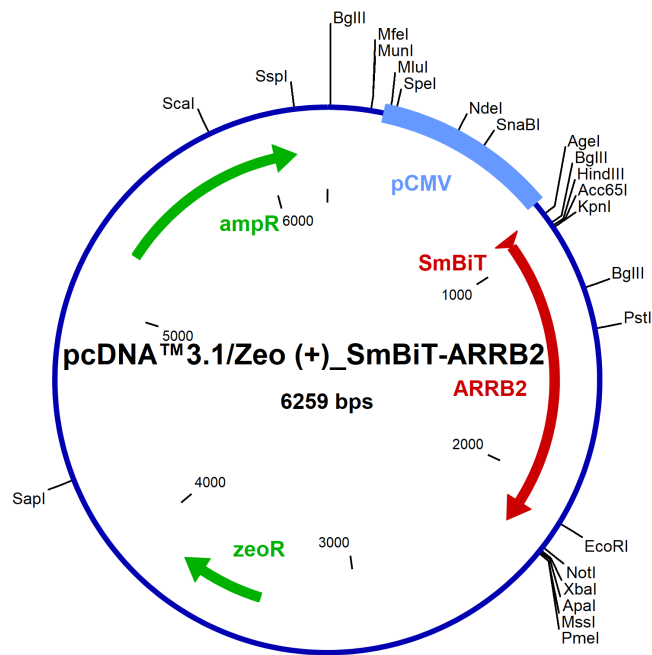


Figure S 6: Plasmid map of pcDNA™3.1/Zeo (+)_SmBiT-ARRB2

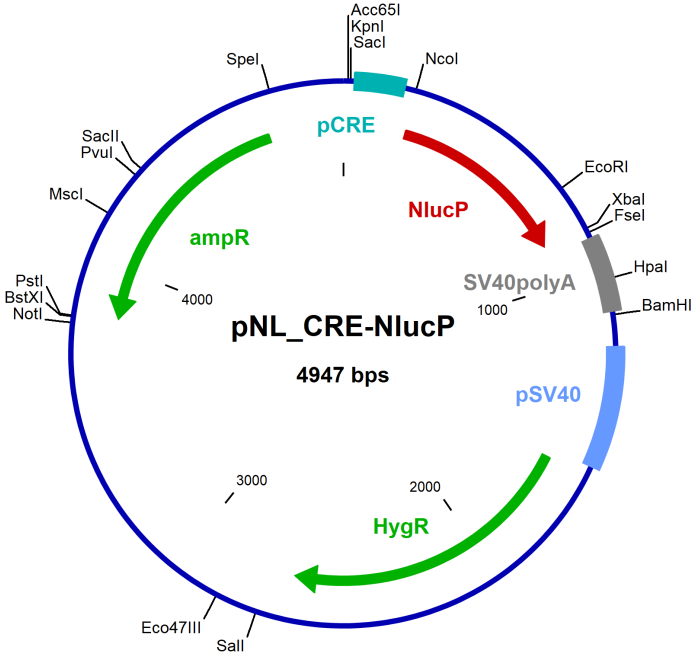


Figure S 7: Plasmid map of pNL_CRE-NlucP

4.B. Adding Substrate By Replacing the Medium

Endurazine™ and Vivazine™ substrates are provided as 100X stocks in organic solvent. Dilute Endurazine™ or Vivazine™ substrate 100-fold in cell culture medium for delivery to the cells. Serum-free medium may decrease Endurazine™ or Vivazine™ solubility, depending on medium type, and may increase cytotoxicity. If possible, include serum in your experiment to promote solubility and cell health. For serum-free conditions, protein supplements, (e.g. albumin) may increase solubility.

Wear gloves when handling Endurazine™ and Vivazine™ stock solutions, and avoid direct contact with skin. Take appropriate precautions when handling serum-containing medium. Consult the SDS for additional safety information.

1. Dilute Endurazine™ or Vivazine™ substrate 100-fold in cell culture medium and mix.

Notes:

1. Replace the cap immediately to avoid evaporation of the volatile organic solvent. Place tube(s) in an ice bucket if uncapped for extended periods.
 2. For continuous measurements in a luminometer, we recommend a buffered medium that will help maintain physiological pH throughout the experiment, unless your luminometer provides CO₂ control (Section 3.D). If measurements will be performed without a lid for several hours, we recommend using 200µl of medium per well (Section 3.D).
 3. FBS can be added up to 10% v/v final, but it will increase autoluminescence (Section 3.F).
 4. Warm medium to 37°C (optional).
2. For adherent cells, aspirate medium from tissue culture plate(s) and replace with the solution from Step 1. For suspension cells, pellet cells at 130 × g for 10 minutes and resuspend pellet with the solution from Step 1.

Notes:

1. For adherent cells, add medium containing Endurazine™ or Vivazine™ substrate slowly to the side of each well to avoid dislodging cells.
 2. For suspension cells, plate at the desired cell density or incubate cells in suspension (see Step 3).
3. If desired, incubate at 37°C to accumulate furimazine in the medium before adding test compounds and control treatments. In general, approximately 1 hour is required for Vivazine™ substrate to reach a peak signal and approximately 2 hours are required for Endurazine™ substrate to reach a stable signal.

Notes:

1. Measure luminescence continuously at 37°C to determine when a signal of sufficient intensity/stability is reached (Section 3.D).
 2. For suspension cells, this incubation can occur prior to cell plating.
 3. Signal intensity for Vivazine™ substrate will be brighter than Endurazine™ substrate at time zero and over the first several hours of a time-course experiment (Section 3.A).
4. Add test compounds and control treatments. For ≥10X stock solutions, use the same medium as Step 1 or similar solution as diluent minus Endurazine™ or Vivazine™ substrate. For less concentrated stock solutions, use a solution containing a 100-fold dilution of Endurazine™ or Vivazine™ substrate as diluent.

Notes:

1. Always include a vehicle control in your experiments for normalization or comparison purposes (Section 3.C).
2. Measure baseline luminescence prior to adding test or control compounds for per-well normalization (Section 3.G).

Figure S 8: Protocol of Nano-Glo® Vivazine™ Live Cell Substrate by Promega. For more information visit <https://www.promega.de/products/luciferase-assays/reporter-assays/nano-glo-extended-live-cell-substrates/?catNum=N2570>

Supplemental Material

4.C. Adding 5X Anti-hIL-6 Antibody Mixture to Assay Wells

If using multiple cell models, each requiring different culture medium, separate 5X Anti-hIL-6 antibody mixtures must be generated in each medium used in the study.

1. Remove the Anti-hIL-6 antibodies from storage immediately before use. Thaw if necessary.
Note: Remove Lumit™ Detection Buffer B from storage at the same time and equilibrate to room temperature if not already thawed. Use a water bath to accelerate buffer warming as necessary. If using the 25ml buffer in Cat. # W6031, you may need to initiate buffer warming further in advance of its use in Section 4.D.
2. Briefly centrifuge the Anti-hIL-6 antibody tubes before opening, then mix by pipetting.
3. Immediately prior to use, prepare a 5X antibody mixture by diluting both antibodies 1:200 into a single volume of prewarmed culture medium. Pipet to mix the antibody solution. To assay a complete 96- or 384-well plate, including some reagent volume for pipetting loss, prepare the 5X antibody mixture as follows:

Reagent	Volume
culture medium	2,376µl
Anti-hIL-6 mAb-SmBiT	12µl
Anti-hIL-6 mAb-LgBiT	12µl

4. Add the 5X Anti-hIL-6 antibody mixture to wells containing cultured cells or standard dilutions, carefully avoiding cross contamination between wells by changing pipette tips if moving from high to low analyte levels.
96-well plate: Dispense 20µl/well of 5X Anti-hIL-6 antibody mixture to 80µl/well of cells or IL-6 standard dilutions.
384-well plate: Dispense 5µl/well of 5X Anti-hIL-6 antibody mixture to 20µl/well of cells or IL-6 standard dilutions.
5. Briefly mix with a plate shaker (e.g., 10 seconds at 250–350rpm).
6. Incubate for 45 minutes at 37°C in a humidified 5% CO₂ incubator.

4.D. Adding Lumit™ Detection Reagent B to Assay Wells

While cells are incubating with the Anti-hIL-6 antibody mixture (Section 4.C), prepare the Lumit™ Detection Reagent B.

1. Equilibrate the required volume of Lumit™ Detection Buffer B to room temperature.
2. Remove the Lumit™ Detection Substrate B from storage and mix. If Lumit™ Detection Substrate B has collected in the cap or on the sides of the tube, briefly centrifuge.
3. Prepare a 1:20 dilution of Lumit™ Detection Substrate B in room temperature Lumit™ Detection Buffer B to create enough volume of Lumit™ Detection Reagent B for the number of wells to be assayed. To assay a 96- or 384-well assay plate, including some reagent volume for pipetting loss, prepare 5X Lumit™ Detection Reagent B as follows:

Reagent	Volume
Lumit™ Detection Buffer B	3,040µl
Lumit™ Detection Substrate B	160µl

Notes:

- a. The 1,000 assay size Lumit™ IL-6 (Human) Immunoassay (Cat. # W6031) contains 25ml of Lumit™ Detection Buffer B and 1.25ml of Lumit™ Detection Substrate B. There is sufficient overfill to prepare Lumit™ Detection Reagent B for analyzing 5 or 10 plates at one time. If Cat. # W6031 is used to assay 10 plates individually, mix 2,375µl of Lumit™ Detection Buffer B + 125µl of Lumit™ Detection Substrate B for each plate.
 - b. Once reconstituted, the Lumit™ Detection Reagent B will lose 10% activity in approximately 3 hours at 20°C. At 4°C, the reconstituted reagent will lose 10% activity in approximately 7 hours.
4. After the incubation in Section 4.C, Step 6, equilibrate the assay plate with cells to room temperature for 15 minutes.
 5. Add room temperature 5X Lumit™ Detection Reagent B to each assay well of the plate:
96-well plate: Dispense 25µl per well.
384-well plate: Dispense 6.25µl per well.
 6. Briefly mix with a plate shaker (e.g., 10 seconds at 300–500rpm).
 7. Incubate at room temperature for 3–5 minutes.
 8. Read luminescence.

Figure S 9: Protocol of Lumit™ IL-6 (Human) Immunoassay by Promega. For more information visit <https://www.promega.de/products/cell-health-assays/inflammation-assay/lumit-il-6-human-immunoassay/?catNum=W6030>

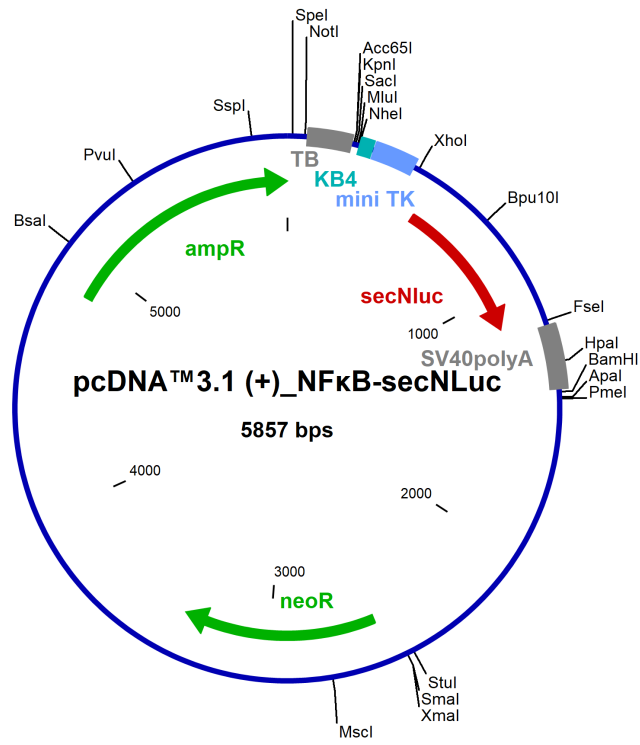


Figure S 10: Plasmid map of pcDNATM 3.1 (+)_NFκB-secNLuc

2. Working Instructions

2.1 Transfection of adherent cells – Standard protocol for a 12-well plate -

i We recommend beginning with the starting points mentioned in the table of section 4 or optimizing by following the optimization protocol.

1. In a 12-well tissue culture plate, seed $1.0 - 4.0 \times 10^5$ (starting point: 2.0×10^5) cells per dish in 1 ml of suitable fresh complete medium.²
2. Incubate the cells at 37°C in a CO₂ incubator until growing area is 90–100% covered. The time required will vary among cell types, but will usually take 18–24 hours.
3. The stock solutions of the METAFECTENE[®] PRO and the DNA or RNA should be at room temperature. Agitate the stock solutions gently before use.

RNA means single stranded RNA (ssRNA), not siRNA!

4. Prepare the following solutions using a cell culture grade 96-well plate or other tubes made of polypropylene, glass or polystyrene (preferentially polypropylene). **Medium must be pipetted first.** Pure solutions must not come into contact with plastic surfaces.

Solution **A**: 0.5 – 1.5 µg of DNA or RNA to 50 µl serum- and antibiotic-free medium or 1xPBS

Solution **B**: 1.0 – 7.0 µl of METAFECTENE[®] PRO to 50 µl serum- and antibiotic-free medium or 1xPBS

5. Mix the solutions gently by carefully pipetting one time.

Ratios will require optimizing based on various factors (see sections 3 and 4). The DNA or RNA lipid ratio has to be kept between 1:2 and 1:7 [µg DNA or RNA : µl METAFECTENE[®] PRO]!

Please note the order of addition in the following step: Add the DNA or RNA solution into the transfection reagent solution and not in reverse!

6. Combine the two solutions, **mix gently by pipetting up and down once** and incubate at room temperature for 15–20 min.

Shear stress may destroy the DNA or RNA lipid complex!

7. After incubation time add as soon as possible the DNA or RNA-lipid complexes dropwise to the cells and swirl the flask with **extreme care**. Incubate at 37°C in a CO₂ incubator.³
8. Depending on cell type and promoter activity, assay cells for gene activity 24–72 h following the start of transfection.

² Numbers of cells to seed depend on cell type and size. Optimization may be necessary, e.g. via determination of a growing curve. Maintain same seeding conditions between experiments.

³ If toxicity is a problem because of very sensitive cells, remove the transfection mixture after 3–6 hours and replace it with medium.

Figure S 11: Protocol of Metafectene[®] Pro by Biontex. For more information visit <https://www.biontex.com/metafectene-pro.html>



4. Nano-Glo® Luciferase Assay System Protocols

4.A. Preparation of the Nano-Glo® Luciferase Assay Reagent

Remove the Nano-Glo® Luciferase Assay Substrate from storage and mix by pipetting. Thaw the Nano-Glo® Luciferase Assay Buffer if stored at –20°C but do **not** exceed 25°C. Prepare the desired amount of reconstituted Nano-Glo® Luciferase Assay Reagent by combining one volume of Nano-Glo® Luciferase Assay Substrate with 50 volumes of Nano-Glo® Luciferase Assay Buffer. For example, if the experiment requires 10ml of reagent, add 200µl of substrate to 10ml of buffer.

Notes:

1. If the Nano-Glo® Luciferase Assay Substrate has collected in the cap or on the sides of the tube, briefly centrifuge tubes containing 200µl or 1ml of substrate in a microcentrifuge. Place 4ml tubes in a swinging bucket rotor and centrifuge at $200 \times g$ for 1 minute.
2. We recommend preparing the Nano-Glo® Luciferase Assay Reagent fresh for each use rather than storing the reagent at any temperature.
3. Once reconstituted, the reagent will lose 10% activity in approximately 8 hours and 50% activity in approximately 2 days at room temperature. The reconstituted reagent may be stored at 4°C with <10% decrease in activity over 2 days.

4.B. Detection of NanoLuc® Luciferase in Mammalian Cells (Lytic Method)

1. Allow all assay components (reagent and sample) to equilibrate to room temperature prior to assay. For example, remove a tissue culture plate from the 37°C, 5% CO₂ incubator and equilibrate it to room temperature for 5–10 minutes.
2. Add a volume of reagent equal to that of the culture medium in each well. Mix for optimal consistency. For 96-well plates, typically 100µl of reagent is added to the cells grown in 100µl of medium. For 384-well plates, typically 30µl of reagent is added to cells grown in 30µl of medium.
3. Wait at least 3 minutes before measuring luminescence. The luminescence intensity will decay gradually, with a signal half-life of approximately 120 minutes at room temperature.

Notes:

1. At high expression levels, the luminescence signal half-life can decrease significantly due to rapid depletion of the furimazine substrate (see Section 5.A). Experimental conditions should be modified to avoid extremely high expression (see Section 5.B).
2. Ensure that the instrument is operating within its linear dynamic range when measuring luminescence (see Section 5.C). Consult with the instrument manufacturer or determine this range empirically. Many instruments will not indicate if values are outside of the linear range.
3. The Nano-Glo® Luciferase Assay System is compatible with a variety of components used in mammalian cell culture experiments, showing minimal differences in luminescence intensity or signal half-life (Figure 5).

Figure S 12: Protocol of Nano-Glo® Luciferase Assay System by Promega. For more information visit https://www.promega.de/products/luciferase-assays/reporter-assays/nano_glo-luciferase-assay-system/?catNum=N1110

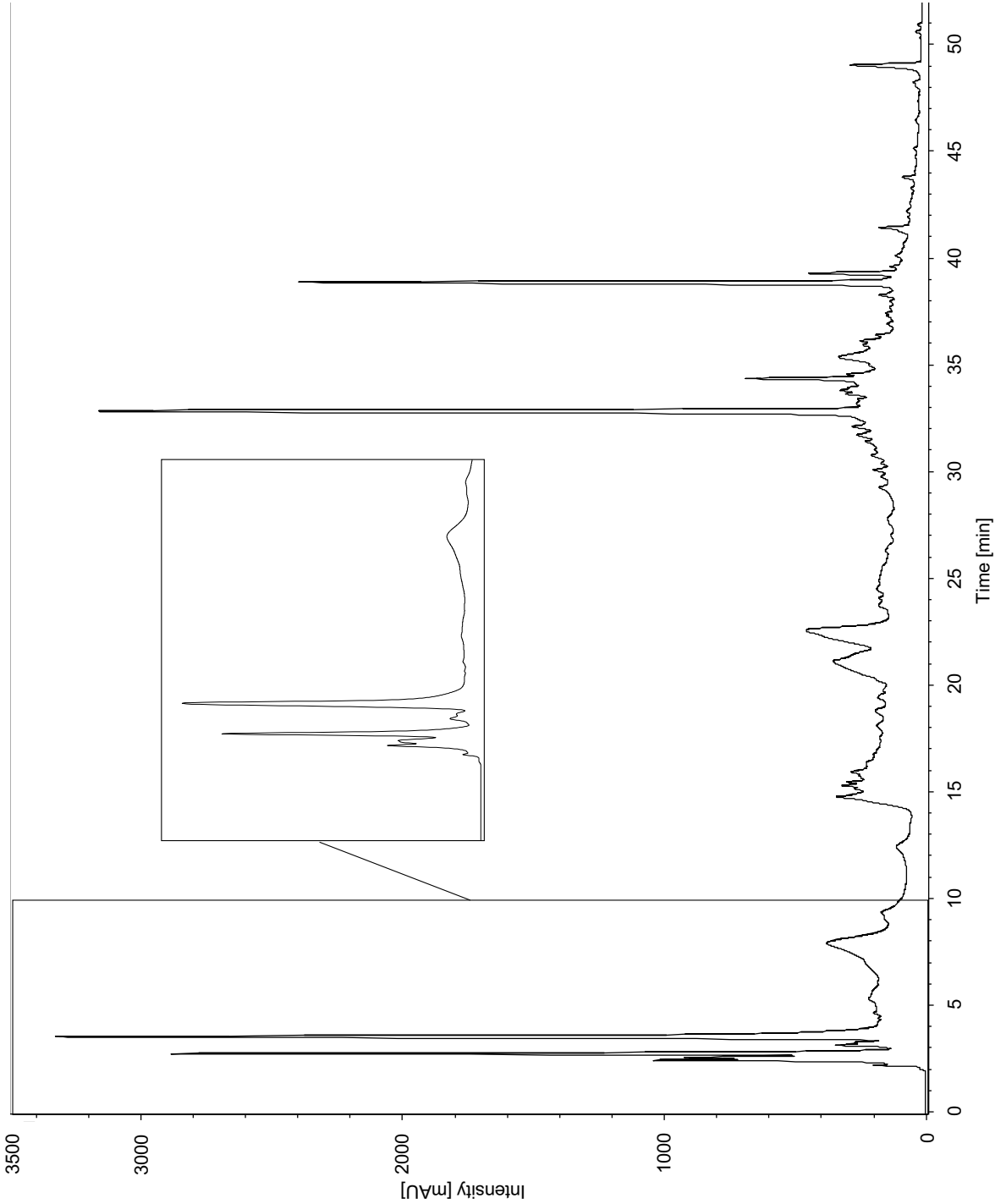


Figure S 13: HPLC chromatogram of EA 575[®] at 205 nm applying the method without phosphoric acid. The zoomed view shows what was collected as fraction I.

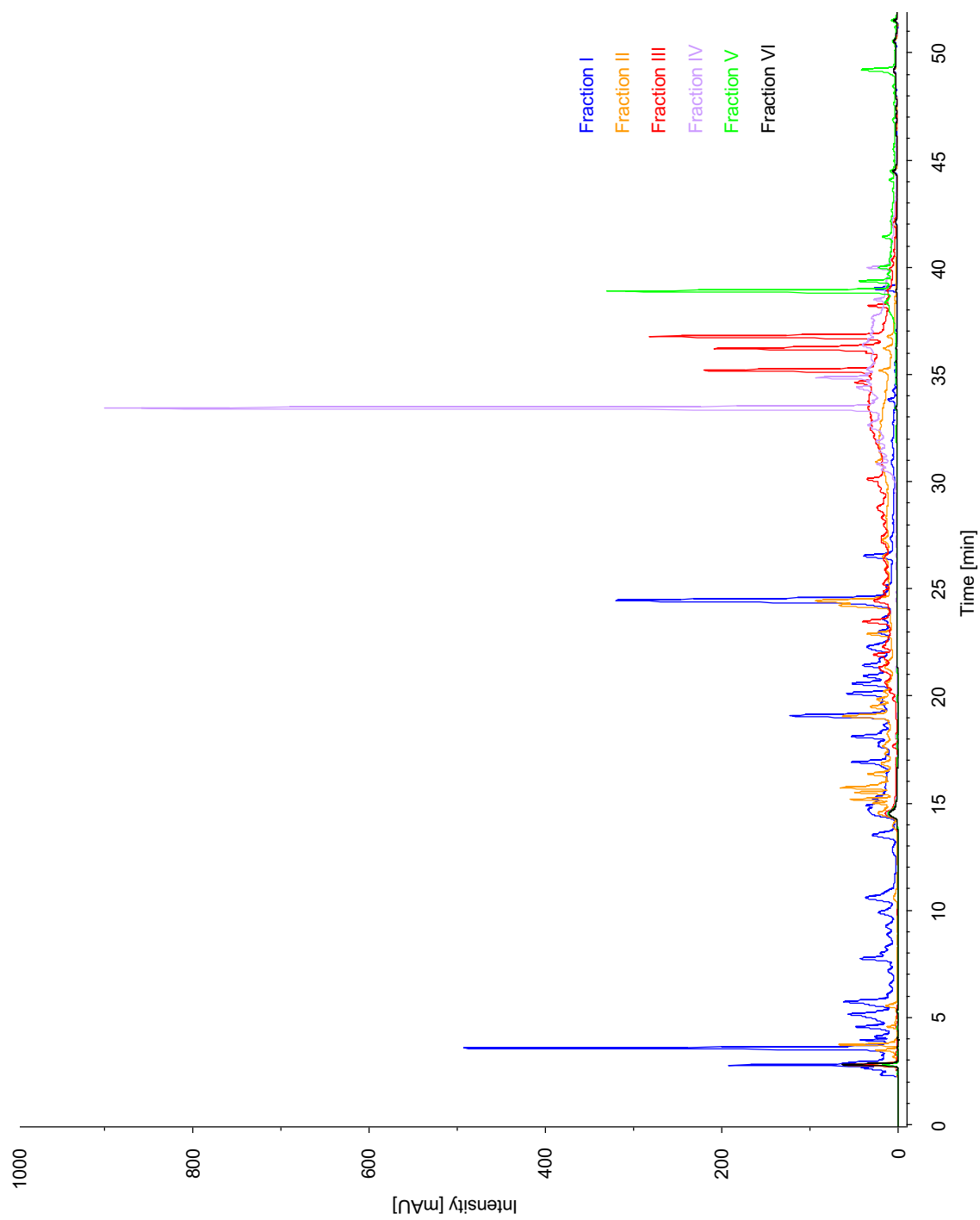


Figure S 14: Overlay of the fraction chromatograms

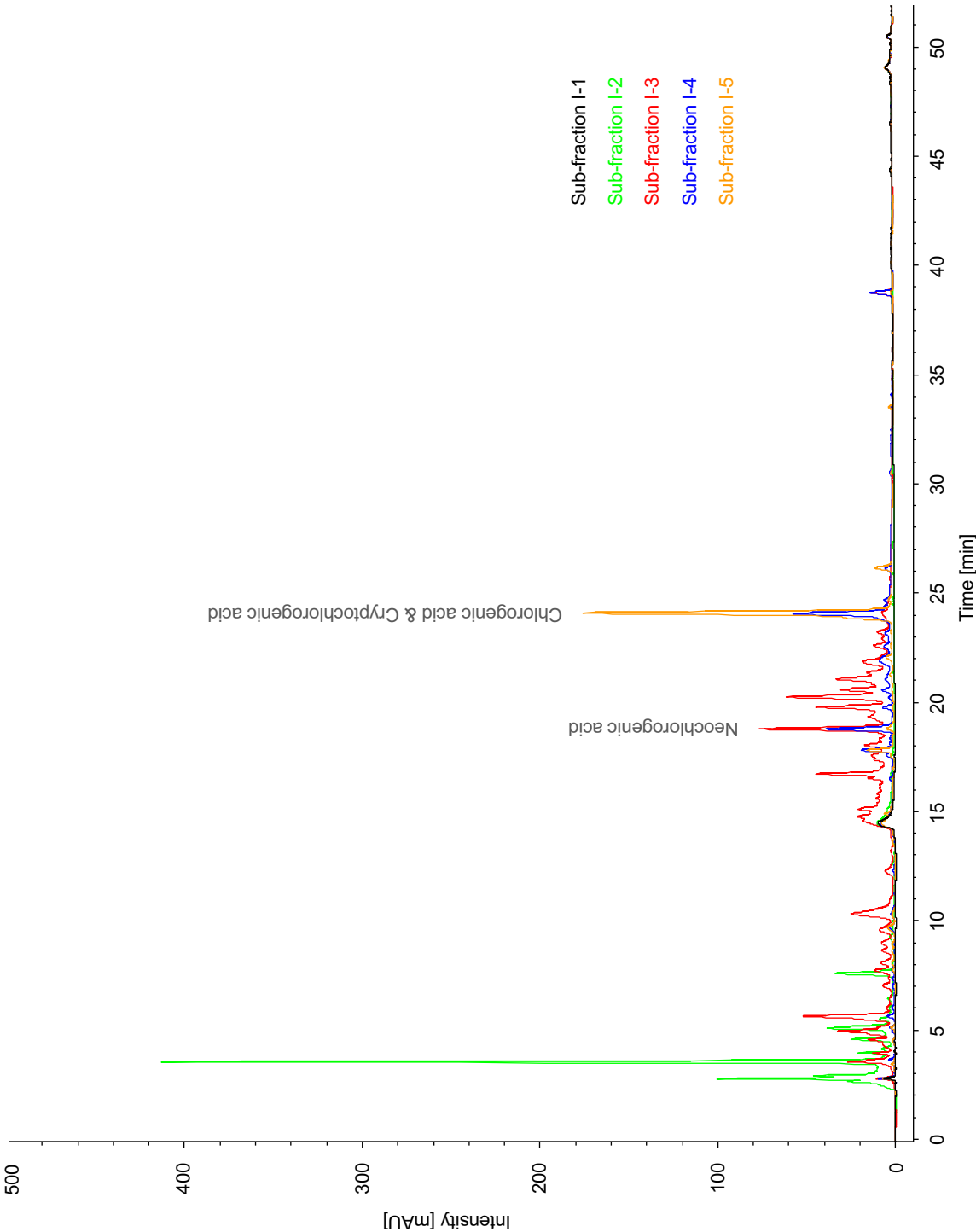


Figure S 15: Overlay of the sub-fraction chromatograms

3.B. Preparing the Nano-Glo® HiBiT Extracellular Reagent

Calculate the amount of Nano-Glo® HiBiT Extracellular Reagent needed to perform the desired experiments. This usually constitutes a volume equal to the total amount of medium in wells, plus any extra required for dispensing. Dilute the LgBiT Protein 1:100 and the Nano-Glo® HiBiT Extracellular Substrate 1:50 into an appropriate volume of room temperature Nano-Glo® HiBiT Extracellular Buffer in a new tube. Mix by inversion.

For example, if 4ml of Nano-Glo® HiBiT Extracellular Reagent is needed, transfer 4ml of Nano-Glo® HiBiT Extracellular Buffer to a 15ml centrifuge tube and add 40µl of LgBiT Protein and 80µl of Nano-Glo® HiBiT Extracellular Substrate.

Notes:

1. The LgBiT Protein stock contains glycerol, which prevents it from freezing at -20°C . The viscosity of this solution may make accurate pipetting difficult. Pipet slowly and avoid excess solution clinging to the outside of the pipette tip. Use a positive displacement pipette, if possible.
2. If the Nano-Glo® HiBiT Extracellular Substrate or LgBiT Protein has collected in the cap or on the sides of the tube, briefly spin the tubes in a microcentrifuge.
3. We recommend preparing the Nano-Glo® HiBiT Extracellular Reagent fresh for each use. Once reconstituted, the reagent will lose about 15% activity over 8 hours and about 60% activity over 24 hours at room temperature. Unused reconstituted reagent may be stored at -80°C , -20°C or 4°C for later use, although there will be some loss of performance relative to freshly prepared reagent. At 4°C , the reconstituted reagent should lose less than 20% activity over 24 hours.

3.C. General Protocol for Adding Nano-Glo® HiBiT Extracellular Reagent to Cells

1. Reconstitute the Nano-Glo® HiBiT Extracellular Reagent as described in Section 3.B.
2. Remove plates containing mammalian cells expressing a HiBiT-tagged protein from the 37°C incubator.
Optional: To minimize well-to-well variability caused by differences in temperature, equilibrate the plate to room temperature (e.g., 5 minutes on a metal block).
3. Add a volume of Nano-Glo® HiBiT Extracellular Reagent equal to the culture medium present in each well, and mix. For example, add 100µl of Nano-Glo® HiBiT Extracellular Reagent to 100µl of cell culture medium.
Note: Mix the samples by gently pipetting samples or placing the plate on an orbital shaker (300–500 rpm) for 3–10 minutes.
4. Measure luminescence 10 minutes after adding reagent. For a HiBiT tag placed within the protein sequence, longer incubation times may be necessary compared to terminal protein tagging. Measure luminescence using settings specific to your instrument. For 96-well plates on GloMax® instruments, integration times of 0.5–2 seconds are recommended. Longer integration times may improve data quality at lower levels of expression. The luminescence intensity will generally decay in a well-mixed sample with a signal half-life of 1–2.5 hours, depending on conditions (see Figure 8, Panel B; Figure 9 Panel B; and Figure 10, Panel B).

Notes:

1. To ensure luminescence is proportional to the amount of HiBiT-tagged protein present, subtract the assay background, especially when measuring low amounts of protein. Include untransfected or mock-transfected cells as background controls in your experiment (see Section 6.I).
2. Placing HiBiT in internal protein positions, like extracellular surface loops, may slow LgBiT and HiBiT equilibration. Increase reagent incubation times to compensate, if necessary.

Figure S 16: Protocol of Nano-Glo® HiBiT Extracellular Detection System by Promega. For more information visit <https://www.promega.de/en/products/protein-detection/protein-quantification/nano-glo-hibit-extracellular-detection-system/?catNum=N2420#protocols>



3.B. Preparing the Nano-Glo® HiBiT Lytic Reagent

Calculate the amount of Nano-Glo® HiBiT Lytic Reagent needed to perform the desired experiments. This volume is usually equal to the total amount of medium in wells plus any extra required for dispensing. Dilute the LgBiT Protein 1:100 and the Nano-Glo® HiBiT Lytic Substrate 1:50 into an appropriate volume of room temperature Nano-Glo® HiBiT Lytic Buffer in a new tube. Mix by inversion.

For example, if 4ml of Nano-Glo® HiBiT Lytic Reagent is needed, transfer 4ml of Nano-Glo® HiBiT Lytic Buffer to a 15ml centrifuge tube and add 40µl of LgBiT Protein and 80µl of Nano-Glo® HiBiT Lytic Substrate.

Notes:

- If the Nano-Glo® HiBiT Lytic Substrate or LgBiT Protein has collected in the cap or on the sides of the tube, briefly spin the tubes in a microcentrifuge.
- The LgBiT Protein stock contains glycerol, which prevents it from freezing at -20°C . The solution viscosity may make accurate pipetting difficult. Pipet slowly and avoid excess solution clinging to the outside of the pipette tip. Use a positive displacement pipette, if possible.
- Because luciferase activity is temperature dependent, the temperature of the samples and reagents should be kept constant while measuring luminescence. We recommend equilibrating reagents to room temperature. For ease of use, store the Nano-Glo® HiBiT Lytic Buffer at room temperature at least a day before experiments. Equilibrate cultured cells to room temperature before adding reagents.
- We recommend preparing the Nano-Glo® HiBiT Lytic Reagent fresh for each use. Once reconstituted, the reagent will lose about 10% activity over 8 hours and about 30% activity over 24 hours at room temperature. Unused reconstituted reagent may be stored at -80°C , -20°C or 4°C for later use, although there will be some loss of performance relative to freshly prepared reagent. At 4°C , the reconstituted reagent should lose less than 10% activity over 24 hours.

3.C. Detecting HiBiT-Tagged Proteins in Mammalian Cells

- Remove plates containing mammalian cells expressing a HiBiT-tagged protein from the incubator and equilibrate to room temperature. Use an opaque, white tissue-culture plate to minimize cross-talk between wells and absorption of the emitted light.
Note: Ensure that the plates used are compatible with the instrument used to measure luminescence.
- Add a volume of Nano-Glo® HiBiT Lytic Reagent equal to the culture medium present in each well, and mix. For optimal results, mix the samples by placing the plate on an orbital shaker (300–600rpm) for 3–10 minutes or by pipetting samples. At a minimum, employ 15–30 seconds of orbital shaking to reduce variability between replicates.
- Wait at least 10 minutes for equilibration of LgBiT and HiBiT in the lysate. Measure luminescence using settings specific to your instrument. When using 96-well plates on the GloMax® instruments, we recommend integration times of 0.5–2 seconds. The luminescence intensity will usually decay with a signal half-life of greater than 3 hours. While 10 minutes of incubation is typically sufficient for maximal signal and low variability, longer incubation times may be necessary for internal fusions of HiBiT (e.g., surface loops) or when the HiBiT-tagged protein is expressed under conditions where the tag is not readily accessible upon cell lysis.

Note: To ensure luminescence is proportional to the amount of HiBiT-tagged protein present, subtract the assay background, especially when measuring low amounts of protein. Include control samples on the assay plate, consisting of cells not expressing HiBiT-tagged proteins (see Section 6.G).

Figure S 17: Protocol of Nano-Glo® HiBiT Extracellular Detection System by Promega. For more information visit <https://www.promega.de/products/protein-detection/protein-quantification/nano-glo-hibit-lytic-detection-system/?catNum=N3030>

RNA isolation

Protocol at a glance (Rev. 07)


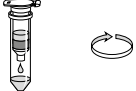

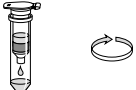
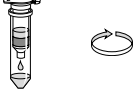
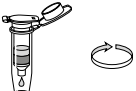
NucleoSpin® RNA Plus XS			
1 Homogenize and lyse sample			100 µL LB1 Homogenize 100 µL LB2
2 Remove gDNA and filtrate lysate			100 x g, 2 min 11,000 x g, 10 s
3 Adjust binding conditions			150 µL BSXS Mix
4 Bind RNA			Load lysate 300 x g, 1 min 11,000 x g, 10 s
5 Wash and dry silica membrane		1 st wash	100 µL MDB 11,000 x g, 10 s
		2 nd wash	500 µL WB2 11,000 x g, 10 s
		3 rd wash	200 µL WB2 < 20,000 x g, 2 min
6 Elute RNA			10–20 µL RNase-free H ₂ O 11,000 x g, 1 min

Figure S 18: Protocol of the NucleoSpin® RNA XS kit by Macherey Nagel. For more information visit <https://www.mn-net.com/de/nucleospin-rna-plus-xs-micro-kit-for-rna-purification-with-dna-removal-column-740990.50>

PROTOCOLS

I. First Strand cDNA Synthesis

After thawing, mix and briefly centrifuge the components of the kit. Store on ice.

1. Add the following reagents into a sterile, nuclease-free tube on ice in the indicated order:

Template RNA	total RNA or poly(A) mRNA or specific RNA	0.1 ng - 5 µg 10 pg - 0.5 µg 0.01 pg - 0.5 µg
Primer	Oligo (dT) ₁₈ primer or Random Hexamer primer or gene-specific primer	1 µL 1 µL 15-20 pmol
Water, nuclease-free		to 12 µL
Total volume		12 µL

2. *Optional.* If the RNA template is GC-rich or contains secondary structures, mix gently, centrifuge briefly and incubate at 65°C for 5 min. Chill on ice, spin down and place the vial back on ice.
3. Add the following components in the indicated order:

5X Reaction Buffer	4 µL	
RiboLock RNase Inhibitor (20 U/µL)	1 µL	
10 mM dNTP Mix	2 µL	
RevertAid M-MuLV RT (200 U/µL)	1 µL	
Total volume		20 µL

4. Mix gently and centrifuge briefly.
5. For oligo(dT)₁₈ or gene-specific primed cDNA synthesis, incubate for 60 min at 42°C. For random hexamer primed synthesis, incubate for 5 min at 25°C followed by 60 min at 42°C. **Note.** For GC-rich RNA templates the reaction temperature can be increased up to 45°C.
6. Terminate the reaction by heating at 70°C for 5 min.

The reverse transcription reaction product can be directly used in PCR applications or stored at -20°C for less than one week. For longer storage, -70°C is recommended

Figure S 19: Protocol of the First Strand cDNA Synthesis Kit by Thermo Fisher Scientific.

For more information visit <https://www.thermofisher.com/order/catalog/product/de/en/K1612>

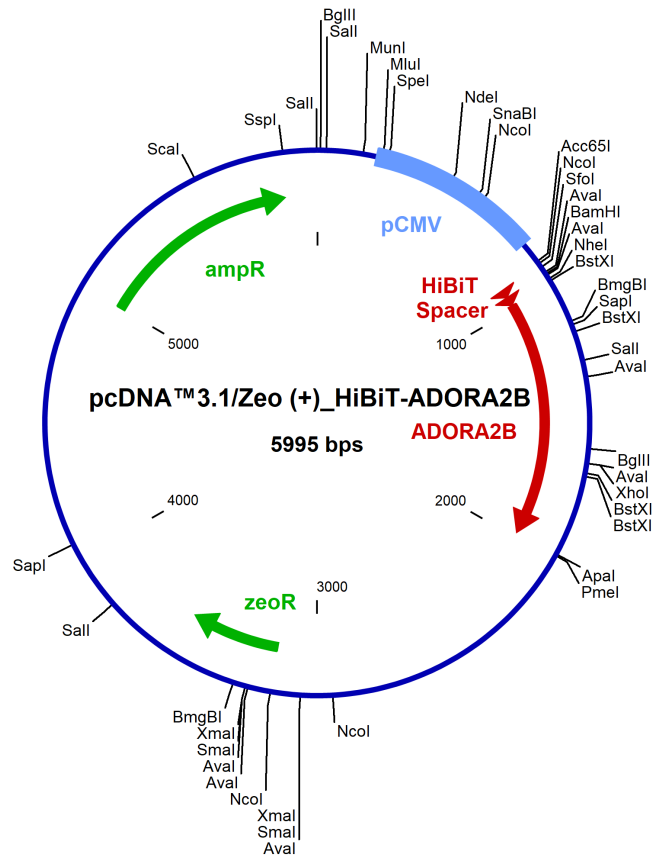


Figure S 20: Plasmid map of pcDNA™ 3.1/Zeo (+)_HiBiT-ADORA2B

Table S 1: PCR cycling parameters

PCR 1		PCR 2		PCR 3		PCR 4	
98 °C / 30 s		98 °C / 120 s		98 °C / 30 s		98 °C / 180 s	
98 °C / 10 s	25×	98 °C / 10 s	25×	98 °C / 10 s	35×	98 °C / 15 s	40×
58 °C / 15 s		68 °C / 20 s		67 °C / 15 s		65 °C / 15 s	
72 °C / 90 s		72 °C / 15 s		72 °C / 30 s		72 °C / 15 s	
72 °C / 120 s		72 °C / 120 s		72 °C / 120 s		72 °C / 120 s	

All PCRs were performed using Q5 High-Fidelity DNA Polymerase.

Table S 2: Presumed substances identified in sub-fraction I-2 via LC-MS/MS (positive ionisation mode)

Measured mass [m/z]	Molecular formula	Presumed substance	MS2 main fragments [m/z]
116.07 [M+H] ⁺	C ₅ H ₉ NO ₂	Proline	70
118.08 [M+H] ⁺	C ₅ H ₁₁ NO ₂	Valine	72, 59, 58, 55
180.09 [M+H] ⁺	C ₆ H ₁₃ NO ₄	<i>Hexosamine</i>	162, 144, 126, 84, 72, 60
355.07 [M+H] ⁺	C ₁₆ H ₁₈ O ₉	<i>Chlorogenic acid</i>	163

Table S 3: Presumed substances identified in sub-fraction I-2 via LC-MS/MS (negative ionisation mode)

Measured mass [m/z]	Molecular formula	Presumed substance	MS2 main fragments [m/z]
115.00 [M-H] ⁻	C ₄ H ₄ O ₄	Maleic acid / Fumaric acid	71
117.02 [M-H] ⁻	C ₄ H ₆ O ₄	Succinic acid	99, 73
133.01 [M-H] ⁻	C ₄ H ₆ O ₅	Malic acid	133, 115, 71
153.02 [M-H] ⁻	C ₇ H ₆ O ₄	Protocatechuic acid	109
173.05 [M-H] ⁻	C ₇ H ₁₀ O ₅	Shikimic acid	155, 129, 111
179.04 [M-H] ⁻	C ₉ H ₈ O ₄	Caffeic acid	135
181.07 [M-H] ⁻	C ₆ H ₁₄ O ₆	<i>Hexitol</i>	163, 101, 89, 85, 73, 71, 59, 55
191.02 [M-H] ⁻	C ₆ H ₈ O ₇	Citric acid	129, 111, 87, 85
191.05 [M-H] ⁻	C ₇ H ₁₁ O ₆	Quinic acid	127, 111, 85
195.05 [M-H] ⁻	C ₆ H ₁₂ O ₇	<i>Hexonic acid</i>	129, 99, 87, 75, 71, 59, 57
209.03 [M-H] ⁻	C ₆ H ₁₀ O ₆	<i>Glucaric acid</i>	191, 85, 71, 59, 57
323.03 [M-H] ⁻	C ₉ H ₁₃ N ₂ O ₉ P	Uridine monophosphate	211, 111, 96, 78
341.11 [M-H] ⁻	C ₁₂ H ₂₂ O ₁₁	<i>Disaccharide</i>	179, 161, 119, 113, 101, 89, 71, 59
353.10 [M-H] ⁻	C ₁₆ H ₁₈ O ₉	<i>Chlorogenic acid</i>	191, 179, 173, 135

Table S 4: Presumed substances identified in sub-fraction I-3 via LC-MS/MS (positive ionisation mode)

Measured mass [m/z]	Molecular formula	Presumed substance	MS2 main fragments [m/z]
124.04 [M+H] ⁺	C ₆ H ₅ NO ₂	Nicotinic acid	96, 80, 78
132.10 [M+H] ⁺	C ₆ H ₁₃ NO ₂	Iso-/Leucine	86
136.06 [M+H] ⁺	C ₅ H ₅ N ₅	Adenine	119
152.06 [M+H] ⁺	C ₅ H ₅ N ₅ O	Guanine	135, 128, 110
182.08 [M+H] ⁺	C ₆ H ₁₃ NO ₄	Tyrosine	165, 136, 123, 119
268.10 [M+H] ⁺	C ₁₀ H ₁₃ N ₅ O ₄	Adenosine	136, 119
284.10 [M+H] ⁺	C ₁₀ H ₁₃ N ₅ O ₅	Guanosine	152, 135, 128, 110
355.07 [M+H] ⁺	C ₁₆ H ₁₈ O ₉	<i>Chlorogenic acid</i>	163

Table S 5: Presumed substances identified in sub-fraction I-3 via LC-MS/MS (negative ionisation mode)

Measured mass [m/z]	Molecular formula	Presumed substance	MS2 main fragments [m/z]
117.02 [M-H] ⁻	C ₄ H ₆ O ₄	Succinic acid	99, 73
133.01 [M-H] ⁻	C ₄ H ₆ O ₅	Malic acid	133, 115, 71
137.02 [M-H] ⁻	C ₇ H ₆ O ₃	Salicylic acid	93, 65
151.04 [M-H] ⁻	C ₈ H ₈ O ₃	Vanillin	136, 108, 92
153.02 [M-H] ⁻	C ₇ H ₆ O ₄	Protocatechuic acid	109
179.04 [M-H] ⁻	C ₉ H ₈ O ₄	Caffeic acid	135
191.02 [M-H] ⁻	C ₆ H ₈ O ₇	Citric acid	129, 111, 87, 85
191.05 [M-H] ⁻	C ₇ H ₁₁ O ₆	Quinic acid	127, 111, 85
341.11 [M-H] ⁻	C ₁₂ H ₂₂ O ₁₁	<i>Disaccharide</i>	179, 161, 119, 113, 101, 89, 71, 59
353.10 [M-H] ⁻	C ₁₆ H ₁₈ O ₉	<i>Chlorogenic acid</i>	191, 179, 135

Substances written in italic letters could also be (stereo-)isomers of this structure.

10 Appendix

10.1 Publikationen und Poster

Publikationen

Meurer F, Häberlein H, Franken S. Ivy Leaves Dry Extract EA 575[®] Has an Inhibitory Effect on the Signalling Cascade of the Adenosine Receptor A_{2B}. *International Journal of Molecular Sciences*. 2023;24(15):12373. doi:10.3390/ijms241512373

Meurer F, Schulte-Michels J, Häberlein H, Franken S. Ivy leaves dry extract EA 575[®] mediates biased β_2 -adrenergic receptor signaling. *Phytomedicine*. 2021;90:153645. doi:10.1016/j.phymed.2021.153645

Bussmann H, Schulte-Michels J, Bingel M, Meurer F, Aatz S, Häberlein F, Franken S, Häberlein H. A comparative study on the influence of an ivy preparation and an ivy/thyme combination on the β_2 -adrenergic signal transduction. *Heliyon*. 2020;6(5):e03960. Published 2020 May 15. doi:10.1016/j.heliyon.2020.e03960

Poster

Meurer F, Häberlein H, Franken S. EA 575[®] wirkt auf Proteinkinasen, die für die Behandlung von Atemwegserkrankungen relevant sind. *Zeitschrift für Phytotherapie*. 2023;44(S 01):25-26. doi:10.1055/s-0043-1769551

Phytotherapiekongress 2023, Bamberg, 15. – 17.06.2023

Meurer F, Schulte-Michels J, Häberlein H, Franken S. Ivy leaves dry extract EA 575[®] enhances G protein/cAMP pathway and simultaneously inhibits GRK2/ β -arrestin 2 pathway leading to a biased β_2 -adrenergic receptor signaling. *Zeitschrift für Phytotherapie*. 2022;43(S 01):44. doi:10.1055/s-0042-1749283

Tetranationale Tagung: Phytotherapie 2022, Zürich, 16. – 17.06.2022

Meurer F, Schulte-Michels J, Häberlein H, Franken S. Ivy leaves dry extract EA 575[®] mediates biased β_2 -adrenergic receptor signaling. *Planta Medica* 2021;87(15):1280. doi:10.1055/s-0041-1736880

69th International Congress and Annual Meeting of the Society for Medicinal Plant and Natural Product Research (GA), virtual conference, 05. – 08.09.2021

Meurer F, Häberlein H, Franken S. Der Efeublätter-Trockenextrakt EA 575[®] inhibiert den Adenosinrezeptor A_{2B}-induzierten cAMP-Anstieg. *Zeitschrift für Phytotherapie*. 2021;42(S 01):23. doi:10.1055/s-0041-1731506

Phytotherapie 2021 - 50 Jahre GPT: Jahreskongress, Bonn, 24. – 26.06.2021

10.2 Danksagung

Zum Schluss möchte ich mich von Herzen bei allen Personen bedanken, die mich während der Zeit meiner Promotion unterstützt haben und immer für mich da waren.

Allen voran Hanns, vielen Dank für die engagierte Betreuung meiner Arbeit und dafür, dass ich mich jederzeit auf deine Unterstützung und auf deinen Rat verlassen konnte.

Vielen Dank auch an Prof. Dr. Gerd Bendas für die freundliche Übernahme meiner Zweitbetreuung.

Ein großer Dank gilt auch Sebastian für die vielen wertvollen Ratschläge zu allen theoretischen und praktischen Fragen sowie für das freundliche Miteinander.

Ich bedanke mich bei meiner Arbeitsgruppe, vor allem Eva, Luisa und Swen. Danke, dass ihr für mich nicht nur Kollegen, sondern Freunde seid. Ihr habt maßgeblich dazu beigetragen, dass ich mich immer gerne an diese Zeit erinnern werde.

Außerdem möchte ich meiner Familie und meinen Freunden danken, insbesondere meiner Mama und meiner Schwester Lisa. Ihr wart immer für mich da und habt mir in der gesamten Zeit den Rücken gestärkt.

Serena, dir gebührt besonderer Dank. Deine Bedeutung ist schwierig in Worte zu fassen, daher einfach danke für alles.

10.3 Eidesstattliche Erklärung

Hiermit versichere ich, Fabio Gian-Luca Meurer, dass ich die vorliegende Arbeit selbstständig angefertigt und keine anderen als die angegebenen Hilfsmittel und Quellen benutzt habe. Ferner erkläre ich, die vorliegende Arbeit an keiner anderen Hochschule als Dissertation eingereicht zu haben. Ich habe noch keinen Promotionsversuch unternommen. Die von mir eingereichte Dissertation habe ich unter Beachtung der Grundsätze zur Sicherung guter wissenschaftlicher Praxis erstellt. Meine Angaben entsprechen der Wahrheit und ich habe diese nach bestem Wissen und Gewissen gemacht.

Bonn, den 25.01.2024

10.4 Zusammenfassung der Publikation nach PromO § 9 (4) und Erklärung zu teil-kumulativer Dissertation

Einige jeweils gekennzeichnete Kapitel dieser Dissertation werden durch die 2023 im International Journal of Molecular Sciences erschienene Publikation „Ivy Leaf Dry Extract EA 575[®] Has an Inhibitory Effect on the Signalling Cascade of Adenosine Receptor A_{2B}” abgedeckt [1]. Diese wurde im Rahmen meiner Promotion erstellt und behandelt den inhibitorischen Effekt des Efeublätter-Trockenextrakts EA 575[®] auf die Signalkaskade des Adenosinrezeptors A_{2B} (A_{2B}AR).

EA 575[®] wird zur Besserung der Beschwerden bei chronisch-entzündlichen Bronchialerkrankungen und akuten Entzündungen der Atemwege mit der Begleiterscheinung Husten angewendet. Der Wirkmechanismus wurde bislang durch die Beeinflussung der β_2 -adrenergen Signaltransduktion erklärt. Die Publikation untersucht einen möglichen Einfluss von EA 575[®] auf den Signalweg des A_{2B}AR, da diesem eine bedeutende und schädliche Rolle bei chronischen inflammatorischen Atemwegserkrankungen zugeschrieben wurde.

Der Einfluss von EA 575[®] auf das A_{2B}AR-Signalling wurde anhand von verschiedenen zellulären Assays untersucht, welche unterschiedliche Prozesse in der Signalkaskade erfassen. Zunächst wurde ein Effekt auf die allgemeine zelluläre Reaktion nach Stimulation des A_{2B}AR mithilfe von Dynamic Mass Redistribution (DMR)-Messungen getestet. Anschließend wurden die Effekte auf den A_{2B}AR-vermittelten Anstieg des cAMP-Spiegels, die Rekrutierung von β -Arrestin 2 zum A_{2B}AR sowie die Aktivierung von cAMP Response Elements (CRE) mittels Luciferase-basierten HEK293-Reporterzelllinien untersucht. Schließlich wurde der Einfluss auf die Freisetzung von IL-6 in Lungenepithelzellen (Calu-3) mithilfe des Lumit[™] Immunoassays ermittelt. Darüber hinaus wurde der Adenosinrezeptor-Subtyp bestimmt, der diese Effekte vermittelt.

Die Ergebnisse der Publikation zeigen einen inhibitorischen Effekt von EA 575[®] auf die A_{2B}AR-vermittelte allgemeine zelluläre Reaktion, den cAMP-Spiegel, die Rekrutierung von β -Arrestin 2 zum A_{2B}AR, die CRE-Aktivierung und die Freisetzung von IL-6. Aufgrund der Tatsache, dass diese Effekte erst nach Inkubationszeiten von mehreren Stunden auftraten, kann der Wirkmechanismus als indirekt bezeichnet werden. Die Publikation ist die erste, die einen inhibitorischen Effekt von EA 575[®] auf den

Signalweg des A_{2B}AR beschreibt. Somit wurde ein neuer Wirkungsmechanismus von EA 575[®] entdeckt und veröffentlicht. Die Ergebnisse der Studie bieten einen Erklärungsansatz für initiale, positive klinische Effekte von EA 575[®] in der adjuvanten Asthmatherapie. Außerdem liefern sie eine Grundlage zur Durchführung weiterer Studien an Tieren oder menschlichen Probanden, um weitere Effekte in der Behandlung von chronischen Atemwegserkrankungen wie Asthma oder COPD zu untersuchen.

Bei der Erstellung dieser Publikation wurden vor allem folgende Beiträge von mir, Fabio Gian-Luca Meurer, geleistet. Die Methodik wurde von mir in Zusammenarbeit mit meinen Betreuern, Prof. Dr. Hanns Häberlein und PD Dr. Sebastian Franken, erarbeitet. Die Validierung, formale Analyse und die Durchführung aller Experimente wurden selbstständig von mir vorgenommen. Die Datenaufbereitung, visuelle Darstellung der Ergebnisse und die Erstellung des Manuskripts der Publikation, insbesondere das Verfassen des ersten Entwurfs, wurden von mir durchgeführt. Die beiden Betreuer und Koautoren der Publikation haben derweil zur Projektverwaltung, der Konzeptualisierung, den Ressourcen, dem Erwerb von Finanzierungsmitteln sowie dem Überprüfen und Überarbeiten des Manuskripts beigetragen. Diese hiermit transparent dargestellte Erklärung der Autorenbeiträge ist ebenfalls Gegenstand der Publikation und kann zusätzlich an entsprechender Stelle innerhalb dieser nachgeschlagen werden.

Die vollständige Publikation ist im Folgenden als Appendix der Dissertation beigefügt. Alle Koautoren sind mit der Verwendung der Inhalte der Publikation für die Dissertation und mit der Darstellung des Eigenbeitrags des Doktoranden, Fabio Gian-Luca Meurer, einverstanden. Ich bestätige, dass ich die in der PromO § 9 (4) festgelegten Vorgaben eingehalten habe.

Bonn, den 25.01.2024

Anhang

Meurer F, Häberlein H, Franken S. Ivy Leaves Dry Extract EA 575[®] Has an Inhibitory Effect on the Signalling Cascade of the Adenosine Receptor A_{2B}. *International Journal of Molecular Sciences*. 2023;24(15):12373. doi:10.3390/ijms241512373



Article

Ivy Leaf Dry Extract EA 575[®] Has an Inhibitory Effect on the Signalling Cascade of Adenosine Receptor A_{2B}

Fabio Meurer, Hanns Häberlein and Sebastian Franken





Article

Ivy Leaf Dry Extract EA 575[®] Has an Inhibitory Effect on the Signalling Cascade of Adenosine Receptor A_{2B}

Fabio Meurer, Hanns Häberlein and Sebastian Franken * 

Institute of Biochemistry and Molecular Biology, Medical Faculty, University of Bonn, 53115 Bonn, Germany; fameur@uni-bonn.de (F.M.); haeberlein@uni-bonn.de (H.H.)

* Correspondence: sfranken@uni-bonn.de

Abstract: Ivy leaf dry extract EA 575[®] is used to improve complaints of chronic inflammatory bronchial diseases and acute inflammation of the respiratory tract accompanied by coughing. Its mechanism of action has so far been explained by influencing β_2 -adrenergic signal transduction. In the present study, we investigated a possible influence on adenosine receptor A_{2B} (A_{2B}AR) signalling, as it has been described to play a significant and detrimental role in chronic inflammatory airway diseases. The influence of EA 575[®] on A_{2B}AR signalling was assessed with measurements of dynamic mass redistribution. Subsequently, the effects on A_{2B}AR-mediated second messenger cAMP levels, β -arrestin 2 recruitment, and cAMP response element (CRE) activation were examined using luciferase-based HEK293 reporter cell lines. Lastly, the impact on A_{2B}AR-mediated IL-6 release in Calu-3 epithelial lung cells was investigated via the Lumit[™] Immunoassay. Additionally, the adenosine receptor subtype mediating these effects was specified, and A_{2B}AR was found to be responsible. The present study demonstrates an inhibitory influence of EA 575[®] on A_{2B}AR-mediated general cellular response, cAMP levels, β -arrestin 2 recruitment, CRE activation, and IL-6 release. Since these EA 575[®]-mediated effects occur within a time frame of several hours of incubation, its mode of action can be described as indirect. The present data are the first to describe an inhibitory effect of EA 575[®] on A_{2B}AR signalling. This may offer an explanation for the beneficial clinical effects of the extract in adjuvant asthma therapy.

Keywords: ivy leaf dry extract; EA 575[®], adenosine receptor A_{2B}



Citation: Meurer, F.; Häberlein, H.; Franken, S. Ivy Leaf Dry Extract EA 575[®] Has an Inhibitory Effect on the Signalling Cascade of Adenosine Receptor A_{2B}. *Int. J. Mol. Sci.* **2023**, *24*, 12373. <https://doi.org/10.3390/ijms241512373>

Academic Editor: Giovanni Pallio

Received: 7 July 2023

Revised: 26 July 2023

Accepted: 26 July 2023

Published: 3 August 2023



Copyright: © 2023 by the authors. Licensee MDPI, Basel, Switzerland. This article is an open access article distributed under the terms and conditions of the Creative Commons Attribution (CC BY) license (<https://creativecommons.org/licenses/by/4.0/>).

1. Introduction

The use of medicinal products containing ivy leaf dry extract EA 575[®] is recommended for the treatment of chronic inflammatory airway diseases and acute respiratory tract inflammation accompanied by coughing [1–4]. Until now, the main mechanism of action has been explained by influencing the β_2 -adrenergic receptor (β_2 -AR). It has been shown that α -hederin identified in EA 575[®] indirectly inhibits the GRK2-mediated phosphorylation of β_2 -AR [5], which is the reason for the decrease in the recruitment of β -arrestin 2 by EA 575[®] [6]. This leads to the inhibition of β_2 -AR internalisation [7–9], which, in turn, results in increased β_2 -adrenergic responsiveness, as evidenced by a corresponding increase in receptor binding and cAMP formation [6,8]. This biased signalling by EA 575[®] provides an explanation for the bronchospasmolytic and secretolytic effects and a reduction in β -arrestin-mediated negative adverse effects [6]. The anti-inflammatory effects of EA 575[®] are substantiated by the β -arrestin-independent inhibition of NF κ B, presumably by the inhibition of I κ B α phosphorylation, leading to decreased IL-6 release [6,10,11].

Since additional receptor classes are involved in the pathogenesis of these respiratory diseases, we investigated other signalling pathways that may be affected by EA 575[®] and might explain its beneficial effects in the treatment of inflammatory airway diseases. Many authors have described the harmful influence of adenosine via its adenosine receptor A_{2B} (A_{2B}AR) in chronic inflammatory airway diseases [12–15] based on the following findings.

Elevated adenosine concentrations were found in the bronchoalveolar lavage fluid (BALF) and exhaled breath condensate (EBC) of patients with chronic respiratory diseases such as asthma and chronic obstructive pulmonary disease (COPD), indicating increased adenosine levels in the lungs [16–19]. These elevations of adenosine were correlated to decreased forced expiratory volumes in 1 s (FEV₁) and higher Global Initiative for Chronic Obstructive Lung Disease (GOLD) stages [19,20]. Inhalation of adenosine or adenosine monophosphate (AMP) causes bronchoconstriction in patients with asthma and COPD but not in healthy subjects [21–23]. Remarkably, elevated transcript levels of A_{2B}AR were recovered from the lung tissues of patients with severe COPD, pulmonary fibrosis, and pulmonary arterial hypertension (PAH) [24,25]. Further elevation of transcript and A_{2B}AR protein levels was determined in the lung tissues of patients with COPD when accompanied by pulmonary hypertension, indicating a correlation with disease severity [26].

Several experiments in mouse models provide additional evidence for the detrimental impact of adenosine and A_{2B}AR on airway diseases such as asthma, COPD, and pulmonary fibrosis. Genetically altered adenosine deaminase (ADA)-deficient mice developed severe pulmonary inflammation and airway remodelling as observed in these disorders [27,28]. Lowering adenosine concentrations via ADA enzyme therapy ameliorates lung injury, indicating a correlation between adenosine levels and inflammation as well as fibrosis in the lung [29,30]. Attenuation of pulmonary inflammation, fibrosis, and airway enlargement can also be achieved by administration of specific A_{2B}AR antagonists [26,31]. Transcript levels of A_{2B}AR were also increased in this model and could be decreased by specific antagonism of A_{2B}AR [28,31,32].

Similar observations were made in another mouse model. Mice treated with bleomycin exhibited elevated levels of adenosine and transcripts of A_{2B}AR in their lungs and developed pulmonary fibrosis and inflammation. This disease progression could be counteracted with specific A_{2B}AR antagonists [31,33].

The proinflammatory and profibrotic cytokine interleukin-6 (IL-6) is associated with the signalling of adenosine via A_{2B}AR and also plays a pivotal role in these pulmonary disorders [13,34]. Patients with asthma exhibit elevated levels of IL-6 in their sputum and BALF compared to healthy subjects [35–37] and compared to asymptomatic asthmatics [38,39], who already have higher serum IL-6 concentrations [40]. A further IL-6 increase in serum and BALF occur after allergen inhalation and during allergic attacks [40,41]. Most remarkably, the sputum IL-6 levels of asthmatics inversely correlate with FEV₁ and peak expiratory flow [37,42,43].

Elevations of IL-6 have also been found in the sputum and serum of patients with COPD compared to healthy controls [44,45], further increasing during exacerbations [46]. As in asthmatics, higher IL-6 levels inversely correlate with lung function [45,46]. Furthermore, correlations with disease severity [47], GOLD stage and BODE index [44], and even mortality [48] have been described.

Correspondingly, genetic IL-6-knockout or anti-IL-6 antibody treatment led to reduced pulmonary inflammation and fibrosis in both of the aforementioned mouse models [49,50]. Further evidence for the deleterious interaction of IL-6 and A_{2B}AR has been provided by experiments using genetic A_{2B}AR-knockouts. While the adenosine receptor agonist NECA caused increased IL-6 secretion in mouse macrophages, reduced IL-6 levels were found in A_{2B}AR-knockout mice [51,52]. Bleomycin-treated mice also exhibited elevated IL-6 levels, which could be decreased by A_{2B}AR-knockout, resulting in improved lung function as well as attenuated pulmonary fibrosis and hypertension [25,33,53]. Moreover, ADA enzyme therapy in ADA-deficient mice was able to reduce IL-6 levels [50].

The present study demonstrates the influence of the ivy leaf dry extract EA 575[®] on adenosine receptor A_{2B} signalling and subsequent IL-6 release. These processes have been described to play a significant and detrimental role in chronic inflammatory pulmonary diseases. The findings may provide an explanation for the positive clinical effects of EA 575[®] in adjuvant asthma therapy by inhibiting A_{2B}AR signalling.

2. Results

2.1. Dynamic Mass Redistribution Measurements

To investigate the influence of the ivy leaf dry extract, EA 575[®], on the cellular reaction evoked by the stimulation of A_{2B}AR, dynamic mass redistribution (DMR) assays were performed. The cellular reaction of HEK cells to 0.5 μM of the A_{2B}AR agonist BAY 60-6583 resulted in a positive wavelength shift mediated by the dynamic mass redistribution of intracellular particles, which was significantly and dose-dependently inhibited up to 45.95 ± 12.36% by pre-incubation with 160–240 μg/mL EA 575[®] for 16 h (Figure 1A).

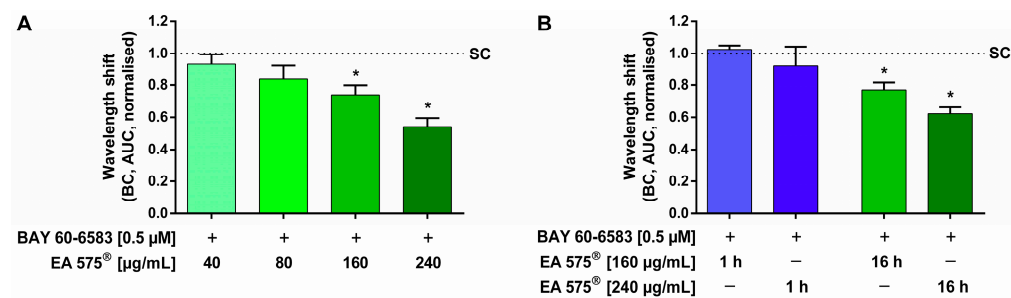


Figure 1. Influence of EA 575[®] (A) and different incubation periods thereof (B) on the cellular reaction of HEK cells evoked by stimulation of A_{2B}AR. Pre-incubation with different concentrations of EA 575[®] was performed for 16 h (A) and 1 or 16 h (B) before cells were stimulated with 0.5 μM BAY 60-6583. The positive wavelength shift mediated by the dynamic mass redistribution of intracellular particles was significantly and dose-dependently inhibited by pre-incubation with 160–240 μg/mL EA 575[®], compared to stimulated control cells not pre-incubated with EA 575[®] (SC) (A). With an incubation time of 1 h, no reduction in BAY 60-6583-mediated wavelength shift was measured. A significant inhibition was only achieved by pre-incubation with 240 μg/mL EA 575[®] for 16 h (B). Data are shown as baseline-corrected (BC) AUC normalised to stimulated control cells not pre-incubated with EA 575[®] (SC). Results represent the mean and SEM ((A): *n* = 5 independent experiments performed in triplicate; (B): *n* = 1 experiment performed in triplicate, * *p* < 0.05).

In order to examine whether the observed effect results from direct inhibition of the receptor, pre-incubation of HEK cells with EA 575[®] was conducted for 1 and 16 h. A reduction in wavelength shifts was exclusively observed with 16 h of pre-incubation time, while a shorter incubation period of 1 h did not alter BAY 60-6583-mediated wavelength shifts (Figure 1B).

2.2. cAMP Measurements

The influence of EA 575[®] on the intracellular cAMP level induced by the stimulation of A_{2B}AR was determined using HEK cells stably expressing luciferase fused with a cAMP binding domain (GloSensor[™], Promega, Mannheim, Germany). Elevation of the second messenger cAMP was elicited by simultaneous stimulation with 1 μM BAY 60-6583 and 1 μM forskolin for one hour. Pre-incubation with 160–240 μg/mL EA 575[®] for 16 h led to a significant and dose-dependent reduction in cAMP levels by up to 39.02 ± 9.92%, compared to stimulated control cells not pre-incubated with EA 575[®] (Figure 2A).

In order to determine if the observed effect was mediated by direct inhibition of the receptor and after what time it occurred, different pre-incubation periods were tested. A pre-incubation time of at least 8 h was required to observe a significant decrease in cAMP levels (Figure 2B).

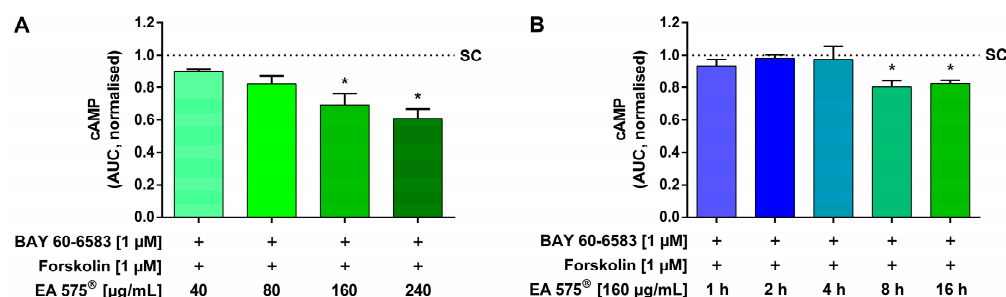


Figure 2. Influence of EA 575[®] (A) and different incubation periods thereof (B) on the intracellular cAMP level in HEK GloSensor[™] cells elicited by stimulation of A_{2B}AR. Prior to co-stimulation with 1 µM BAY 60-6583 and 1 µM forskolin, pre-incubation with different concentrations of EA 575[®] was performed for 16 h (A) and for 1–16 h with 160 µg/mL EA 575[®] (B). The A_{2B}AR-induced cAMP increase was significantly and dose-dependently inhibited by pre-incubation with 160–240 µg/mL EA 575[®], compared to stimulated control cells not pre-incubated with EA 575[®] (SC) (A). Pre-incubation for at least 8 h was necessary to cause a significant decrease in cAMP levels (B). Data are presented as AUC normalised to stimulated control cells not pre-incubated with EA 575[®] (SC). Results represent the mean and SEM ($n = 3$ independent experiments performed in triplicate, * $p < 0.05$).

2.3. Measurements of β -Arrestin 2 Recruitment

To investigate another possible process involved in the inhibition of A_{2B}AR by EA 575[®], measurements of β -arrestin 2 recruitment were performed. HEK cells transiently expressing A_{2B}AR-LgBiT and SmBiT- β -arrestin 2 generated a luminescence signal after stimulation with the unspecific adenosine receptor agonist NECA or BAY 60-6583, indicating β -arrestin 2 recruitment to A_{2B}AR. Pre-incubation with 160 µg/mL EA 575[®] for 16 h led to significant inhibition of both NECA- and BAY 60-6583-mediated β -arrestin 2 recruitment by $16.90 \pm 4.69\%$ and $9.31 \pm 4.82\%$, respectively (Figure 3).

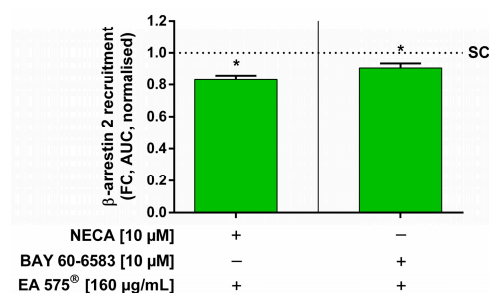


Figure 3. Influence of EA 575[®] on the recruitment of β -arrestin 2 to the A_{2B}AR in transiently transfected HEK cells induced by stimulation with NECA or BAY 60-6583. Pre-incubation with 160 µg/mL EA 575[®] was conducted for 16 h before cells were stimulated with 10 µM NECA or 10 µM BAY 60-6583. EA 575[®] was able to significantly inhibit the recruitment of β -arrestin 2 to the A_{2B}AR induced by both NECA and BAY 60-6583. Data are shown as AUC of the fold change (FC) after stimulation normalised to equally stimulated control cells not pre-incubated with EA 575[®] (SC). Results represent the mean and SEM ($n = 3$ independent experiments performed in triplicate, * $p < 0.05$).

2.4. Measurements of CRE Activation

The influence of EA 575[®] on cAMP response elements (CRE) was investigated using HEK cells transiently expressing NanoLuc[®]-PEST under the control of a promoter with cAMP response elements.

The impact of EA 575[®] on adenosine-mediated CRE activation was examined first. Compared to stimulated control cells not pre-incubated with EA 575[®], pre-incubation with 80–240 µg/mL EA 575[®] for 16 h led to a significant reduction by a maximum of $24.23 \pm 9.38\%$ of the CRE activation mediated by stimulation with 100 µM adenosine

(Figure 4A). Pre-incubation with EA 575[®] also specifically inhibited A_{2B}AR-mediated CRE activation by 10 μ M BAY 60-6583 in a dose-dependent manner up to $20.18 \pm 2.67\%$, being significant at 80–240 μ g/mL (Figure 4B).

Since adenosine is a non-specific agonist binding to all adenosine receptor subtypes, identification of the receptor accountable for the observed effect was addressed next. For this purpose, cells were pre-incubated with the A_{2B}AR-specific antagonist PSB-603 or the A_{2A}AR-specific antagonist SCH 442416 for one hour prior to stimulation with 100 μ M adenosine. PSB-603 was able to significantly inhibit the adenosine-mediated CRE activation by $33.37 \pm 6.63\%$ at a concentration of 1 μ M, while SCH 442416 significantly reduced the CRE activation by $54.11 \pm 7.90\%$ at a concentration of 10 μ M. Lower concentrations of both antagonists did not show a significant reduction in the signal, whereas 0.1 μ M SCH 442416 significantly increased CRE activation by $34.64 \pm 12.25\%$ (Figure 4C).

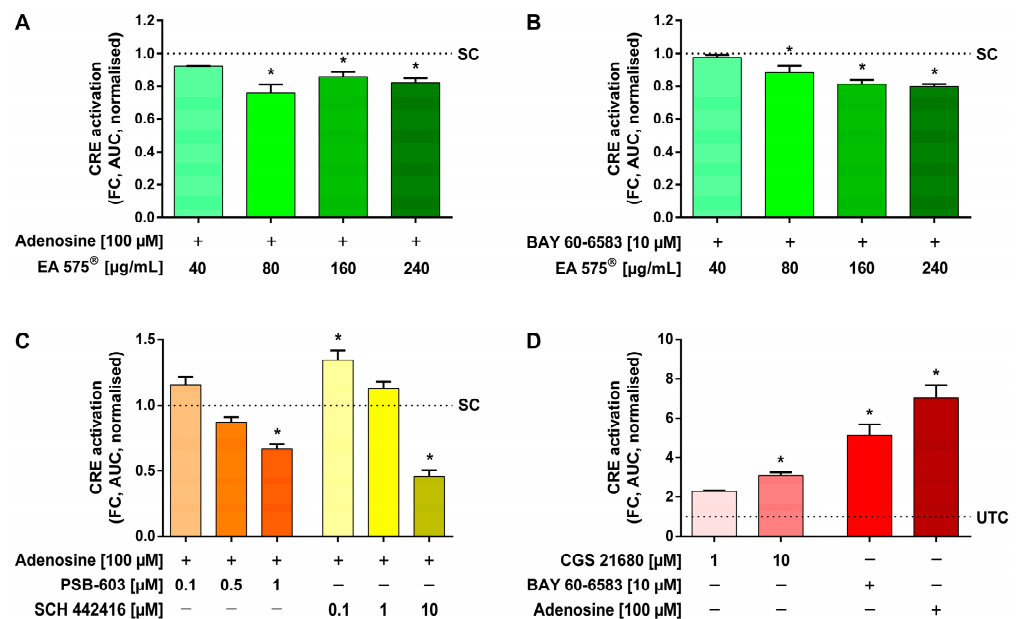


Figure 4. Influence of EA 575[®] (A,B) or the antagonists PSB-603 and SCH 442416 (C) on the CRE activation in transiently transfected HEK cells mediated by stimulation with adenosine (A,C) or BAY 60-6583 (B). Pre-incubation with 40–240 μ g/mL EA 575[®] was conducted for 16 h (A,B) or with 0.1–10 μ M of the antagonists for 2 h (C) before cells were stimulated by adding 100 μ M adenosine (A,C) or 10 μ M BAY 60-6583 (B). The non-specifically mediated CRE activation was significantly inhibited by pre-incubation with 80–240 μ g/mL EA 575[®] (A) or 1 μ M PSB-603 (C), compared to stimulated control cells not pre-incubated with EA 575[®] (SC). SCH 442416 also significantly reduced the CRE activation at a concentration of 10 μ M, whereas this effect could not be observed at lower concentrations of both antagonists. Instead, 0.1 μ M SCH 442416 slightly increased the CRE activation (C). The inhibition of the specific A_{2B}AR-mediated CRE activation was achieved by pre-incubation with 80–240 μ g/mL EA 575[®] (B). Influence of the A_{2A}AR agonist CGS 21680 and, in comparison, BAY 60-6583 and adenosine on the CRE activation in transiently transfected HEK cells (D). Stimulation was performed with 1–10 μ M CGS 21680, 10 μ M BAY 60-6583, or 100 μ M adenosine. The A_{2A}AR-mediated CRE activation was significantly increased by 10 μ M CGS 21680 compared with completely untreated control cells (UTC), but to a lesser extent than that mediated by A_{2B}AR or non-specifically using adenosine (D). Data are shown as AUC of the fold change (FC) after stimulation normalised to stimulated control cells not pre-incubated with EA 575[®] (SC) (A–C) or completely untreated control cells (UTC) (D). Results represent the mean and SEM ($n = 3$ independent experiments performed in triplicate, * $p < 0.05$).

CRE activation could also be mediated by stimulation with 10 μ M of the A_{2A}AR agonist CGS 21680, resulting in a significant 3.10 ± 0.24 -fold increase in the luminescence signal compared to completely untreated control cells. Nevertheless, this A_{2A}AR stimulation

elicited a smaller effect than 10 μM BAY 60-6583, which showed a 5.14 ± 0.93 -fold elevation, and 100 μM adenosine, for which the signal was highest with a 7.06 ± 1.09 -fold increase (Figure 4D).

2.5. IL-6 Measurements

IL-6 release of Calu-3 cells was provoked by stimulation with 100 μM adenosine and measured as luminescence using the LumitTM IL-6 (Human) Immunoassay by Promega.

The influence of EA 575[®] on this non-specifically mediated IL-6 release was investigated. Compared to stimulated control cells not pre-incubated with EA 575[®], pre-incubation with 80–240 $\mu\text{g}/\text{mL}$ EA 575[®] for 16 h led to a significant and dose-dependent reduction by up to $33.73 \pm 10.76\%$ of the adenosine-mediated IL-6 release (Figure 5A). Also, when pre-incubating with 40–240 $\mu\text{g}/\text{mL}$ EA 575[®], BAY 60-6583-mediated IL-6 release was significantly inhibited up to $36.36 \pm 2.16\%$ in a dose-dependent manner (Figure 5B).

Receptor-specific antagonists PSB-603 and SCH 442416 were employed to identify the specific receptor subtype involved in the induction of adenosine-mediated IL-6 release. PSB-603 was able to significantly inhibit the adenosine-mediated IL-6 release by $22.56 \pm 8.19\%$ at a concentration of 1 μM , whereas SCH 442416 increased the concentration of IL-6 even further by up to $24.99 \pm 9.57\%$ (Figure 5C).

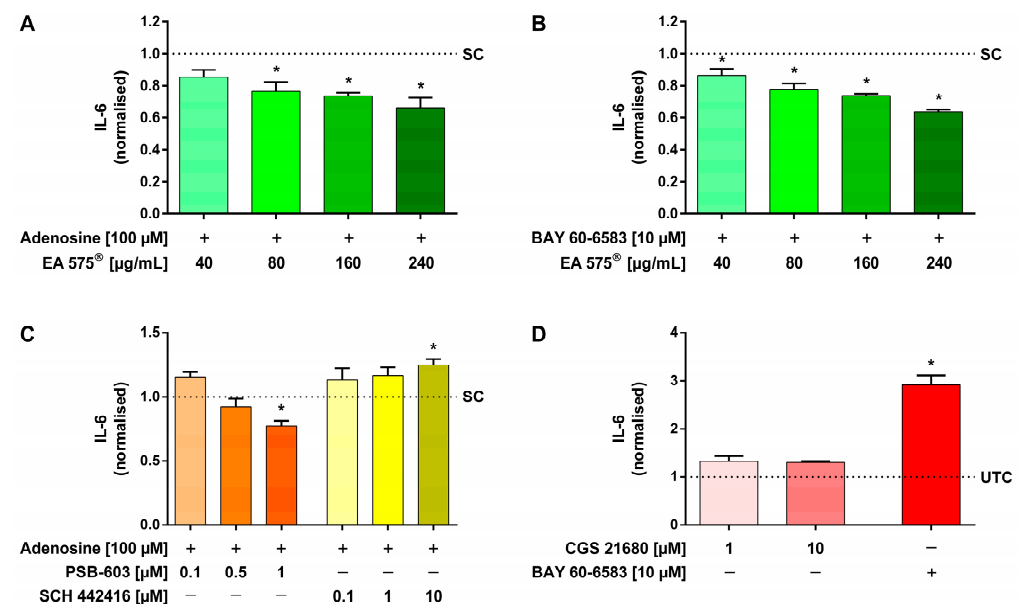


Figure 5. Influence of EA 575[®] (A,B) or the antagonists PSB-603 and SCH 442416 (C) on the IL-6 release of Calu-3 cells mediated by stimulation with adenosine (A,C) or BAY 60-6583 (B). Pre-incubation with 40–240 $\mu\text{g}/\text{mL}$ EA 575[®] was conducted for 16 h (A,B) or with 0.1–10 μM of the antagonists for 1 h (C) before cells were stimulated by adding 100 μM adenosine (A,C) or 10 μM BAY 60-6583 (B) for another 24 h. The non-specifically mediated IL-6 release was significantly and dose-dependently inhibited by pre-incubation with 80–240 $\mu\text{g}/\text{mL}$ EA 575[®] (A) or 1 μM PSB-603 (C), compared to stimulated control cells not pre-incubated with EA 575[®] (SC). SCH 442416, however, increased the concentration of IL-6 even further. (C). The inhibition of the specific A_{2B}AR-mediated IL-6 release was achieved by pre-incubation with 40–240 $\mu\text{g}/\text{mL}$ EA 575[®] (B). Influence of the A_{2A}AR agonist CGS 21680 and, in comparison, BAY 60-6583 on the IL-6 release of Calu-3 cells (D). Stimulation was performed with 1–10 μM CGS 21680 or 10 μM BAY 60-6583 for 24 h. The A_{2A}AR-mediated IL-6 release was slightly, but neither significantly nor dose-dependently, increased compared to completely untreated control cells (UTC) (D). Results represent the mean normalised to stimulated control cells not pre-incubated with EA 575[®] (SC) (A–C) or completely untreated control cells (UTC) (D) and SEM ($n = 3$ independent experiments performed in triplicate, * $p < 0.05$).

In another approach, stimulation was performed with 10 μ M BAY 60-6583, resulting in a 2.91 ± 0.35 -fold increase in IL-6 release, while A_{2A} AR agonist CGS 21680 had no significant effect, showing a maximal 1.33 ± 0.20 -fold IL-6 increase, compared to completely untreated control cells (Figure 5D).

2.6. Measurements of NF κ B Transcriptional Activity

In order to evaluate whether the observed effect of an IL-6 release via adenosine receptors in Calu-3 cells was NF κ B-dependent, the influence of adenosine receptor agonists on NF κ B transcriptional activity was investigated using an NF κ B reporter gene cell line. Calu-3 cells stably expressing a secreted NanoLuc[®] under the control of an NF κ B-binding sequence reacted with a 1.62 ± 0.11 -fold increase in the luminescence signal to stimulation with 25 ng/mL TNF α for 3 h. However, neither 10–100 μ M adenosine, nor 1–10 μ M NECA, nor 1–10 μ M BAY 60-6583 showed any effect on the NF κ B transcriptional activity (Figure 6).

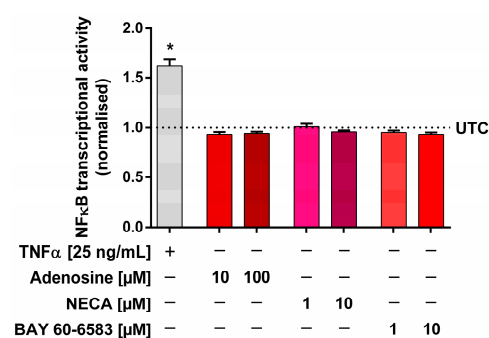


Figure 6. Influence of different adenosine receptor agonists on NF κ B transcriptional activity. Calu-3 cells stably expressing a secreted NanoLuc[®] under control of an NF κ B binding sequence were stimulated for 3 h. An amount of 25 ng/mL TNF α was used as positive control, resulting in a significant increase in the luminescence signal. Amounts of 10–100 μ M adenosine, 1–10 μ M NECA, or 1–10 μ M BAY 60-6583 did not show any effect on the NF κ B transcriptional activity. Results represent the mean normalised to completely untreated control cells (UTC) and SEM ($n = 3$ independent experiments performed in triplicate, * $p < 0.05$).

3. Discussion

In the present study, we further explored the mechanism of action of the ivy leaf dry extract EA 575[®] to explain its positive effects on inflammatory airway diseases [2–4]. Since adenosine receptor A_{2B} (A_{2B} AR) plays an essential role in the pathogenesis of chronic inflammatory airway diseases such as asthma, COPD, and pulmonary fibrosis [12–15], we investigated a possible effect of EA 575[®] on this receptor.

We first examined a possible impact of EA 575[®] on the cellular response of HEK cells to stimulation of the A_{2B} AR using DMR measurements. This label-free technology is well-suited for an initial investigation of the general influence of ligands on GPCR signalling due to its capability to provide a holistic overview of the complex cellular response [54]. We observed the dose-dependent inhibition of the cellular reaction to A_{2B} AR stimulation by EA 575[®]. This effect was observed after 16 h of pre-incubation, while no impact was seen after a short incubation time of 1 h, indicating indirect inhibition of A_{2B} AR.

To further specify the influenced cellular response observed in the DMR experiments, second messenger cAMP was assessed. In alignment with the DMR results, a corresponding decrease in cAMP levels was observed after pre-treatment with EA 575[®] under A_{2B} AR stimulatory conditions. A similar effect was shown for the highly selective A_{2B} AR antagonist PSB-603 using the same cAMP biosensor technology [55]. Next, we challenged the required minimum incubation time period and found that at least 8 h of EA 575[®] pre-incubation was necessary to mediate a reduction in cAMP levels. Such long incubation periods are unlikely to be in accordance with a direct mode of action, as these ligands typically compete for receptor binding sites within minutes. PSB-603, for example, requires

a pre-incubation period of only 30 min in this assay [55]. These findings confirm that EA 575[®] is able to inhibit the A_{2B}AR signalling pathway and that this can be explained by an indirect mechanism of action. Since adenosine receptors are ubiquitously expressed in humans, this could be advantageous over orthosteric antagonism in terms of adverse effects [56]. To our knowledge, the present study is the first to show the influence of an ivy extract on adenosine receptor A_{2B}.

To further investigate the mode of action of EA 575[®] on A_{2B}AR and to determine whether it also influences other downstream signalling pathways, the recruitment of β -arrestin 2 to A_{2B}AR was examined. For this purpose, a slightly modified assay system recently described by Saecker et al. was used [57]. In this system, A_{2B}AR is tagged with LgBiT and β -arrestin 2 with SmBiT. When β -arrestin 2 recruitment occurs specifically to A_{2B}AR, luminescence is generated by reversible complementation of a nanoluciferase. Stimulation was performed using the unspecific adenosine receptor agonist NECA, as well as the specific A_{2B}AR agonist BAY 60-6583. Since A_{2B}AR is the only receptor tagged with LgBiT in this system, the effects detected after stimulation with NECA can also be considered specific for this receptor in this case. EA 575[®] caused a reduction in β -arrestin 2 recruitment to A_{2B}AR and thus affected the receptor signalling in an inhibitory manner in several ways. This is remarkable as under β_2 -AR stimulatory conditions, EA 575[®] inhibits β -arrestin 2 recruitment while enhancing G protein/cAMP signalling [6].

In the downstream signalling cascade of G_s protein-coupled receptors such as A_{2B}AR, cAMP causes phosphorylation of cAMP response element-binding protein via PKA, PKC, and ERK, and can thereby activate cAMP response elements (CRE) located in promoter regions, thus affecting the transcriptional activity of genes [58–61]. Since EA 575[®] reduced cAMP levels under A_{2B}AR stimulatory conditions, subsequent inhibition of CRE was expected. Indeed, EA 575[®] inhibited CRE activation mediated both non-specifically by adenosine as well as A_{2B}AR-specifically by BAY 60-6583. A similar result was found for a specific A_{2B}AR antagonist, which reduced the NECA-mediated phosphorylation of CRE binding protein [62].

One of the genes regulated by CRE, encoding IL-6, plays a crucial role in several inflammatory and airway diseases, such as asthma and COPD [34]. The IL-6 promoter region contains several elements that activate IL-6 expression, one of which is a CRE [63–67]. The release of IL-6 and other inflammatory and chemotactic mediators, in turn, can be mediated by adenosine via the A_{2B}AR signalling pathway, and CRE might be at least one important factor in this signalling cascade [68,69]. Since EA 575[®] inhibits both A_{2B}AR signalling and CRE activation, an effect on IL-6 release seemed plausible. Therefore, we tested the potential effect of EA 575[®] on the adenosine-mediated IL-6 release in Calu-3 cells. It was found that EA 575[®], in fact, reduces the adenosine-mediated release of IL-6, indicating a possible reduction in IL-6-mediated airway inflammation and fibrosis. This inhibition of A_{2B}AR-mediated IL-6 release could also be reproduced with the specific agonist BAY 60-6583.

This is a new finding that complements the previously published decrease in IL-6 release by EA 575[®] via inhibition of NF κ B. In our experiments, we were able to demonstrate that neither adenosine, NECA, nor BAY 60-6583 influenced NF κ B transcriptional activity in Calu-3 cells. Although the IL-6 promoter region contains an NF κ B binding element [70,71], the release of IL-6 via adenosine receptors is not mediated by this promoter element. This is in line with the results published by Sitaraman et al., who showed that the NF κ B binding site, in contrast to the CRE binding site, is not important for adenosine-mediated IL-6 release [69]. Similarly, Zhong et al. found that NECA does not affect NF κ B-mediated transcription but rather affects CRE-mediated transcription [68]. Therefore, in this case, EA 575[®] affects IL-6 release via another mechanism, which could be the inhibition of CRE.

Additionally, we wanted to specify which adenosine receptor subtype is responsible for the observed effects in the IL-6 and CRE activation assays. Therefore, we investigated the inhibition of the adenosine-mediated CRE activation and IL-6 release with the A_{2A}AR antagonist SCH 442416 or the A_{2B}AR antagonist PSB-603, as these are the predominantly

expressed adenosine receptor subtypes in the cell types we used [72–74]. Only PSB-603 reduced both CRE activation and IL-6 release after stimulation with adenosine. In contrast, SCH 442416 caused the inhibition of CRE activation but simultaneously led to a slight increase in IL-6 release. In addition, CGS 21680, a specific A_{2A} AR agonist, was shown to increase CRE activation in a dose-dependent manner but had no effect on IL-6 release. These data suggest that A_{2A} AR signalling activates CRE but does not result in an increase in IL-6. This might be because IL-6 is regulated not only by the cAMP response element but also by several other elements, as mentioned above. These findings suggest that adenosine mediates IL-6 release through CRE activation via A_{2B} AR. Furthermore, adenosine mediates IL-6 release only in concentrations as high as 10–100 μ M [61,68,69,75]. Considering the affinities of adenosine to the different receptor subtypes (EC_{50} : $A_1 = 0.31 \mu$ M, $A_{2A} = 0.73 \mu$ M, $A_{2B} = 23.5 \mu$ M, $A_3 = 0.29 \mu$ M) [76], this also suggests mediation via A_{2B} AR. Taken together, published receptor-affinity data and our results indicate that adenosine-induced IL-6 release is mediated through the A_{2B} AR signalling pathway. These findings disagree with those of Sun et al., who stated that A_{2A} AR, but not A_{2B} AR, is responsible for adenosine-mediated IL-6 release [61], but are consistent with data from Sitaraman et al. and Zhong et al., who both identified A_{2B} AR as being responsible for adenosine-mediated IL-6 release [68,69,75]. Although not particularly distinguishing between the two receptors, several other studies have provided additional evidence for the A_{2B} AR-mediated inhibition of IL-6 release. Elevated IL-6 levels in ADA-deficient and bleomycin-treated mice were reduced by the administration of a specific A_{2B} AR antagonist [31,33]. Additionally, a NECA-mediated increase in IL-6 was reduced by antagonists of A_{2B} AR in these models [33,50]. A reduction in NECA-mediated IL-6 elevation by A_{2B} AR antagonists was also shown in macrophages [24,52]. Secretion of IL-6 after treating pulmonary arterial smooth muscle cells of PAH patients with BAY 60-6583 under hypoxic conditions was also reduced by a specific antagonist of A_{2B} AR [25].

Moreover, A_{2A} AR signalling is described as anti-inflammatory and lung protective, which basically matches our results, suggesting that this receptor does not contribute to IL-6 release but rather attenuates it [12–14]. Nevertheless, our findings differ from others in terms of the influence of A_{2A} AR on IL-6. There have been reports of both increases [77] as well as reductions [78–81] by the stimulation of A_{2A} AR with CGS 21680, whereas other research, similar to our study, found no effect [82,83]. Furthermore, the genetic knockout of A_{2A} AR in mice led to higher expressions of IL-6 in one study [84] but did not affect IL-6 in another study examining an ADA/ A_{2A} AR double knockout [85]. However, in other studies, antagonism of A_{2A} AR caused the elevation of IL-6 levels, matching our findings [79,80,82].

Several factors may account for these controversial findings. First, the effect of adenosine may be dependent on its concentration and the stage of the disease. At low levels, adenosine activates high-affinity receptors such as A_{2A} AR, triggering anti-inflammatory pathways. In highly inflammatory environments and chronic disease states such as asthma or COPD, higher levels of adenosine are released. Adenosine concentrations have been estimated to reach about 200 μ M in the lungs of asthmatics [16]. At such high concentrations, low-affinity A_{2B} AR is activated, which may lead to further exacerbation of airway inflammation [15]. Inhibition of A_{2B} AR is therefore considered beneficial in chronic inflammatory airway diseases [12–14]. In a guinea pig model of asthma, antagonism of A_{2B} AR ameliorated the changes provoked by an allergen challenge, whereas A_{2A} AR antagonism deteriorated them [86]. A_{2B} AR antagonism also proved beneficial in mouse models of chronic lung diseases as it attenuated bronchoconstriction, airway inflammation, pulmonary fibrosis, and airspace enlargement [26,31,33,87].

In conclusion, this offers a possible explanation for the positive clinical effects of the extract in adjuvant asthma therapy by means of a possible reduction in adenosine-mediated inflammation and bronchoconstriction [88]. Still, further research is necessary to fully understand the mechanisms of action of this versatile extract. It is still unclear which constituents play a role in the observed effects. It has been shown that a fraction of an ivy leaf

extract enriched in phenolics and flavonoids elicits anti-inflammatory properties [89,90]. Since some of the enriched substances have also been identified in EA 575[®], future investigations should be performed with the pure compounds. However, the results presented here provide a rationale for further studies in animals or human subjects to prove further effects regarding chronic airway diseases such as asthma or COPD.

4. Materials and Methods

4.1. Chemicals

Ivy leaf dry extract EA 575[®] (DER 5-7.5:1, 30% ethanol; batch number 14B0310) was received from Engelhard Arzneimittel (Niederdorfelden, Germany) and is well characterised by 17 ingredients from the natural product classes of flavonoids, saponins, and dicaffeoylquinic acids identified via LC-MS analysis [7]. All reagents for luciferase assays were received from Promega (Mannheim, Germany) if not stated otherwise. Coelenterazine h was obtained from Prolume (Pinetop-Lakeside, AZ, USA). Adenosine, BAY 60-6583, forskolin, 5'-N-Ethylcarboxamidoadenosine (NECA), and SCH 442416 were obtained from Sigma-Aldrich (Crailsheim, Germany). TNF α was received from Merck (Darmstadt, Germany). PSB-603 and CGS 21680 were obtained from Biomol (Hamburg, Germany).

4.2. Cell Culture

Human embryonic kidney cells (HEK293), subsequently called HEK cells, were obtained from DSMZ (No. ACC 305; Braunschweig, Germany). HEK cells and all constructed clones were cultivated at 37 °C with 5% CO₂ in DMEM supplemented with 100 units/mL penicillin, 100 μ g/mL streptomycin, and 10% fetal bovine serum (FBS) (all obtained from Thermo Fisher Scientific, Waltham, MA, USA). Cells were subcultured 1:10 every 3–4 days in 10 cm cell culture dishes.

Calu-3 cells were obtained from ATCC (HTB-55; Manassas, VA, USA). Calu-3 cells and all constructed clones were cultivated at 37 °C with 5% CO₂ in DMEM/F-12 supplemented with GlutaMAX[™], 100 units/mL penicillin, 100 μ g/mL streptomycin, and 15% FBS (all obtained from Thermo Fisher Scientific). Cells were subcultured 1:5 every 5–7 days in 10 cm cell culture dishes.

4.3. Dynamic Mass Redistribution Measurements

Dynamic mass redistribution (DMR) measurements were performed using the Corning Epic[®] biosensor. HEK GloSensor[™] cells were seeded at a density of 3000 cells per well in a 384-well plate by Corning (#5042; Corning, NY, USA) and allowed to grow for at least 24 h in full growth medium. Pre-incubation was performed with 40, 80, 160, or 240 μ g/mL EA 575[®] for up to 16 h. After pre-incubation, the medium was replaced by HBSS supplemented with 20 mM HEPES and the cells were allowed to equilibrate at 37 °C for one hour. A baseline of 10 measurement points was recorded before stimulation was performed using a CyBi[®]-SELMA semi-automatic pipetting system (Analytik Jena AG, Jena, Germany) at 37 °C. Subsequently, the wavelength shift mediated by the dynamic mass redistribution of intracellular particles was measured for another 70 min.

4.4. cAMP Measurements

The establishment of HEK cells expressing a cAMP sensor and the measurement of cAMP were performed as described by Bussmann et al. [8]. Briefly, pre-incubation was carried out with 40, 80, 160, or 240 μ g/mL EA 575[®] for up to 16 h in full growth medium. After pre-incubation, the medium was changed to a substrate solution containing 4% GloSensor[™] cAMP reagent stock solution in HEPES-buffered DMEM. Cells were incubated at 37 °C for one hour and subsequently equilibrated at room temperature in the plate reader (Tecan Infinite[®] 200 PRO, Tecan, Männedorf, Switzerland) for another hour. Stimulation was performed with 1 μ M BAY 60-6583 and 1 μ M forskolin simultaneously, and cAMP increase was measured as luminescence for one hour after stimulation.

4.5. Measurements of β -Arrestin 2 Recruitment

The plasmid coding for human adenosine receptor A_{2B} ($A_{2B}AR$) fused to the N-terminus of Large BiT (LgBiT) was generated by initially removing the region coding for YFP of the vector *pEYFP-N1-A2BR*, which was a gift from Robert Tarran (Addgene plasmid # 37202; <http://n2t.net/addgene:37202> (accessed 13 November 2019); RRID:Addgene_37202) [91], using BamHI/NotI. The open reading frame coding for LgBiT was amplified via PCR (forward primer: 5'-GATCGGATCCAAGTGGTAGCGGGGTCTTTACCCTG-3'; reverse primer: 5'-GATCGCGGCCGCTAGCTACCACCGCATCC-3'). The PCR product was cut with BamHI/NotI and inserted into the vector via ligation.

For expression of rat β -arrestin 2 with an N-terminal Small BiT (SmBiT), the coding sequence was taken from *pECFP-N1-r β -arrestin-2* (a gift from M. Bouvier, Montreal, QC, Canada) by restriction with NheI/SalI. The fragment was introduced into *pcDNATM3.1/Zeo⁽⁺⁾* Mammalian Expression Vector (Invitrogen, Waltham, MA, USA) containing the information for the SmBiT via NheI and XhoI sites.

HEK cells were co-transfected to transiently express $A_{2B}AR$ -LgBiT and SmBiT- β -arrestin 2 using branched polyethylenimine (PEI) (Sigma-Aldrich). For this purpose, cells were seeded in a 6-well plate at a density of 350,000 cells per well and allowed to grow for one day. For each DNA, 1.5 μ g was diluted into 200 μ L of 150 mM NaCl, then 7.5 μ L of a 1 mg/mL PEI solution was added, and the mixture was vortexed immediately for 10 s. After 10 min at RT, the DNA/PEI mixture was added to the cells and incubated for 24 h. The transiently transfected cells were seeded in a 96-well plate at a density of 15,000 cells per well and allowed to grow for one day in full growth medium. Pre-incubation was carried out with 160 μ g/mL EA 575[®] for 16 h.

In general, measurements of recruitment of β -arrestin 2 to $A_{2B}AR$ were performed as recently described by Saecker et al. for $A_{1}AR$ [57]. Briefly, pre-incubation medium was replaced by a solution of 2.5 μ M coelenterazine h in HBSS supplemented with 20 mM HEPES. A baseline of 3 measurement points was recorded before stimulation was performed. Subsequently, luminescence corresponding to the recruitment of β -arrestin 2 was measured for another 27 min using a Spark[®] plate reader by Tecan.

4.6. Measurements of CRE Activation

The plasmid expressing NanoLuc[®]-PEST (NlucP) from a promoter with cAMP response elements (CRE) was received by Promega. HEK cells were transfected to transiently express this construct using PEI, as described above. Transiently transfected HEK cells were seeded in a 96-well plate at a density of 20,000 cells per well and allowed to grow for one day in fully supplemented medium. Pre-incubation was conducted with 40, 80, 160, or 240 μ g/mL EA 575[®] in full growth medium for 16 h. Pre-incubation with antagonists was carried out for only two hours, simultaneously with the substrate incubation. Nano-Glo[®] VivazineTM Live Cell Substrate (Promega) was prepared according to the manufacturer's instructions using HEPES-buffered medium, and cells were incubated with the substrate for 2 h at 37 °C in a Tecan Spark[®] plate reader already measuring luminescence. Stimulation was then performed by adding adenosine, BAY 60-6583, or CGS 21680, and measurement was performed for another 22 h.

4.7. IL-6 Measurements

Measurement of IL-6 release was performed using the LumitTM IL-6 (Human) Immunoassay by Promega. Calu-3 cells were seeded in a 96-well plate at a density of 20,000 cells per well and allowed to grow for at least two days to a confluency of 80–90% in full growth medium. Pre-incubation was carried out with 40, 80, 160, or 240 μ g/mL EA 575[®] in DMEM/F-12 without phenol red supplemented with GlutaMAXTM and 5% FBS for 16 h. Pre-incubation with antagonists was conducted for only one hour. IL-6 release was then provoked by adding adenosine, BAY 60-6583, or CGS 21680 for the following 24 h. Subsequently, the measurement of IL-6 was performed according to the manufacturer's instructions using a Tecan Spark[®] plate reader.

4.8. Measurements of NFκB Transcriptional Activity

For the generation of a secreted NanoLuc[®] expression construct under the control of an NFκB binding sequence, the *pNFκB-d2EGFP* vector (Clontech, Mountain View, CA, USA) was used as a first template. Destabilised GFP was removed from the vector by PCR (forward primer: 5'-TCGGATATCTCGAGCCGGAATTCGGGGAAGCTTC-3'; reverse primer: 5'-GTTTCAGGGGGAGGTGTG-3') and restriction with BamHI/XhoI. The open reading frame coding for the secreted NanoLuc[®] was cut from *pNL1.3[secNluc]* vector (Promega) using BamHI/XhoI and introduced into the vector via ligation.

In a second step, this secreted NanoLuc[®] expression construct, under the control of an NFκB binding sequence, was cloned into the *pcDNATM3.1⁽⁺⁾* Mammalian Expression Vector (Invitrogen). Therefore, the CMV promoter was removed from the vector by restriction with BamHI/BglII and re-ligation. Then, the vector was re-cut with NotI/XhoI. The insert was isolated out of the plasmid generated in the first step using NotI/SalI and introduced into the vector via ligation.

Calu-3 cells were transfected using Metafectene[®] Pro (Biontex, Munich, Germany) according to the manufacturer's instructions. For the selection of successfully transfected cells, the medium was changed to fully supplemented DMEM/F-12 containing 600 µg/mL G418 (Thermo Fisher Scientific).

Cells were seeded in a 96-well plate at a density of 25,000 cells per well and allowed to grow for at least two days to a confluency of 80–90% in full growth medium. Before stimulating with TNFα, adenosine, NECA, or BAY 60-6583 for 3 h, cells were starved overnight. Measurement of NFκB transcriptional activity was performed in a Tecan Spark[®] plate reader using the Nano-Glo[®] Luciferase Assay System (Promega) according to the manufacturer's instructions.

4.9. Statistical Analysis

For statistical analysis, one-way analysis of variance (ANOVA) with Dunnett's multiple comparisons test was performed using Prism software version 6.01 (GraphPad Software, San Diego, CA, USA). Results were considered to be significant for *p*-values of <0.05.

Author Contributions: Conceptualisation, H.H. and S.F.; methodology, F.M., H.H. and S.F.; software, F.M.; validation, F.M.; formal analysis, F.M.; investigation, F.M.; resources, H.H. and S.F.; data curation, F.M.; writing—original draft preparation, F.M.; writing—review and editing, H.H. and S.F.; visualisation, F.M.; supervision, H.H. and S.F.; project administration, H.H. and S.F.; funding acquisition, H.H. and S.F. All authors have read and agreed to the published version of the manuscript.

Funding: This study was supported by a grant from Engelhard Arzneimittel GmbH & Co. KG, Niederdorfelden, Germany, grant number H-061.0037.

Institutional Review Board Statement: Not applicable.

Informed Consent Statement: Not applicable.

Data Availability Statement: All relevant data are contained within the article.

Conflicts of Interest: The authors declare no conflict of interest. The funders had no role in the design of the study, in the collection, analyses, or interpretation of data, in the writing of the manuscript, or in the decision to publish the results.

References

1. Kardos, P.; Dinh, Q.T.; Fuchs, K.H.; Gillissen, A.; Klimek, L.; Koehler, M.; Sitter, H.; Worth, H. Guidelines of the German Respiratory Society for Diagnosis and Treatment of Adults Suffering from Acute, Subacute and Chronic Cough. *Pneumologie* **2019**, *73*, 143–180. [[CrossRef](#)] [[PubMed](#)]
2. Lang, C.; Röttger-Lüer, P.; Staiger, C. A Valuable Option for the Treatment of Respiratory Diseases: Review on the Clinical Evidence of the Ivy Leaves Dry Extract EA 575[®]. *Planta Med.* **2015**, *81*, 968–974. [[CrossRef](#)] [[PubMed](#)]
3. Schaefer, A.; Ludwig, F.; Giannetti, B.M.; Bulitta, M.; Wacker, A. Efficacy of Two Dosing Schemes of a Liquid Containing Ivy Leaves Dry Extract EA 575 versus Placebo in the Treatment of Acute Bronchitis in Adults. *ERJ Open Res.* **2019**, *5*, 52–57. [[CrossRef](#)]

4. Schaefer, A.; Kehr, M.S.; Giannetti, B.M.; Bulitta, M.; Staiger, C. A Randomized, Controlled, Double-Blind, Multi-Center Trial to Evaluate the Efficacy and Safety of a Liquid Containing Ivy Leaves Dry Extract (EA 575[®]) vs. Placebo in the Treatment of Adults with Acute Cough. *Pharmazie* **2016**, *71*, 504–509. [[CrossRef](#)]
5. Schulte-Michels, J.; Wolf, A.; Aatz, S.; Engelhard, K.; Sieben, A.; Martinez-Osuna, M.; Häberlein, F.; Häberlein, H. α -Hederin Inhibits G Protein-Coupled Receptor Kinase 2-Mediated Phosphorylation of B2-Adrenergic Receptors. *Phytomedicine* **2016**, *23*, 52–57. [[CrossRef](#)]
6. Meurer, F.; Schulte-Michels, J.; Häberlein, H.; Franken, S. Ivy Leaves Dry Extract EA 575[®] Mediates Biased B2-Adrenergic Receptor Signaling. *Phytomedicine* **2021**, *90*, 153645. [[CrossRef](#)]
7. Greunke, C.; Hage-Hülsmann, A.; Sorkalla, T.; Keksel, N.; Häberlein, F.; Häberlein, H. A Systematic Study on the Influence of the Main Ingredients of an Ivy Leaves Dry Extract on the B2-Adrenergic Responsiveness of Human Airway Smooth Muscle Cells. *Pulm. Pharmacol. Ther.* **2015**, *31*, 92–98. [[CrossRef](#)]
8. Bussmann, H.; Schulte-Michels, J.; Bingel, M.; Meurer, F.; Aatz, S.; Häberlein, F.; Franken, S.; Häberlein, H. A Comparative Study on the Influence of an Ivy Preparation and an Ivy/Thyme Combination on the B2-Adrenergic Signal Transduction. *Heliyon* **2020**, *6*, e03960. [[CrossRef](#)]
9. Sieben, A.; Prenner, L.; Sorkalla, T.; Wolf, A.; Jakobs, D.; Runkel, F.; Häberlein, H. α -Hederin, but Not Hederacoside c and Hedera-genin from Hedera Helix, Affects the Binding Behavior, Dynamics, and Regulation of B2- Adrenergic Receptors. *Biochemistry* **2009**, *48*, 3477–3482. [[CrossRef](#)]
10. Schulte-Michels, J.; Runkel, F.; Gokorsch, S.; Häberlein, H. Ivy Leaves Dry Extract EA 575[®] Decreases LPS-Induced IL-6 Release from Murine Macrophages. *Pharmazie* **2016**, *71*, 158–161. [[CrossRef](#)]
11. Schulte-Michels, J.; Keksel, C.; Häberlein, H.; Franken, S. Anti-Inflammatory Effects of Ivy Leaves Dry Extract: Influence on Transcriptional Activity of NF κ B. *Inflammopharmacology* **2019**, *27*, 339–347. [[CrossRef](#)] [[PubMed](#)]
12. Li, X.; Berg, N.K.; Mills, T.; Zhang, K.; Eltzschig, H.K.; Yuan, X. Adenosine at the Interphase of Hypoxia and Inflammation in Lung Injury. *Front. Immunol.* **2021**, *11*, 604944. [[CrossRef](#)] [[PubMed](#)]
13. Le, T.T.T.; Berg, N.K.; Harting, M.T.; Li, X.; Eltzschig, H.K.; Yuan, X. Purinergic Signaling in Pulmonary Inflammation. *Front. Immunol.* **2019**, *10*, 1633. [[CrossRef](#)] [[PubMed](#)]
14. Zhou, Y.; Schneider, D.J.; Blackburn, M.R. Adenosine Signaling and the Regulation of Chronic Lung Disease. *Pharmacol. Ther.* **2009**, *123*, 105–116. [[CrossRef](#)]
15. Blackburn, M.R. Too Much of a Good Thing: Adenosine Overload in Adenosine-Deaminase-Deficient Mice. *Trends Pharmacol. Sci.* **2003**, *24*, 66–70. [[CrossRef](#)]
16. Driver, A.G.; Kukoly, C.A.; Ali, S.; Mustafa, S.J. Adenosine in Bronchoalveolar Lavage Fluid in Asthma. *Am. Rev. Respir. Dis.* **1993**, *148*, 91–97. [[CrossRef](#)]
17. Huszár, É.; Vass, G.; Vizi, É.; Csoma, Z.; Barát, E.; Molnár-Világos, G.; Herjavec, I.; Horváth, I. Adenosine in Exhaled Breath Condensate in Healthy Volunteers and in Patients with Asthma. *Eur. Respir. J.* **2002**, *20*, 1393–1398. [[CrossRef](#)]
18. Esther, C.R.; Boysen, G.; Olsen, B.M.; Collins, L.B.; Ghio, A.J.; Swenberg, J.W.; Boucher, R.C. Mass Spectrometric Analysis of Biomarkers and Dilution Markers in Exhaled Breath Condensate Reveals Elevated Purines in Asthma and Cystic Fibrosis. *Am. J. Physiol. Lung Cell. Mol. Physiol.* **2009**, *296*, L987. [[CrossRef](#)]
19. Esther, C.R.; Lazaar, A.L.; Bordonali, E.; Qaqish, B.; Boucher, R.C. Elevated Airway Purines in COPD. *Chest* **2011**, *140*, 954–960. [[CrossRef](#)]
20. Vizi, É.; Huszár, É.; Csoma, Z.; Böszörményi-Nagy, G.; Barát, E.; Horváth, I.; Herjavec, I.; Kollai, M. Plasma Adenosine Concentration Increases during Exercise: A Possible Contributing Factor in Exercise-Induced Bronchoconstriction in Asthma. *J. Allergy Clin. Immunol.* **2002**, *109*, 446–448. [[CrossRef](#)]
21. Cushley, M.; Tattersfield, A.; Holgate, S. Inhaled Adenosine and Guanosine on Airway Resistance in Normal and Asthmatic Subjects. *Br. J. Clin. Pharmacol.* **1983**, *15*, 161–165. [[CrossRef](#)]
22. Mann, J.S.; Holgate, S.T.; Renwick, A.G.; Cushley, M.J. Airway Effects of Purine Nucleosides and Nucleotides and Release with Bronchial Provocation in Asthma. *J. Appl. Physiol.* **1986**, *61*, 1667–1676. [[CrossRef](#)]
23. Oosterhoff, Y.; De Jong, J.W.; Jansen, M.A.M.; Koeter, G.H.; Postma, D.S. Airway Responsiveness to Adenosine 5'-Monophosphate in Chronic Obstructive Pulmonary Disease Is Determined by Smoking. *Am. Rev. Respir. Dis.* **1993**, *147*, 553–558. [[CrossRef](#)] [[PubMed](#)]
24. Zhou, Y.; Murthy, J.N.; Zeng, D.; Belardinelli, L.; Blackburn, M.R. Alterations in Adenosine Metabolism and Signaling in Patients with Chronic Obstructive Pulmonary Disease and Idiopathic Pulmonary Fibrosis. *PLoS ONE* **2010**, *5*, e9224. [[CrossRef](#)]
25. Mertens, T.C.J.; Hanmandlu, A.; Tu, L.; Phan, C.; Collum, S.D.; Chen, N.Y.; Weng, T.; Davies, J.; Liu, C.; Eltzschig, H.K.; et al. Switching-Off Adora2b in Vascular Smooth Muscle Cells Halts the Development of Pulmonary Hypertension. *Front. Physiol.* **2018**, *9*, 555. [[CrossRef](#)]
26. Karmouty-Quintana, H.; Weng, T.; Garcia-Morales, L.J.; Chen, N.Y.; Pedroza, M.; Zhong, H.; Molina, J.G.; Bunge, R.; Bruckner, B.A.; Xia, Y.; et al. Adenosine A2B Receptor and Hyaluronan Modulate Pulmonary Hypertension Associated with Chronic Obstructive Pulmonary Disease. *Am. J. Respir. Cell Mol. Biol.* **2013**, *49*, 1038–1047. [[CrossRef](#)] [[PubMed](#)]
27. Blackburn, M.R.; Datta, S.K.; Kellems, R.E. Adenosine Deaminase-Deficient Mice Generated Using a Two-Stage Genetic Engineering Strategy Exhibit a Combined Immunodeficiency. *J. Biol. Chem.* **1998**, *273*, 5093–5100. [[CrossRef](#)]

28. Chunn, J.L.; Young, H.W.J.; Banerjee, S.K.; Colasurdo, G.N.; Blackburn, M.R. Adenosine-Dependent Airway Inflammation and Hyperresponsiveness in Partially Adenosine Deaminase-Deficient Mice. *J. Immunol.* **2001**, *167*, 4676–4685. [[CrossRef](#)] [[PubMed](#)]
29. Blackburn, M.R.; Volmer, J.B.; Thrasher, J.L.; Zhong, H.; Crosby, J.R.; Lee, J.J.; Kellems, R.E. Metabolic Consequences of Adenosine Deaminase Deficiency in Mice Are Associated with Defects in Alveogenesis, Pulmonary Inflammation, and Airway Obstruction. *J. Exp. Med.* **2000**, *192*, 159–170. [[CrossRef](#)] [[PubMed](#)]
30. Chunn, J.L.; Molina, J.G.; Mi, T.; Xia, Y.; Kellems, R.E.; Blackburn, M.R. Adenosine-Dependent Pulmonary Fibrosis in Adenosine Deaminase-Deficient Mice. *J. Immunol.* **2005**, *175*, 1937–1946. [[CrossRef](#)] [[PubMed](#)]
31. Sun, C.-X.; Zhong, H.; Mohsenin, A.; Morschl, E.; Chunn, J.L.; Molina, J.G.; Belardinelli, L.; Zeng, D.; Blackburn, M.R. Role of A2B Adenosine Receptor Signaling in Adenosine-Dependent Pulmonary Inflammation and Injury. *J. Clin. Investig.* **2006**, *116*, 2173–2182. [[CrossRef](#)]
32. Chunn, J.L.; Mohsenin, A.; Young, H.W.J.; Lee, C.G.; Elias, J.A.; Kellems, R.E.; Blackburn, M.R. Partially Adenosine Deaminase-Deficient Mice Develop Pulmonary Fibrosis in Association with Adenosine Elevations. *Am. J. Physiol. Lung Cell. Mol. Physiol.* **2006**, *290*, L579–L587. [[CrossRef](#)]
33. Karmouty-Quintana, H.; Zhong, H.; Acero, L.; Weng, T.; Melicoff, E.; West, J.D.; Hemnes, A.; Grenz, A.; Eltzschig, H.K.; Blackwell, T.S.; et al. The A2B Adenosine Receptor Modulates Pulmonary Hypertension Associated with Interstitial Lung Disease. *FASEB J.* **2012**, *26*, 2546–2557. [[CrossRef](#)] [[PubMed](#)]
34. Rincon, M.; Irvin, C.G. Role of IL-6 in Asthma and Other Inflammatory Pulmonary Diseases. *Int. J. Biol. Sci.* **2012**, *8*, 1281–1290. [[CrossRef](#)] [[PubMed](#)]
35. Marini, M.; Vittori, E.; Hollemborg, J.; Mattoli, S. Expression of the Potent Inflammatory Cytokines, Granulocyte-Macrophage-Colony-Stimulating Factor and Interleukin-6 and Interleukin-8, in Bronchial Epithelial Cells of Patients with Asthma. *J. Allergy Clin. Immunol.* **1992**, *89*, 1001–1009. [[CrossRef](#)]
36. Mattoli, S.; Mattoso, V.L.; Soloperto, M.; Allegra, L.; Fasoli, A. Cellular and Biochemical Characteristics of Bronchoalveolar Lavage Fluid in Symptomatic Nonallergic Asthma. *J. Allergy Clin. Immunol.* **1991**, *87*, 794–802. [[CrossRef](#)]
37. Neveu, W.A.; Allard, J.L.; Raymond, D.M.; Bourassa, L.M.; Burns, S.M.; Bunn, J.Y.; Irvin, C.G.; Kaminsky, D.A.; Rincon, M. Elevation of IL-6 in the Allergic Asthmatic Airway Is Independent of Inflammation but Associates with Loss of Central Airway Function. *Respir. Res.* **2010**, *11*, 28. [[CrossRef](#)] [[PubMed](#)]
38. Konno, S.I.; Gonokami, Y.; Kurokawa, M.; Kawazu, K.; Asano, K.; Okamoto, K.I.; Adachi, M. Cytokine Concentrations in Sputum of Asthmatic Patients. *Int. Arch. Allergy Immunol.* **1996**, *109*, 73–78. [[CrossRef](#)] [[PubMed](#)]
39. Broide, D.H.; Lotz, M.; Cuomo, A.J.; Coburn, D.A.; Federman, E.C.; Wasserman, S.I. Cytokines in Symptomatic Asthma Airways. *J. Allergy Clin. Immunol.* **1992**, *89*, 958–967. [[CrossRef](#)]
40. Yokoyama, A.; Kohno, N.; Fujino, S.; Hamada, H.; Inoue, Y.; Fujioka, S.; Ishida, S.; Hiwada, K. Circulating Interleukin-6 Levels in Patients with Bronchial Asthma. *Am. J. Respir. Crit. Care Med.* **1995**, *151*, 1354–1358. [[CrossRef](#)]
41. Tillie-Leblond, I.; Pugin, J.; Marquette, C.H.; Lamblin, C.; Saulnier, F.; Brichet, A.; Wallaert, B.; Tonnel, A.B.; Gosset, P. Balance between Proinflammatory Cytokines and Their Inhibitors in Bronchial Lavage from Patients with Status Asthmaticus. *Am. J. Respir. Crit. Care Med.* **1999**, *159*, 487–494. [[CrossRef](#)]
42. Dixon, A.E.; Raymond, D.M.; Suratt, B.T.; Bourassa, L.M.; Irvin, C.G. Lower Airway Disease in Asthmatics with and without Rhinitis. *Lung* **2008**, *186*, 361–368. [[CrossRef](#)]
43. Morjaria, J.B.; Babu, K.S.; Vijayanand, P.; Chauhan, A.J.; Davies, D.E.; Holgate, S.T. Sputum IL-6 Concentrations in Severe Asthma and Its Relationship with FEV1. *Thorax* **2011**, *66*, 537. [[CrossRef](#)] [[PubMed](#)]
44. Attaran, D.; Lari, S.M.; Towhidi, M.; Marallu, H.G.; Ayatollahi, H.; Khajehdaluae, M.; Ghanei, M.; Basiri, R. Interleukin-6 and Airflow Limitation in Chemical Warfare Patients with Chronic Obstructive Pulmonary Disease. *Int. J. Chronic Obstr. Pulm. Dis.* **2010**, *5*, 335–340. [[CrossRef](#)]
45. Eickmeier, O.; Huebner, M.; Herrmann, E.; Zissler, U.; Rosewich, M.; Baer, P.C.; Buhl, R.; Schmitt-Grohé, S.; Zielen, S.; Schubert, R. Sputum Biomarker Profiles in Cystic Fibrosis (CF) and Chronic Obstructive Pulmonary Disease (COPD) and Association between Pulmonary Function. *Cytokine* **2010**, *50*, 152–157. [[CrossRef](#)]
46. Donaldson, G.C.; Seemungal, T.A.R.; Patel, I.S.; Bhowmik, A.; Wilkinon, T.M.A.; Hurst, J.R.; MacCallum, P.K.; Wedzicha, J.A. Airway and Systemic Inflammation and Decline in Lung Function in Patients with COPD. *Chest* **2005**, *128*, 1995–2004. [[CrossRef](#)]
47. Hacievliyagil, S.S.; Gunen, H.; Mutlu, L.C.; Karabulut, A.B.; Temel, I. Association between Cytokines in Induced Sputum and Severity of Chronic Obstructive Pulmonary Disease. *Respir. Med.* **2006**, *100*, 846–854. [[CrossRef](#)]
48. Celli, B.R.; Locantore, N.; Yates, J.; Tal-Singer, R.; Miller, B.E.; Bakke, P.; Calverley, P.; Coxson, H.; Crim, C.; Edwards, L.D.; et al. Inflammatory Biomarkers Improve Clinical Prediction of Mortality in Chronic Obstructive Pulmonary Disease. *Am. J. Respir. Crit. Care Med.* **2012**, *185*, 1065–1072. [[CrossRef](#)]
49. Saito, F.; Tasaka, S.; Inoue, K.I.; Miyamoto, K.; Nakano, Y.; Ogawa, Y.; Yamada, W.; Shiraishi, Y.; Hasegawa, N.; Fujishima, S.; et al. Role of Interleukin-6 in Bleomycin-Induced Lung Inflammatory Changes in Mice. *Am. J. Respir. Cell Mol. Biol.* **2008**, *38*, 566–571. [[CrossRef](#)]
50. Pedroza, M.; Schneider, D.J.; Karmouty-Quintana, H.; Coote, J.; Shaw, S.; Corrigan, R.; Molina, J.G.; Alcorn, J.L.; Galas, D.; Gelinis, R.; et al. Interleukin-6 Contributes to Inflammation and Remodeling in a Model of Adenosine Mediated Lung Injury. *PLoS ONE* **2011**, *6*, e22667. [[CrossRef](#)] [[PubMed](#)]

51. Ryzhov, S.; Zaynagetdinov, R.; Goldstein, A.E.; Novitskiy, S.V.; Blackburn, M.R.; Biaggioni, I.; Feoktistov, I. Effect of A2B Adenosine Receptor Gene Ablation on Adenosine-Dependent Regulation of Proinflammatory Cytokines. *J. Pharmacol. Exp. Ther.* **2008**, *324*, 694–700. [[CrossRef](#)] [[PubMed](#)]
52. Philip, K.; Mills, T.W.; Davies, J.; Chen, N.Y.; Karmouty-Quintana, H.; Luo, F.; Molina, J.G.; Amione-Guerra, J.; Sinha, N.; Guha, A.; et al. HIF1A Up-Regulates the ADORA2B Receptor on Alternatively Activated Macrophages and Contributes to Pulmonary Fibrosis. *FASEB J.* **2017**, *31*, 4745–4758. [[CrossRef](#)] [[PubMed](#)]
53. Karmouty-Quintana, H.; Philip, K.; Acero, L.F.; Chen, N.Y.; Weng, T.; Molina, J.G.; Luo, F.; Davies, J.; Le, N.B.; Bunge, I.; et al. Deletion of ADORA2B from Myeloid Cells Dampens Lung Fibrosis and Pulmonary Hypertension. *FASEB J.* **2015**, *29*, 50–60. [[CrossRef](#)]
54. Schröder, R.; Janssen, N.; Schmidt, J.; Kebig, A.; Merten, N.; Hennen, S.; Müller, A.; Blättermann, S.; Mohr-Andrä, M.; Zahn, S.; et al. Deconvolution of Complex G Protein–Coupled Receptor Signaling in Live Cells Using Dynamic Mass Redistribution Measurements. *Nat. Biotechnol.* **2010**, *28*, 943–949. [[CrossRef](#)] [[PubMed](#)]
55. Goulding, J.; May, L.T.; Hill, S.J. Characterisation of Endogenous A2A and A2B Receptor-Mediated Cyclic AMP Responses in HEK 293 Cells Using the GloSensor™ Biosensor: Evidence for an Allosteric Mechanism of Action for the A2B-Selective Antagonist PSB 603. *Biochem. Pharmacol.* **2018**, *147*, 55–66. [[CrossRef](#)] [[PubMed](#)]
56. Barresi, E.; Martini, C.; Da Settimo, F.; Greco, G.; Taliani, S.; Giacomelli, C.; Trincavelli, M.L. Allosterism vs. Orthosterism: Recent Findings and Future Perspectives on A2B AR Physio-Pathological Implications. *Front. Pharmacol.* **2021**, *12*, 652121. [[CrossRef](#)]
57. Saecker, L.; Häberlein, H.; Franken, S. Investigation of Adenosine A1 Receptor-Mediated β -Arrestin 2 Recruitment Using a Split-Luciferase Assay. *Front. Pharmacol.* **2023**, *14*, 1172551. [[CrossRef](#)]
58. Montminy, M.R.; Bilezikjian, L.M. Binding of a Nuclear Protein to the Cyclic-AMP Response Element of the Somatostatin Gene. *Nature* **1987**, *328*, 175–178. [[CrossRef](#)]
59. Montminy, M.R.; Sevarino, K.A.; Wagner, J.A.; Mandel, G.; Goodman, R.H. Identification of a Cyclic-AMP-Responsive Element within the Rat Somatostatin Gene. *Proc. Natl. Acad. Sci. USA* **1986**, *83*, 6682–6686. [[CrossRef](#)]
60. Yamamoto, K.K.; Gonzalez, G.A.; Biggs, W.H.; Montminy, M.R. Phosphorylation-Induced Binding and Transcriptional Efficacy of Nuclear Factor CREB. *Nature* **1988**, *334*, 494–498. [[CrossRef](#)]
61. Sun, Y.; Wu, F.; Sun, F.; Huang, P. Adenosine Promotes IL-6 Release in Airway Epithelia. *J. Immunol.* **2008**, *180*, 4173–4181. [[CrossRef](#)] [[PubMed](#)]
62. Du, X.; Ou, X.; Song, T.; Zhang, W.; Cong, F.; Zhang, S.; Xiong, Y. Adenosine A2B Receptor Stimulates Angiogenesis by Inducing VEGF and ENOS in Human Microvascular Endothelial Cells. *Exp. Biol. Med.* **2015**, *240*, 1472–1479. [[CrossRef](#)] [[PubMed](#)]
63. Ray, A.; LaForge, K.S.; Sehgal, P.B. On the Mechanism for Efficient Repression of the Interleukin-6 Promoter by Glucocorticoids: Enhancer, TATA Box, and RNA Start Site (Inr Motif) Occlusion. *Mol. Cell. Biol.* **1990**, *10*, 5736–5746. [[CrossRef](#)] [[PubMed](#)]
64. Ray, A.; Sassone-Corsi, P.; Sehgal, P.B. A Multiple Cytokine- and Second Messenger-Responsive Element in the Enhancer of the Human Interleukin-6 Gene: Similarities with c-Fos Gene Regulation. *Mol. Cell. Biol.* **1989**, *9*, 5537–5547. [[CrossRef](#)]
65. Krueger, J.; Ray, A.; Tamm, I.; Sehgal, P.B. Expression and Function of Interleukin-6 in Epithelial Cells. *J. Cell. Biochem.* **1991**, *45*, 327–334. [[CrossRef](#)]
66. Ray, A.; Tatter, S.B.; May, L.T.; Sehgal, P.B. Activation of the Human “Beta 2-Interferon/Hepatocyte-Stimulating Factor/Interleukin 6” Promoter by Cytokines, Viruses, and Second Messenger Agonists. *Proc. Natl. Acad. Sci. USA* **1988**, *85*, 6701–6705. [[CrossRef](#)]
67. Zhang, Y.; Lin, J.X.; Vilcek, J. Synthesis of Interleukin 6 (Interferon-B2/B Cell Stimulatory Factor 2) in Human Fibroblasts Is Triggered by an Increase in Intracellular Cyclic AMP. *J. Biol. Chem.* **1988**, *263*, 6177–6182. [[CrossRef](#)]
68. Zhong, H.; Belardinelli, L.; Maa, T.; Feoktistov, I.; Biaggioni, I.; Zeng, D. A2B Adenosine Receptors Increase Cytokine Release by Bronchial Smooth Muscle Cells. *Am. J. Respir. Cell Mol. Biol.* **2004**, *30*, 118–125. [[CrossRef](#)]
69. Sitaraman, S.V.; Merlin, D.; Wang, L.; Wong, M.; Gewirtz, A.T.; Si-Tahar, M.; Madara, J.L. Neutrophil-Epithelial Crosstalk at the Intestinal Luminal Surface Mediated by Reciprocal Secretion of Adenosine and IL-6. *J. Clin. Investig.* **2001**, *107*, 861–869. [[CrossRef](#)]
70. Libermann, T.A.; Baltimore, D. Activation of Interleukin-6 Gene Expression through the NF-Kappa B Transcription Factor. *Mol. Cell. Biol.* **1990**, *10*, 2327–2334. [[CrossRef](#)]
71. Shimizu, H.; Mitomo, K.; Watanabe, T.; Okamoto, S.; Yamamoto, K. Involvement of a NF-Kappa B-like Transcription Factor in the Activation of the Interleukin-6 Gene by Inflammatory Lymphokines. *Mol. Cell. Biol.* **1990**, *10*, 561–568. [[CrossRef](#)] [[PubMed](#)]
72. Cobb, B.R.; Ruiz, F.; King, C.M.; Fortenberry, J.; Greer, H.; Kovacs, T.; Sorscher, E.J.; Clancy, J.P. A2 Adenosine Receptors Regulate CFTR through PKA and PLA2. *Am. J. Physiol. Lung Cell. Mol. Physiol.* **2002**, *282*, 12–25. [[CrossRef](#)] [[PubMed](#)]
73. Szkotak, A.J.; Ng, A.M.L.; Man, S.F.P.; Baldwin, S.A.; Cass, C.E.; Young, J.D.; Duszyk, M. Coupling of CFTR-Mediated Anion Secretion to Nucleoside Transporters and Adenosine Homeostasis in Calu-3 Cells. *J. Membr. Biol.* **2003**, *192*, 169–179. [[CrossRef](#)] [[PubMed](#)]
74. Atwood, B.K.; Lopez, J.; Wager-Miller, J.; Mackie, K.; Straiker, A. Expression of G Protein-Coupled Receptors and Related Proteins in HEK293, AtT20, BV2, and N18 Cell Lines as Revealed by Microarray Analysis. *BMC Genom.* **2011**, *12*, 14. [[CrossRef](#)]
75. Zhong, H.; Belardinelli, L.; Maa, T.; Zeng, D. Synergy between A2B Adenosine Receptors and Hypoxia in Activating Human Lung Fibroblasts. *Am. J. Respir. Cell Mol. Biol.* **2005**, *32*, 2–8. [[CrossRef](#)]

76. Fredholm, B.B.; IJzerman, A.P.; Jacobson, K.A.; Linden, J.; Müller, C.E. International Union of Basic and Clinical Pharmacology. LXXXI. Nomenclature and Classification of Adenosine Receptors—An Update. *Pharmacol. Rev.* **2011**, *63*, 1–34. [[CrossRef](#)] [[PubMed](#)]
77. Geraghty, N.J.; Adhikary, S.R.; Watson, D.; Sluyter, R. The A2A Receptor Agonist CGS 21680 Has Beneficial and Adverse Effects on Disease Development in a Humanised Mouse Model of Graft-versus-Host Disease. *Int. Immunopharmacol.* **2019**, *72*, 479–486. [[CrossRef](#)] [[PubMed](#)]
78. Pei, H.; Linden, J. Adenosine Influences Myeloid Cells to Inhibit Aeroallergen Sensitization. *Am. J. Physiol. Lung Cell. Mol. Physiol.* **2016**, *310*, L985–L992. [[CrossRef](#)]
79. Zheng, X.; Wang, D. The Adenosine A2A Receptor Agonist Accelerates Bone Healing and Adjusts Treg/Th17 Cell Balance through Interleukin 6. *Biomed. Res. Int.* **2020**, *2020*, 2603873. [[CrossRef](#)]
80. Tang, L.M.; Wang, Y.P.; Wang, K.; Pu, L.Y.; Zhang, F.; Li, X.C.; Kong, L.B.; Sun, B.C.; Li, G.Q.; Wang, X.H. Protective Effect of Adenosine A2A Receptor Activation in Small-for-Size Liver Transplantation. *Transpl. Int.* **2007**, *20*, 93–101. [[CrossRef](#)]
81. Rogachev, B.; Ziv, N.Y.; Mazar, J.; Nakav, S.; Chaimovitz, C.; Zlotnik, M.; Douvdevani, A. Adenosine Is Upregulated during Peritonitis and Is Involved in Downregulation of Inflammation. *Kidney Int.* **2006**, *70*, 675–681. [[CrossRef](#)] [[PubMed](#)]
82. Zhang, L.; Franchini, M.; Wehrli Eser, M.; Dip, R. Enhanced IL-6 Transcriptional Response to Adenosine Receptor Ligands in Horses with Lower Airway Inflammation. *Equine Vet. J.* **2012**, *44*, 81–87. [[CrossRef](#)] [[PubMed](#)]
83. Schwaninger, M.; Neher, M.; Viegas, E.; Schneider, A.; Spranger, M. Stimulation of Interleukin-6 Secretion and Gene Transcription in Primary Astrocytes by Adenosine. *J. Neurochem.* **1997**, *69*, 1145–1150. [[CrossRef](#)]
84. McColl, S.R.; St-Onge, M.; Dussault, A.-A.; Laflamme, C.; Bouchard, L.; Boulanger, J.; Pouliot, M. Immunomodulatory Impact of the A2A Adenosine Receptor on the Profile of Chemokines Produced by Neutrophils. *FASEB J.* **2006**, *20*, 187. [[CrossRef](#)]
85. Mohsenin, A.; Mi, T.; Xia, Y.; Kellems, R.E.; Chen, J.F.; Blackburn, M.R. Genetic Removal of the A2A Adenosine Receptor Enhances Pulmonary Inflammation, Mucin Production, and Angiogenesis in Adenosine Deaminase-Deficient Mice. *Am. J. Physiol. Lung Cell. Mol. Physiol.* **2007**, *293*, L753–L761. [[CrossRef](#)] [[PubMed](#)]
86. Pejman, L.; Omrani, H.; Mirzamohammadi, Z.; Shahbazfar, A.A.; Khalili, M.; Keyhanmanesh, R. The Effect of Adenosine A2A and A2B Antagonists on Tracheal Responsiveness, Serum Levels of Cytokines and Lung Inflammation in Guinea Pig Model of Asthma. *Adv. Pharm. Bull.* **2014**, *4*, 131–138. [[CrossRef](#)] [[PubMed](#)]
87. Mustafa, S.J.; Nadeem, A.; Fan, M.; Zhong, H.; Belardinelli, L.; Zeng, D. Effect of a Specific and Selective A2B Adenosine Receptor Antagonist on Adenosine Agonist AMP and Allergen-Induced Airway Responsiveness and Cellular Influx in a Mouse Model of Asthma. *J. Pharmacol. Exp. Ther.* **2007**, *320*, 1246–1251. [[CrossRef](#)]
88. Zeil, S.; Schwanebeck, U.; Vogelberg, C. Tolerance and Effect of an Add-on Treatment with a Cough Medicine Containing Ivy Leaves Dry Extract on Lung Function in Children with Bronchial Asthma. *Phytomedicine* **2014**, *21*, 1216–1220. [[CrossRef](#)]
89. Shokry, A.A.; El-Shiekh, R.A.; Kamel, G.; Bakr, A.F.; Ramadan, A. Bioactive Phenolics Fraction of *Hedera helix* L. (Common Ivy Leaf) Standardized Extract Ameliorates LPS-Induced Acute Lung Injury in the Mouse Model through the Inhibition of Proinflammatory Cytokines and Oxidative Stress. *Heliyon* **2022**, *8*, e09477. [[CrossRef](#)]
90. Shokry, A.A.; El-Shiekh, R.A.; Kamel, G.; Bakr, A.F.; Sabry, D.; Ramadan, A. Anti-Arthritic Activity of the Flavonoids Fraction of Ivy Leaves (*Hedera helix* L.) Standardized Extract in Adjuvant Induced Arthritis Model in Rats in Relation to Its Metabolite Profile Using LC/MS. *Biomed. Pharmacother.* **2022**, *145*, 112456. [[CrossRef](#)]
91. Watson, M.J.; Worthington, E.N.; Clunes, L.A.; Rasmussen, J.E.; Jones, L.; Tarran, R. Defective Adenosine-Stimulated CAMP Production in Cystic Fibrosis Airway Epithelia: A Novel Role for CFTR in Cell Signaling. *FASEB J.* **2011**, *25*, 2996–3003. [[CrossRef](#)] [[PubMed](#)]

Disclaimer/Publisher’s Note: The statements, opinions and data contained in all publications are solely those of the individual author(s) and contributor(s) and not of MDPI and/or the editor(s). MDPI and/or the editor(s) disclaim responsibility for any injury to people or property resulting from any ideas, methods, instructions or products referred to in the content.